

ENHANCED PRODUCTION CONSIDERING TEMPERATURE EFFECTS ON NEW

HYBRIDOMAS FOR BOVINE NATURAL KILLER CELL

MONOCLONAL ANTIBODIES

By

A. NATASHA GODWIN

A thesis submitted in partial fulfillment of
the requirements for the degree of

MASTER OF SCIENCE IN CHEMICAL ENGINEERING

WASHINGTON STATE UNIVERSITY

School of Chemical Engineering and Bioengineering

DECEMBER 2008

To the Faculty of Washington State University:

The members of the Committee appointed to examine the thesis of A. NATASHA GODWIN find it satisfactory and recommend that it be accepted.

Chair

ACKNOWLEDGMENTS

I would like to thank my advisor, Dr. Van Wie, for his knowledgeable advice and help with editing both my manuscript and my thesis. You have always believed in me and my capabilities and pushed me to finish even when I had my doubts. I would also like to thank Dr. Davis and Mary Jo Hamilton for their tremendous help in teaching me all the techniques and skills I used in my research. Without your extensive knowledge and support I would have been lost. To the other members of my committee, Dr. Reeves and Dr. Abu-Lail, I offer my thanks for your belief in my research and the many encouraging words given to me during our committee meetings. I am also grateful to the ladies in the main office, Diana, Jo Ann, and Senja. Without your help I would have never been paid or have been able to order the materials I needed or to have even been able to work the copy machine. Plus, walks to the office offered a nice break from my daily routine with a friendly conversation and sometimes even a cookie.

To the many friends I have made here in Pullman, I thank you the most for making this a home away from home. I knew no one when I moved here four years ago but I will be leaving with the many wonderful friendships we have made. Thank you all for the love and support you have given me and, most of all, thanks for the memories.

Last, but not least, I would like to thank my family for all of their emotional and financial support. I am a long way from home but you always make me feel like you are right here with me. Without you none of this would have been possible.

ENHANCED PRODUCTION CONSIDERING TEMPERATURE EFFECTS ON NEW
HYBRIDOMAS FOR BOVINE NATURAL KILLER CELL
MONOCLONAL ANTIBODIES

Abstract

By A. Natasha Godwin, M.S.

Washington State University

December 2008

Chair: Bernard J. Van Wie

Demand for monoclonal antibodies (mAbs) has led to the improvement of mammalian cell culture processes taking into account reactor design and specific mAb production rate of the cell line. The creation of a continuous centrifugal bioreactor (CCBR) allows for increased volumetric productivity by maintaining a high density cell culture, 10^8 cells/mL, while lowering the cell culture temperature increases the specific mAb production rate. This thesis contains a manuscript prepared for submission to *Journal of Veterinary Immunology and Immunopathology* in which I describe the creation of new hybridoma cell lines secreting mAb to bovine natural killer (NK) cells. The recent development of a mAb to the bovine orthologue of the activating NK receptor NKp46 allowed us to develop a flow cytometric method for clustering and characterizing additional mAbs reactive with bovine NK cells. Cluster 1 mAbs, NK64A and NK93A, recognize an orthologue of the stress protein gp96 expressed on NK cells and granulocytes. Cluster 2 mAbs, NK29A, NK42A, NK47A, NK86A, NK134A, and NK137A,

recognize a yet undetermined molecule expressed on activated NK cells and subsets of $\alpha\beta$ and $\gamma\delta$ T cells. The NK64A hybridoma was utilized in studies of the effect of cell culture temperature on cell growth and specific mAb production using the CCBR and a kinetic model for predicting glucose, ammonium, lactate, and mAb concentrations. Batch studies were performed at temperatures of 31, 33, 35, 37, and 39°C; and for the temperature range 35 to 39°C it was found that the growth rate was essentially constant, $0.052 \text{ hr}^{-1} \pm 0.001$, but decreased to 0.036 hr^{-1} for 33°C and 0.026 hr^{-1} for 31°C. The specific mAb production rate increased by 120% at 33°C and 100% at 31°C compared to 37°C. Culture of the NK64A hybridoma in the CCBR at 37 and 33°C resulted in decreased growth rates compared to batch studies, 0.0039 hr^{-1} and 0.011 hr^{-1} respectively, indicating cell density inhibition for this cell line. Yield coefficients were adjusted to improve fit of the kinetic model to the CCBR data. These results indicate the need to study each cell line in order to determine the optimum cell culture conditions.

TABLE OF CONTENTS

	Page
ACKNOWLEDGEMENTS.....	iii
ABSTRACT.....	iv
LIST OF TABLES.....	ix
LIST OF FIGURES.....	x
CHAPTER	
1. GENERAL INTRODUCTION.....	1
2. USE OF FLOW CYTOMETRY TO IDENTIFY AND CHARACTERIZE MONOCLONAL ANTIBODIES SPECIFIC FOR BOVINE NATURAL KILLER CELLS	
2.1. Title Page.....	10
2.2. Abstract.....	11
2.3. Introduction.....	12
2.4. Materials and Methods.....	14
2.4.1. Generation of bovine NK cells.....	14
2.4.2. Generation of anti-NK monoclonal antibodies.....	14
2.4.3. Generation of T cell subsets.....	15
2.4.4. Monoclonal antibodies.....	16
2.4.5. Preparation of cells for flow cytometry.....	17
2.4.6. Flow cytometry.....	18
2.4.7. 2-DE and Western blotting.....	18
2.4.8. MS/MS analysis.....	19

2.5. Results.....	20
2.5.1. Preparation of NK cells for immunization and mAb characterization.....	20
2.5.2. Identification and clustering of antibodies recognizing molecules expressed on NK cells.....	20
2.5.3. Cross-comparison of NK mAbs.....	23
2.5.4. Cluster 2 recognizes subsets of T cells.....	25
2.5.5. Cluster 1 mAbs recognize the bovine orthologue of stress protein gp96.....	29
2.6. Discussion.....	29
2.7. Acknowledgments.....	32
2.8. References.....	33
3. EFFECT OF CULTURE TEMPERATURE ON MONOCLONAL ANTIBODY PRODUCTION BY THE NK64A HYBRIDOMA IN BATCH AND HIGH-DENSITY CULTURES.....	35
3.1. Introduction.....	35
3.2. Theory.....	37
3.2.1. Kinetic modeling.....	37
3.2.2. Bioreactor settling velocities and porosities.....	38
3.3. Materials and Methods.....	40
3.3.1. Culture medium.....	40
3.3.2. Cell line.....	41
3.3.3. Batch cultures.....	41
3.3.4. Inhibition studies.....	42
3.4. CCBR.....	43

3.4.1. Construction.....	43
3.4.2. Startup.....	45
3.4.3. Sampling.....	45
3.4.4. Reactor runs.....	46
3.5. Analysis.....	47
3.5.1. Cell concentration and viability assay.....	47
3.5.2. Glucose assay.....	47
3.5.3. Lactate assay.....	47
3.5.4. Ammonium assay.....	48
3.5.5. Monoclonal antibody assay.....	48
3.6. Results and Discussion.....	49
3.6.1. Inhibition studies.....	49
3.6.2. Temperature studies.....	50
3.6.3. Temperature dependencies of yield coefficients.....	59
3.6.4. Modeling of batch culture.....	61
3.6.5. Model of CCBR culture.....	64
3.6.6. Model fit to reactor runs.....	69
3.7. Conclusions.....	79
3.8. References.....	82
4. GENERAL CONCLUSIONS AND FUTURE WORK.....	84

LIST OF TABLES

CHAPTER TWO

1. MAbs for common T cell markers and the anti-CD335 mAb for NK cells
used to characterize and cluster the new NK mAbs.....17
2. New NK mAbs were placed into clusters based on their expression patterns.....22

CHAPTER THREE

1. Cell growth parameters determined from batch temperature studies.....59

LIST OF FIGURES

CHAPTER 2

1. Representative single fluorescent dot plot profiles of a peripheral blood mononuclear cell preparation labeled with the mAbs indicated.....20
2. Single fluorescent dot plot profiles of a rHuIL-15 stimulated NK cell preparation labeled with the mAbs indicated.....22
3. Cross-comparison of NK mAbs using two-color FC analysis and a preparation of rHuIL-15 stimulated NK cells.....24
4. Phenotypic analysis of Cluster 2 positive cells using three-color FC on a preparation of cells comprised of rHuIL-15 stimulated NK cells and concanavalin A stimulated T cell blasts (3:1 cell ratio respectively).....25
5. Further characterization of T cell subsets labeled by Cluster 2 mAbs using purified cultures of CD3⁺ (A-F) or TcR1⁺ (G-L) T cells separated from splenic leukocytes using MACS columns and mAbs to either CD3 (A-F) or the TcR1 δ chain (G-L).....27
6. 2-DE and immunoblot analysis of NK cell lysates.....28

CHAPTER 3

1. Schematic of bioreactor and direction of forces acting on the cells.....39
2. Flow profile of the CCBR cell culture system.....44
3. Results of ammonium ion and lactate inhibition experiments.....49
4. Live cell concentration profiles for the five temperature experiments.....51
5. Glucose concentrations for the five temperature experiments.....52

6. Lactate concentrations for the five temperature experiments.....	53
7. Ammonium ion concentrations for the five temperature experiments.....	54
8. Monoclonal antibody concentrations for the five temperature experiments.....	55
9. Yield coefficients and growth rate as a function of cell culture temperature.....	58
10. Arrhenius plot for literature values.....	60
11. Arrhenius plot for NK64A hybridoma.....	61
12. Model fit for cell and glucose concentration in 75 mL batch culture.....	62
13. Model fit for mAb, lactate, and ammonium ion concentration in 75 mL batch culture.....	63
14. Model predictions for cell and glucose concentrations during NK64A culture in the CCBR at 37°C with an initial cell concentration of 2.50×10^7 cells/mL.....	65
15. Model predictions for ammonium, lactate, and mAb production during NK64A culture in the CCBR at 37°C with an initial cell concentration of 2.50×10^7 cells/mL.....	66
16. Model predictions for cell and glucose concentrations during NK64A culture in the CCBR at 33°C with an initial cell concentration of 2.50×10^7 cells/mL.....	67
17. Model predictions for ammonium, lactate, and mAb production during NK64A culture in the CCBR at 33°C with an initial cell concentration of 2.50×10^7 cells/mL.....	68
18. pH and temperature profiles for reactor run 1 at 37°C.....	70
19. Model fit to the cell and glucose concentration data obtained from reactor run 1 at 37°C using the growth rate observed in the reactor and the yield coefficients from the 37°C batch study.....	71
20. Model fit to the lactate and ammonium concentration data obtained from reactor run 1 at 37°C using the growth rate observed in the reactor and the yield coefficients from the 37°C batch study.....	72

21. Model fit to the cell and glucose concentration data obtained from reactor run 1 using the growth rate observed in the reactor and adjusted yield coefficients for glucose, lactate, and ammonium.....	73
22. Model fit to the lactate and ammonium concentration data obtained from reactor run 1 using the growth rate observed in the reactor and adjusted yield coefficients for glucose, lactate, and ammonium.....	74
23. pH and temperature profiles for reactor run 2 at 33°C.....	75
24. Model fit to the cell and glucose concentration data obtained from reactor run 2 at 33°C using the growth rate observed in the reactor and the yield coefficients from the 33°C batch study.....	76
25. Model fit to the lactate and ammonium concentration data obtained from reactor run 2 at 33°C using the growth rate observed in the reactor and the yield coefficients from the 33°C batch study.....	77
26. Model fit to the cell and glucose concentration data obtained from reactor run 2 using the growth rate observed in the reactor and adjusted yield coefficients for glucose, lactate, and ammonium.....	78
27. Model fit to the lactate and ammonium concentration data obtained from reactor run 2 using the growth rate observed in the reactor and adjusted yield coefficients for glucose, lactate, and ammonium.....	79

DEDICATION

This thesis is dedicated to my parents, Randy and Ann Godwin, and my late sister,
Miranda Godwin. I love you all very much.

CHAPTER ONE

GENERAL INTRODUCTION

Natural killer (NK) cells are large, granular lymphocytes of bone marrow origin with the ability to spontaneously lyse target cells such as tumor cells, cells that have been infected with bacteria, viruses, or parasites, and normal cells that are MHC-disparate (Delgi-Esposti and Smyth 2005; Moretta et al. 2008; Zhang et al. 2006). They also have the ability to produce large quantities of cytokines such as IFN- γ , TNF, GM-CSF, IL-10, IL-13, and IL-5 and chemokines of the MIP-1 family (Delgi-Esposti and Smyth 2005; Diefenbach and Raulet 2001; Lanier 2000; Raulet et al. 2001; Zhang et al. 2006). NK cells are part of the innate immune system and therefore do not require prior activation or immunization to respond and require no proliferation phase following infection (Moretta et al. 2008; Raulet et al. 2001; Zhang et al. 2006). NK cells are able to discriminate between target and non-target cells using inhibitory and activating receptors expressed on their surface similar to the receptors on B and T cells; however, NK receptors do not undergo gene rearrangement (Diefenbach and Raulet 2001; Moretta et al. 2008; Raulet et al. 2001). Some NK inhibitory receptors focus on the recognition of MHC class I molecules, which are present on healthy cells and thus prevents NK cell attack against these cells (Delgi-Esposti and Smyth 2005; Moretta et al. 2008; Natarajan et al. 2002). Loss or downregulation of MHC class I molecules is common in infected or tumor transformed cells and results in activation of NK cells and subsequent lysis of the target cell. This is known as the “missing self hypothesis” (Karre 2008; Lanier 2008). Cells that have lost or downregulated expression of MHC class I molecules can no longer engage the inhibitory receptors on NK cells that recognize MHC class I and are therefore

susceptible to lysis providing that an activating receptor is also engaged. Activating receptors recognize host-derived or pathogen-encoded ligands that are often expressed on infected cells (Moretta et al. 2008). The balance between these activating and inhibitory receptors determines the outcome of the NK cell – target cell interaction.

In cattle, NK-like cells were first discovered based on their ability to lyse certain target cells without prior antigen stimulation and the ability to produce cytokines such as IFN- γ after pathogen infection (Boysen et al. 2006b; Denis et al. 2007). These cells were characterized as being CD3⁻CD2⁺ lymphocytes with little to no expression of CD8 and CD11b (Endsley et al. 2006). Recent investigations (Storset et al. 2004) have led to the development of a mAb that recognizes bovine NKp46 (CD335), a cell-activating receptor that in humans is found solely on NK cells. CD335⁺ cells constitute ~5% of the mononuclear cell population in bovine peripheral blood (Kulberg et al. 2004). Further studies (Boysen et al. 2006a; Denis et al. 2007; Goff et al. 2006; Klevar et al. 2007; Maley et al. 2006; Olsen et al. 2005) have shown that NK cells play a pivotal role in the early stages of many common bovine infections, including *Neospora caninum*, *Babesia bovis*, *Mycobacterium bovis*, and *Mycobacterium avium* subsp. *paratuberculosis*, through the production of IFN- γ . The development of the anti-CD335 antibody has led to the discovery that bovine NK cells can be either CD2⁺ or CD2⁻. The CD335⁺CD2⁻ phenotype constitutes 20% of the CD335⁺ cells found in peripheral blood and is more activated in circulation with stronger IFN- γ producing capabilities (Boysen et al. 2006b). Another recent study (Boysen et al. 2007) shows that NK cells present in the lymph nodes of healthy calves are CD16⁺ but express little to no CD2. These lymph node-derived NK cells have a higher expression of the activation markers CD44 and CD25

than NK cells found in blood. The development of additional mAbs to molecules expressed on the surface of bovine NK cells through the use of hybridoma cells will facilitate further research into the role that NK cells play in the innate immunity of cattle.

Culturing hybridoma cells for the production of mAb typically includes using batch, fed-batch, or various perfusion systems each with their own advantages and disadvantages. Batch and fed-batch systems are the most common systems employed in industry for large scale production due to the ease of scale-up and simplicity of operation (Birch and Racher 2006; Farid 2006; Jain and Kumar 2008). Stirred-tank reactors operated in fed-batch mode can increase the viability of cells over the traditional batch culture by the addition of concentrated key nutrients and mixing to help maintain a homogeneous environment (Butler 2005; Jain and Kumar 2008). However, stirred-tank reactors are limited to a maximum cell density of 20×10^6 cells/mL provided that cells are returned to the culture from the spent medium (Detzel et al. 2008). To increase cell densities, perfusion systems such as hollow fiber bioreactors (HFBRs) and packed bed bioreactors (PBRs) have been developed. In these systems the cells are supplied with a continuous flow of fresh medium while being immobilized to prevent washout through the use of capillaries in the case of the HFBR or porous micro-carrier beads in the PBR leading to cell densities as high as 10^8 cells/mL (Detzel et al. 2008; Jain and Kumar 2008). Disadvantages of HFBRs and PBRs include higher contamination risks from longer cycle times, membrane fouling, and diffusional limitations leading to heterogeneous product formation (Detzel et al. 2008; Farid 2006).

In an effort to overcome these problems a continuous centrifugal bioreactor (CCBR) was developed. The CCBR immobilizes cells through the balance of centrifugal forces

with opposing drag and buoyant forces allowing for cell densities as high as 3.2×10^8 cells/mL (Detzel et al. 2008; Van Wie et al. 1991; Van Wie et al. 1986). Cells are suspended in a homogeneous fluidized bed where the continuous flow of fresh medium provides adequate transport of key nutrients to the cells and removal of harmful waste products. A kinetic model has also been developed for the CCBR that accurately predicts the nutrient and metabolite concentrations within the culture providing a useful tool for maintaining optimum conditions over the duration of the culture (Detzel et al. 2008).

In addition to improvements in the design of the reactor system used to culture hybridoma cells, improvements in the specific mAb production of the hybridoma can also be made in order to maximize production while minimizing costs. Varying the temperature at which the cells are cultured has been shown to be a promising method for increasing the specific mAb production. The standard temperature for mammalian cell culture is 37°C and studies have shown no cell growth occurs when the temperature is dropped to 29°C or raised to 42°C but in the range of $32\text{-}39^\circ\text{C}$ cells are still viable and the specific mAb production rate can be increased or decreased depending on the cell line (Bloemkolk et al. 1992; Chuppa et al. 1997; Fox et al. 2004; Sureshkumar and Mutharasan 1991; Yoon et al. 2004; Yoon et al. 2003). Increasing the cell culture temperature to $38\text{-}39^\circ\text{C}$ increases the cellular metabolism thus increasing glucose consumption and metabolite production as well as increasing mAb production for the rat-mouse-mouse trioma S4B6 (Bloemkolk et al. 1992) and the mouse-mouse hybridoma 14-4-4S (Sureshkumar and Mutharasan 1991). The specific growth rate for the S4B6 trioma also increased with temperature from an average value of 0.030 hr^{-1} at 37°C to 0.054 hr^{-1} at 38°C while the specific growth rate of the 14-4-4S hybridoma was found to be

relatively constant only increasing from 0.045 hr^{-1} to 0.048 hr^{-1} with a temperature increase from 37 to 39°C. For both cell lines a decrease in temperature to 35°C resulted in essentially the same growth rate as 37°C but an 8% decrease in specific mAb production. A further decrease to 33-34°C lowered the specific growth rate by 24-28% for both lines while the specific mAb production remained unchanged for the trioma but decreased an additional 36% for the hybridoma (Bloemkolk et al. 1992; Sureshkumar and Mutharasan 1991). Studies with Chinese hamster ovary cells have seen both decreases and increases in specific mAb production rates with a decrease in temperature from 37 to 32°C with some cell lines increasing production as much as 2- to 25-fold (Chuppa et al. 1997; Fox et al. 2004; Yoon et al. 2004; Yoon et al. 2003). These results indicate that the effect of temperature on specific mAb production rate is cell line dependent and in many instances knowing the optimal temperature could prove to be a relatively easy way to increase production of mAbs.

- Birch J, Racher A. 2006. Antibody production. *Advanced Drug Delivery Reviews* 58:671-685.
- Bloemkolk J, Gray M, Merchant F, Mosmann T. 1992. Effect of temperature on hybridoma cell cycle and mAb production. *Biotechnology and Bioengineering* 40:427-431.
- Boysen P, Gunnes G, Pende D, Valheim M, Storset A. 2007. Natural killer cells in lymph nodes of healthy calves express CD16 and show both cytotoxic and cytokine-producing properties. *Developmental and Comparative Immunology* In press.
- Boysen P, Klevar S, Olsen I, Storset A. 2006a. The protozoan Neospora caninum directly triggers bovine NK cells to produce gamma interferon and to kill infected fibroblasts. *Infection and Immunity* 74(2):953-960.
- Boysen P, Olsen I, Berg I, Kulberg S, Johansen G, Storset A. 2006b. Bovine CD2-/NKp46+ cells are fully functional natural killer cells with a high activation status. *BMC Immunology* 7(10).
- Butler M. 2005. Animal cell cultures: recent achievements and perspectives in the production of biopharmaceuticals. *Applied Microbiology and Biotechnology* 68:283-291.
- Chuppa S, Tsai Y, Yoon S, Shackelford S, Rozales C, Bhat R, Tsay G, Matanguihan C, Konstantinov K, Naveh D. 1997. Fermentor temperature as a tool for control of high-density perfusion cultures of mammalian cells. *Biotechnology and Bioengineering* 55(2):328-338.
- Delgi-Esposti M, Smyth K. 2005. Close encounters of different kinds: dendritic cells and NK cells take centre stage. *Nature Reviews* 5:112-124.
- Denis M, Keen D, Parlane N, Storset A, Buddle B. 2007. Bovine natural killer cells restrict the replication of *Mycobacterium bovis* in bovine macrophages and enhance IL-12 release by infected macrophages. *Tuberculosis* 87(1):53-62.
- Detzel C, Mason D, Davis W, Van Wie B. 2008. Optimization of a centrifugal bioreactor for high population density hybridoma culture. *Biotechnology Progress* Submitted.
- Diefenbach A, Raulet D. 2001. Strategies for target cell recognition by natural killer cells. *Immunological Reviews* 181:170-184.
- Endsley J, Endsley M, Estes D. 2006. Bovine natural killer cells acquire cytotoxic/effector activity following activation with IL-12/15 and reduce *Mycobacterium bovis* BCG in infected macrophages. *Journal of Leukocyte Biology* 79(1):71-79.
- Farid S. 2006. Established bioprocesses for producing antibodies as a basis for future planning. *Advances in Biochemical Engineering/Biotechnology* 101:1-42.
- Fox S, Patel U, Yap M, Wang D. 2004. Maximizing interferon- γ production by chinese hamster ovary cells through temperature shift optimization: Experimental and modeling. *Biotechnology and Bioengineering* 85(2):177-184.
- Goff W, Storset A, Johnson W, Brown W. 2006. Bovine splenic NK cells synthesize IFN- γ in response to IL-12-containing supernatants from *Babesia bovis*-exposed monocyte cultures. *Parasite Immunology* 28:221-228.

- Jain E, Kumar A. 2008. Upstream processes in antibody production: Evaluation of critical parameters. *Biotechnology Advances* 26:46-72.
- Karre K. 2008. Natural killer cell recognition of missing self. *Nature Immunology* 9(5):477-480.
- Klevar S, Kulberg S, Boysen P, Storset A, Moldal T, Björkman C, Olsen I. 2007. Natural killer cells act as early responders in an experimental infection with *Neospora caninum* in calves. *International Journal for Parasitology* 37:329-339.
- Kulberg S, Boysen P, Storset A. 2004. Reference values for relative numbers of natural killer cells in cattle blood. *Developmental and Comparative Immunology* 28:941-948.
- Lanier L. 2000. The origin and functions of natural killer cells. *Clinical Immunology* 95(1):S14-S18.
- Lanier L. 2008. Up on the tightrope: natural killer cell activation and inhibition. *Nature Immunology* 9(5):495-502.
- Maley S, Buxton D, Macaldowie C, Anderson I, Wright S, Bartley P, Esteban-Redondo I, Hamilton C, Storset A, Innes E. 2006. Characterization of the immune response in the placenta of cattle experimentally infected with *Neospora caninum* in early gestation. *Journal of Comparative Pathology* 135:130-141.
- Moretta A, Marcenaro E, Parolini S, Ferlazzo G, Moretta L. 2008. NK cells at the interface between innate and adaptive immunity. *Cell Death and Differentiation* 15:226-233.
- Natarajan K, Dimasi N, Wang J, Mariuzza R, Margulies D. 2002. Structure and function of natural killer cell receptors: Multiple molecular solutions to self, nonself discrimination. *Annual Review of Immunology* 20:853-885.
- Olsen I, Boysen P, Kulberg S, Hope J, Jungersen G, Storset A. 2005. Bovine NK cells can produce interferon in response to the secreted mycobacterial proteins ESAT-6 and MPP14 but not in response to MPB70. *Infection and Immunity* 73(9):5628-5635.
- Raulet D, Vance R, McMahon C. 2001. Regulation of the natural killer cell receptor repertoire. *Annual Review of Immunology* 19:291-330.
- Storset A, Kulberg S, Berg I, Boysen P, Hope J, Dissen E. 2004. NKp46 defines a subset of bovine leukocytes with natural killer cell characteristics. *European Journal of Immunology* 34:669-676.
- Sureshkumar G, Mutharasan R. 1991. The influence of temperature on a mouse-mouse hybridoma growth and monoclonal antibody production. *Biotechnology and Bioengineering* 37:292-295.
- Van Wie B, Brouns T, Elliott M, Davis W. 1991. A novel continuous centrifugal bioreactor for high-density cultivation of mammalian and microbial cells. *Biotechnology and Bioengineering* 38:1190-1202.
- Van Wie B, Elliott M, Lee J. 1986. Development and characterization of a continuous centrifugal bio-reactor. *Biotechnology and Bioengineering Symposium* 17:335-344.
- Yoon S, Hwang S, Lee G. 2004. Enhancing effect of low culture temperature on specific antibody productivity of recombinant chinese hamster ovary cells: Clonal variation. *Biotechnology Progress* 20:1683-1688.

- Yoon S, Kim S, Lee G. 2003. Effect of low culture temperature on specific productivity and transcription level of anti-4-1BB antibody in recombinant chinese hamster ovary cells. *Biotechnology Progress* 19:1383-1386.
- Zhang C, Zhang J, Tian Z. 2006. The regulatory effect of natural killer cells: Do "NK-reg cells" exist? *Cellular and Molecular Immunology* 3(4):241-254.

Chapter 2 of this thesis contains a publishable manuscript prepared for submission to the *Journal of Veterinary Immunology and Immunopathology*, in which we describe the development and characterization of monoclonal antibodies specific for molecules expressed on the surface of bovine natural killer cells through the use of an anti-CD335 mAb and flow cytometric analysis. Many authors contributed to this manuscript, however, a significant majority of the writing and experimentation was performed by me, A.N. Godwin. William C. Davis designed the majority of the experiments and aided in interpreting the results. Mary Jo Hamilton contributed to the execution of the experiments by teaching the proper techniques for cell culture, blood separation, cell fusions, ELISA, and flow cytometry preparation. Wendell C. Johnson performed the MACS separation of CD3 and TcR1 cells as well as their culture and flow cytometry analysis and wrote the corresponding methods section. William L. Goff had a substantial financial contribution to the MACS separation work and aided in editing the manuscript. Keun S. Seo performed the 2-DE and MS/MS analysis and wrote the corresponding methods section. Greg A. Bohach had a substantial financial contribution to the 2-DE work. Anne K. Storset provided anti-CD335 mAb and helped with the interpretation of the results as well as editing of the manuscript. Finally, my advisor Bernard J. Van Wie assisted in interpreting the results and editing the manuscript.

CHAPTER TWO

USE OF FLOW CYTOMETRY TO IDENTIFY AND CHARACTERIZE MONOCLONAL ANTIBODIES SPECIFIC FOR BOVINE NATURAL KILLER CELLS

A. Natasha Godwin^a, William C. Davis^b, Mary Jo Hamilton^b, Wendell C. Johnson^c, William L.
Goff^c, Keun S. Seo^d, Greg A. Bohach^d, Anne K. Storset^e, Bernard J. Van Wie^a

^aSchool of Chemical Engineering and Bioengineering,
Washington State University, Pullman, WA 99164-2710, USA

^bCollege of Veterinary Medicine, ^cUSDA-ADRU,
Washington State University, Pullman, WA 99164-7040, USA

^dDepartment of Microbiology, Molecular Biology and Biochemistry,
University of Idaho, Moscow, ID 83844, USA

^eDepartment of Food Safety and Infection Biology,
Norwegian School of Veterinary Science, Oslo, Norway

Keywords: Bovine, NK cells, T cells, CD335, NKp46, gp96, IL-15

Prepared for submission to *Journal of Veterinary Immunology and Immunopathology*

2.2. Abstract

Study of natural killer (NK) cells in cattle has been constrained due to the lack of monoclonal antibodies (mAbs) specific for molecules expressed on NK cells. To address this problem, we used a mAb specific for the bovine orthologue of NKp46 (CD335) to develop a flow cytometric (FC) method for clustering and characterizing additional mAbs reactive with molecules expressed on NK cells. Two clusters of mAbs were identified by FC from a set of hybridomas produced from mice immunized with a highly enriched preparation of NK cells (purity ~99%). The mAbs in Cluster 1, NK64A and NK93A, recognize an orthologue of gp96, a stress protein uniquely expressed on bovine NK cells and granulocytes. The mAbs in Cluster 2, NK29A, NK42A, NK47A, NK86A, NK134A, and NK137A, recognize a yet undefined molecule expressed on activated NK cells and subsets of $\alpha\beta$ and $\gamma\delta$ T cells. The availability of a mAb to CD335 has enabled the development of a flow cytometric strategy to accelerate identification of additional mAbs to molecules uniquely expressed on bovine NK cells.

2.3. Introduction

Natural killer (NK) cells are a heterogeneous population of lymphocytes that play multiple roles in innate immunity (Diefenbach and Raulet, 2001; Lanier, 2000; Moretta et al., 2008; Zhang et al., 2006). NK or NK-like cells have been identified in most mammals including primates, rodents, and ruminants as well as in birds and fish (Endsley et al., 2006). NK cells have the ability to lyse certain target cells which lack MHC I expression due to viral infection, stress, or tumor transformation and require no prior antigen contact to do so (Delgi-Esposti and Smyth, 2005; Moretta et al., 2008; Zhang et al., 2006). NK cells have also been shown to be an important producer of gamma interferon (IFN- γ) during the early stages of pathogen infection which helps drive the development of a Type1 immune response. They have also been shown to influence B cell differentiation and immunoglobulin (Ig) isotype switching (Delgi-Esposti and Smyth, 2005; Endsley et al., 2006; Raulet et al., 2001; Zhang et al., 2006). In addition to IFN- γ , NK cells can also produce large quantities of the cytokines TNF, GM-CSF, IL-10, IL-13, and IL-5 as well as chemokines of the MIP-1 family (Delgi-Esposti and Smyth, 2005; Diefenbach and Raulet, 2001; Lanier, 2000; Raulet et al., 2001; Zhang et al., 2006).

NK cells are able to discriminate between target and non-target cells using inhibitory and activating receptors expressed on the NK surfaces. The majority of NK receptors focus on the recognition of classical and non-classical MHC molecules (Diefenbach and Raulet, 2001; Lanier, 2005; Moretta et al., 2008). There are currently three gene families of MHC class I-recognizing inhibitory receptors: Ly49 in rodents and killer cell immunoglobulin-like receptors (KIR) in humans that recognize classical MHC class I molecules, and CD94/NKG2 that recognize non-classical MHC class I molecules. These inhibitory receptors contain immunoreceptor tyrosine-based inhibition motifs (ITIM) in their cytoplasmic domain. Upon ligand binding, the ITIM

residues are tyrosine phosphorylated and recruit the src homology 2-containing tyrosine phosphatases SHP-1 and SHP-2 which inhibits NK cell activation. Activating NK receptors for MHC class I molecules are also encoded by the Ly49, KIR, and CD94/NKG2 gene families. In addition to the MCH class I specific activating receptors there are two other groups of NK activating receptors: the non-MHC-specific receptors NKG2D, NKR-P1A, NKR-P1C, NKp46, NKp44, and NKp30; and the co-activating receptors CD2, CD16, CD28, CD40L, 2B4, and DNAM-1. These activating receptors do not contain ITIMs in their cytoplasmic domains. They all associate noncovalently with small adapter signaling proteins such as DAP12. DAP12 has an immunoreceptor tyrosine-based activation motif (ITAM) which is phosphorylated upon binding of the activation ligand and recruits the cytoplasmic tyrosine kinases ZAP70 or syk (Diefenbach and Raulet, 2001; Lanier, 2000, 2005; Moretta et al., 2008; Natarajan et al., 2002). It is the balance of activating and inhibitory signals that leads to the outcome of the NK-target cell interaction.

In cattle, NK-like cells were first described as CD3⁻CD2⁺ lymphocytes with the ability to lyse certain target cells without prior antigen stimulation and the ability to produce cytokines such as IFN- γ after pathogen infection (Boysen et al., 2006b; Denis et al., 2007). NK-like cells have also been identified, based on negative selection, using markers not commonly found on NK cells such as CD8 and CD11b (Endsley et al., 2006). However, though NK-like cells have been identified in cattle, the lack of mAbs truly specific for NK cells has constrained research. To date only one mAb has been developed for use in the study of bovine NK cells. The AKS1 mAb recognizes the bovine orthologue of NKp46 (CD335), a cell-activating receptor that in humans is found solely on NK cells. The anti-CD335 mAb has facilitated characterization and

isolation of NK cells in peripheral blood, and the liver, spleen, lung, and lymph node (Storset et al., 2004).

Additional bovine NK-specific antibodies are clearly needed to facilitate further characterization and elucidation of the role that NK cells play in the innate immunity in cattle. In this report we describe the use of anti-CD335 mAb and a flow cytometric (FC) method to identify and characterize additional mAbs that recognize molecules expressed on NK cells.

2.4. Materials and methods

2.4.1. Generation of bovine NK cells

Bovine peripheral blood mononuclear cells (PBMC) were isolated from fresh anti-coagulated blood by density gradient separation on Accu-Paque™ (1.086 g/L) (Accu-Paque, Accurate Chemicals, NY). The PBMCs were collected from the interface and washed with PBS-20% acid citrate dextrose (ACD). Residual erythrocytes were lysed with Tris buffered NH₄Cl (0.87%). The cells were then cultured in Dulbecco's Modified Eagle Medium (DMEM) supplemented with 10% Calf Bovine Serum (CBS) (Hyclone, Logan, UT), 2 mM L- glutamine, 100 units/mL penicillin, 100 µg/mL streptomycin, 10 mM HEPES buffer, 3 x 10⁻⁵ M 2-mercapto-ethanol, and 1 µg/mL recombinant human interleukine-15 (rHuIL-15) (R&D Systems, Minneapolis, MN). All medium ingredients were purchased from Invitrogen (Carlsbad, CA) unless stated otherwise. To determine the percentage of cells in culture that were NK cells, the cells were labeled with either anti-CD335 (AKS1) or anti-CD3 (MM1A) mAbs (MacHugh et al., 1998; Storset et al., 2004) and then examined by FC.

2.4.2. Generation of anti-NK monoclonal antibodies

Three female BALB/c mice were hyper-immunized with a culture of bovine NK cells (~99% purity) as previously described (Hamilton and Davis, 1995). Seventy-two hours prior to being

ethanized, the mice were boosted by i.v. injection through the tail vein. The spleens were harvested and cryopreserved in CBS with 10% dimethyl sulfoxide (DMSO) until needed for fusion. The X63 murine myeloma cell line was used as the fusion partner and 1.2×10^8 spleen cells were fused with 4.8×10^7 myeloma cells according to the standard protocol and distributed into eleven 96-well culture plates (Hamilton and Davis, 1995). After seven days, supernatants were collected and screened by FC for the presence of antibody using whole blood or cultures enriched for NK cells. All positive cultures were expanded into 12 well culture plates. All hybridomas producing mAbs of potential interest were cryopreserved. Supernatants from the cultures were collected and frozen for further analysis. The isotype of mAbs was determined with kits from EY Laboratories, Inc. (San Mateo, CA).

2.4.3. *Generation of T cell subsets*

Two Holstein-Friesian calves were obtained at 8-12 weeks of age and maintained according to the American Association for Laboratory Animal Care procedures with an acceptable bovine ration, water and mineral block provided *ad libitum*. The spleen of each animal was surgically marsupialized to facilitate aspiration of spleen cells (Varma and Shatry, 1980). The procedure has proven to be an efficient means for obtaining sequential samples from a single animal without demonstrable consequences to splenic phenotypic ratios or basal levels of cellular activity (Goff et al., 2002). Splenic aspirates were aseptically collected in syringes containing ACD under local anesthesia and processed into a single-cell suspension using a tissue homogenizer. Splenic cell suspensions or peripheral blood were layered onto Hypaque-Ficoll (Sigma-Aldrich, St. Louis, MO) and centrifuged for 30 minutes at 1500 g and 4°C. Cells were collected from the interface and washed in 50 mL DMEM for 7 minutes at 1500 g and 4°C. The cells were suspended with DMEM and washed twice at 400 g for 7 minutes and 4°C to remove

platelets, which remained in the supernatant. The final pellets were suspended in Iscove's medium (Invitrogen, Carlsbad, CA) containing 25 mM HEPES, 2 mM glutamine, 10 µg/mL gentamycin, 50 µM mercaptoethanol, 15% endotoxin-free fetal bovine serum (FBS) (< 0.06 EU/mL as assayed by Limulus amoebocyte lysate gelation) (Hyclone, Logan, UT) and essential and non-essential amino acids (Invitrogen) (Iscove's/FBS medium). To generate cultures of T cell subsets, CD3⁺ cells or γδ T cells were purified from spleen cells with MACS™ columns (Miltenyi Biotec, Auburn, CA) per the manufacturer's protocol prior to incubation with cytokines. Briefly, 1 x 10⁸ cells were washed into PBS supplemented with 0.5% BSA, 2 mM EDTA (PBS-BE), suspended to 1 mL and incubated with 6 µg of either mAb MM1A (anti-CD3) or GB21A (TcR1, δ chain specific (Davis et al., 1996)) for 15 minutes at 4°C. The cells were washed once with PBS-BE at 400 g at 4°C suspended in PBS-BE and incubated, as before, with goat anti-mouse IgG coupled to superparamagnetic nano-sized and biodegradable MACS MicroBeads (Miltenyi Biotec, Auburn, CA) and passed over LS MACS columns placed in the magnetic field of a MACS Separator. The columns were flushed with PBS-BE and then removed from the magnet. The positively selected cells were released from the columns into Iscove's/FBS medium. A purity of > 98% was routinely achieved as evaluated by staining for CD3 or TcR1 and subsequent FC analysis. Purified cells were cultured for two weeks in Iscove's/FBS medium supplemented with 20 ng/mL rHuIL-15 at 37°C and 5% CO₂ as previously described (Goff et al., 2006).

2.4.4. *Monoclonal antibodies*

The mAbs used to characterize and cluster the new NK mAbs are listed in Table 1.

Cluster	mAb	Ig Isotype
CD335	AKS1	G1
CD3	MM1A	G1
TcR1 δ	GB21A	G2b
CD2	CACT31A	M
CD4	ILA11A	G2a
CD8	7C2B	G2a

Table 1: MAbs for common T cell markers and the anti-CD335 mAb for NK cells used to characterize and cluster the new NK mAbs.

2.4.5. Preparation of cells for flow cytometry

For single color FC, 50 μ L of appropriately diluted mAbs were added to the wells of conical bottom 96-well microtiter plates (Corning, NY). Following addition of cells (10^5 cells in 50 μ L of FC first wash buffer [FWB, PBS containing 20% ACD and 0.5% horse serum]) the plates were incubated on ice for 15 minutes and then centrifuged. Supernatants were removed by flicking of the plates. The cells were washed with 3 cycles of centrifugation and resuspension in FWB. The cells were then incubated with an appropriately diluted polyclonal goat anti-mouse IgG/IgM second step antibodies conjugated to fluorescein (Caltag Laboratories, CA) for an additional 15 minutes. Following incubation, the cells were washed twice with second wash buffer (SWB, PBS containing 20% ACD) and fixed in 2% formaldehyde in PBS and either screened immediately or kept in the refrigerator for later analysis. For multi-color FC, cells were added to wells containing 2 or 3 mAbs of different isotype and incubated and washed as described. The second step reagents used were isotype specific goat anti-mouse immunoglobulins conjugated with fluorescein (FL), phycoerythrin (PE), Cy5, or PE-Cy5 (Caltag Laboratories, CA). When the mAbs were all of the same isotype (IgG1), Zenon™ One Mouse

IgG1 labeling kits were used (Molecular Probes, OR). Zenon-Fab fragments of IgG1 specific goat anti-mouse antibody conjugated with different fluorochromes (FL, PE, Cy5, or PE-Cy5) were used according to the manufacturer's instructions. Briefly, 5 μ L of a Zenon-Fab reagent was added to 50 μ L of cell culture supernatant or ascites containing the respective mAbs and incubated for 5 minutes at room temperature. Following incubation, 5 μ L of Zenon-Fab blocking reagent, a nonspecific mouse IgG used to complex unbound Fab fragments, was added. The mixture was incubated an additional 5 minutes. The Zenon-Fab labeled antibodies were then mixed and added to the cell preparations and incubated on ice for 15 minutes. The cell preparations were processed as described and fixed in 2% PBS-buffered formaldehyde.

2.4.6. *Flow cytometry*

FC analysis was performed using a Becton Dickinson FACSort equipped with a MAC computer and Cell Quest software (BD Immunocytometry Systems, San Jose, CA). FCS Express software (DeNovo Software, Ontario, CA) was used to analyze the data.

2.4.7. *2-DE and Western blotting*

Whole cell lysate was prepared using lysis buffer containing 7 M urea (Bio-Rad laboratories, Hercules, CA), 2 M thiourea (Bio-Rad laboratories), 2% ASB-14 (Sigma, St. Louis, MO), 0.5% Triton X-100 (Sigma), 2 mM tributylphosphine (Bio-Rad), and 0.1% bromophenol blue. Cell lysate was further treated with a protein inhibitor cocktail (GE Healthcare) for 5 minutes on ice, followed by nuclease treatment (GE Healthcare) for 15 minutes at room temperature. Whole cell lysate was centrifuged at 45,000 g for 30 minutes and then the supernatant was subjected to 2-dimensional gel electrophoresis (2-DE). Cell lysates were supplemented with 2% IPG-buffer (pH 3-11, GE Healthcare). Two hundred microliters of samples were loaded into a swelling tray, then IPG strips (ImmobilineTM Drystrip gels, pH 3-11 non-linear, GE Healthcare) were overlaid

and allowed to rehydrate for 24 hours in duplicate. First dimensions (isoelectric focusing) were performed in three running phase (Phase 1; 300 V/0.01 h, Phase 2; 3500 V/1.50 h, and Phase 3; 3500 V/4.00 h) using a Multiphor II unit (GE Healthcare). After equilibration and alkylation with DTT (0.01 mM) and (15 mM) iodoacetamide in equilibration solution (50 mM Tris-HCl, pH 6.8, 6 M urea, 30% glycerol, and 1% SDS), respectively, the IPG strips were embedded onto 12.5% polymerized slab gel using 0.5% agarose. A second dimension (SDS-PAGE) was then conducted in 12.5% poly-acrylamide gels with constant current at 8 mA for overnight. One gel was stained with Coomassie blue G 250 (Bio-Rad, Hercules, CA) and the other gel was transferred to polyvinylidene difluoride membrane (PVDF, Millipore Corp.). After blocking with 2% skim milk in Tween-Tris buffered saline [TTBS: 20 mM Tris-HCl (pH 7.4), 150 mM NaCl, 0.05 % Tween 20] for 2 hours, membranes were incubated with NK93A mAb (1:500,000) in TTBS for an additional 2 hours. Membranes were washed and incubated with peroxidase-conjugated anti-mouse IgG (1:5000; GE Healthcare) in TTBS for 1 hour. Chemiluminescence detection was conducted with a kit (Pierce, Rockford, IL). To ensure that equal amount of protein samples were loaded, membranes were stripped and re-probed with rabbit-anti-bovine β actin, and visualized as described above using peroxidase-conjugated anti-rabbit IgG (1:5000; GE Healthcare) in TTBS for 1 hour.

2.4.8. *MS/MS analysis*

A spot identified in the immuno-blotted membrane was excised from the Coomassie Blue stained gel and digested with trypsin (Worthington, Lakewood, NJ) as previously described (Shevchenko et al., 2002). Trypsin digested peptides were separated by matrix-assisted laser desorption ionization (MALDI) and nanoelectrospray LC-MS/MS using a Nanoacquity Ultra Performance Liquid Chromatograph (Waters, Milford, MA). Peptide spectra were acquired by

Quadrupole-TOF Premier mass spectrometer equipped with a Nano-ESI source (Waters).

Spectra were analyzed by the Mascot search engine. Probability-based protein identification was performed by searching the sequence databases using mass spectrometry data (Perkins et al., 1999).

2.5. Results

2.5.1. Preparation of NK cells for immunization and mAb characterization

Initial studies comparing the capacity of rHuIL-2 and bovine IL-2 (Storset et al., 2004) and rHuIL-15 revealed culture of PBMC in rHuIL-15 yielded preparations of cells highly enriched for NK cells. The procedure was repeated for the present study with purities of cultures stimulated with rHuIL-15 ranging from 30 to 99% based on FC analysis of cell preparations labeled with anti-CD335. A preparation of ~99% pure NK cells from the rHuIL-15 stimulated cultures was used for immunization and production of mAbs to molecules expressed on NK cells.

2.5.2. Identification and clustering of antibodies recognizing molecules expressed on NK cells

Screening of the primary supernatants from the fusion with PBMC using single fluorescence FC analysis yielded 158 hybridomas producing antibodies that recognized molecules expressed on NK cells, B cells, T cells, granulocytes, and monocytes. Twenty-nine of the hybridomas that appeared to recognize molecules exclusively expressed on NK cells were selected for further analysis. Two-color FC on resting PBMCs revealed that the mAbs NK64A and NK93A recognize a molecule expressed on granulocytes and a small subset of lymphocytes (Fig. 1G). Analysis of the mAbs NK29A, NK42A, NK47A, NK86A, NK134A, and NK137A revealed they recognize a molecule expressed on a small subset of lymphocytes but not on granulocytes (Fig. 1H).

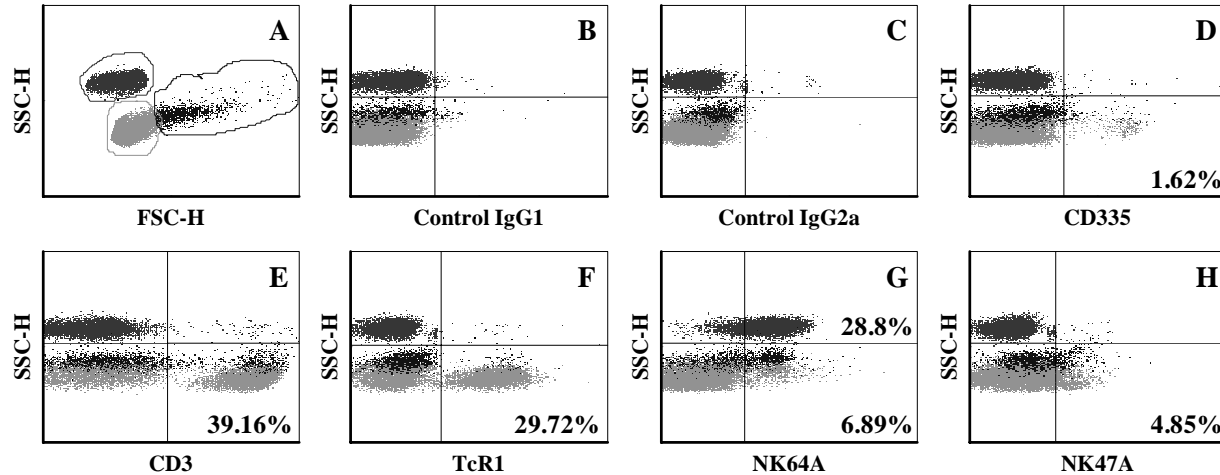


Fig. 1. Representative single fluorescent dot plot profiles of a peripheral blood mononuclear cell preparation labeled with the mAbs indicated. A side light scatter (SSC) vs. forward light scatter (FSC) dot plot was used to gate and color code the major populations of cells: dark gray for granulocytes, light gray for resting lymphocytes and black for activated lymphocytes (A). The cells in panels B and C were used as isotype controls. Panels D, E, and F show the percentage of cells that are NK cells, CD3⁺ T cells, and $\gamma\delta$ T cells respectively. Panel G shows that NK64A labels the majority of the granulocyte population and a subset of lymphocytes. Panel H shows that NK47A also labels a subset of lymphocytes but does not label granulocytes. Few resting NK cells express the Cluster 2 molecule.

Based on this differential, the hybridomas producing mAbs detecting molecules with similar patterns of expression were clustered for further analysis. The selected hybridomas were cloned to establish cell lines as previously described. Two hybridomas (NK64A and NK93A) were placed in Cluster 1 and six (NK29A, NK42A, NK47A, NK86A, NK134A, and NK137A) were placed in Cluster 2 (Table 2).

mAb	Ig Isotype	Lymphocytes	Granulocytes	Cluster
NK64A	G1	+	+	1
NK93A	G1	+	+	1
NK29A	G1	+	-	2
NK42A	G1	+	-	2
NK47A	G2a	+	-	2
NK86A	G1	+	-	2
NK134A	G2a	+	-	2
NK137A	G1	+	-	2

Table 2: New NK mAbs were placed into clusters based on their expression patterns.

To determine if the molecules being recognized by each cluster are expressed on activated cells, rHuIL-15 stimulated cultures of NK cells were used. In the NK enriched cultures ~58% of the cells were NK (Fig. 2C) while the remainder of the cells were CD3⁺ T cells (Fig. 2D). Figure 2E shows that the molecule recognized by mAbs in Cluster 1 is expressed on activated NK cells and is not expressed on CD3⁺ T cells. MAbs in Cluster 2, on the other hand, labeled both activated NK cells and some CD3⁺ T cells (Fig. 2F).

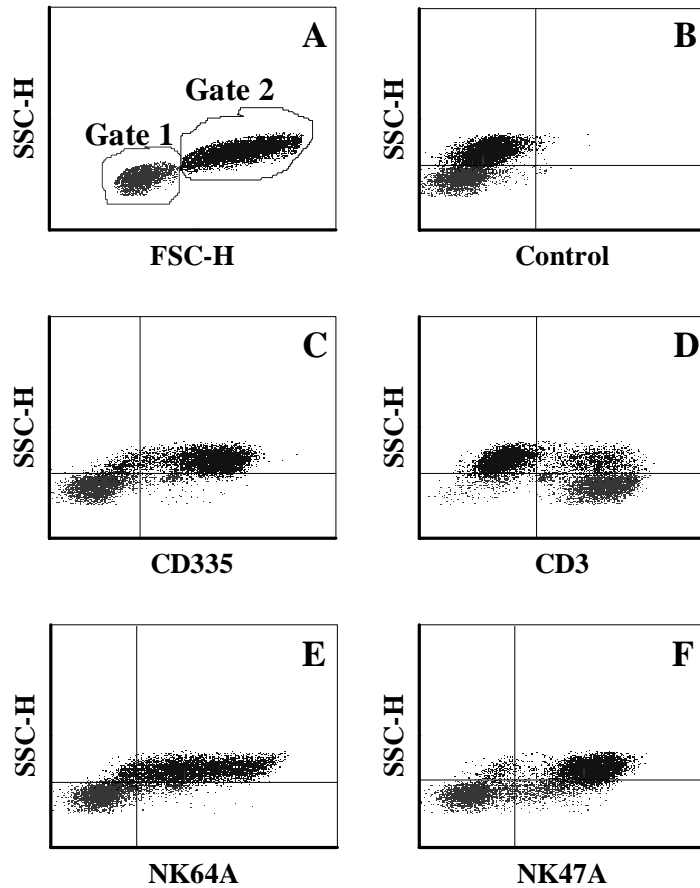


Fig. 2. Single fluorescent dot plot profiles of a rHuIL-15 stimulated NK cell preparation labeled with the mAbs indicated. A side light scatter (SSC) vs. forward light scatter (FSC) dot plot was used to gate and color code the two populations of cells: gray for the smaller resting cells (Gate 1) and black for the larger activated cells (Gate 2) (A). Approximately 52% of the cell preparation is positive for CD335, showing the majority of cells in Gate 2 are NK cells, (C) while the remainder are CD3⁺ T cells present in Gate 1 (D). NK64A only labeled the cells in Gate 2, NK cells, (E). NK47A also labeled the cells in Gate 2 as well as a subset present in Gate 1 (F).

2.5.3. Cross-comparison of NK mAbs

Two-color flow cytometry using rHuIL-15 enriched NK cell cultures was used to cross compare mAbs and show whether they recognize the same or different molecules. Comparison of Cluster 1 mAbs, (NK64A and NK93A, IgG1), using fluorochrome conjugated Zenon-Fab fragments (Fig. 3B) showed the mAbs recognize the same molecule, i.e., labeling with the two

mAbs yielded a tight diagonal pattern of labeling indicating the mAbs recognize different epitopes on the same molecule on the surface of NK cells. In contrast, comparison of labeling with anti-CD335 showed the mAbs do not react with NKp46. Dual labeling yielded a diffuse pattern indicating the mAbs recognize different molecules (Fig. 3C). Cross comparison of labeling with the mAbs in Cluster 2 showed the mAbs recognize the same molecule (Fig. 3E). The comparison also showed the molecule recognized by Cluster 2 is expressed on all NK cells (Fig. 3F) and a subset of CD3⁺ T cells (Fig. 3G). Comparison of the labeling pattern of mAbs in Cluster 1 with mAbs in Cluster 2 yielded a diffuse pattern of labeling indicating that the mAbs recognized different molecules (Fig. 3H).

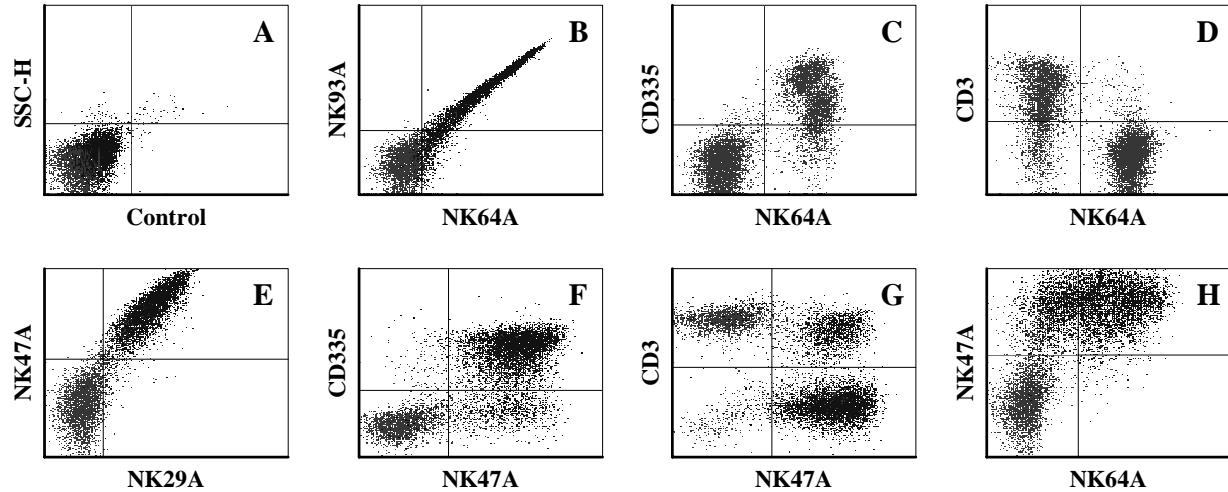


Fig. 3. Cross-comparison of NK mAbs using two-color FC analysis and a preparation of rHuIL-15 stimulated NK cells. Zenon-Fab fragments were used to label the mAbs in profiles B, C, and D since both mAbs in each comparison are IgG1. The two Cluster 1 mAbs recognize the same molecule on the NK cell surface (B, inferred from the tight diagonal labeling pattern). The molecule detected was not CD335 (C, inferred from the loose cloud labeling pattern). The labeling showed the Cluster 1 molecule is not expressed on CD3⁺ T cells (D). Cluster 2 mAbs recognize a different molecule than Cluster 1 on the NK cell surface, but all Cluster 2 mAbs recognize the same molecule (E, loose diagonal pattern of labeling consistent with the mAbs recognizing the same molecule). The molecule detected is expressed on all NK cells (F) and a subset of CD3⁺ T cells (G). The molecule detected with Cluster 2 mAbs is expressed on all Cluster 1⁺ cells and a subset of Cluster 1⁻ cells (H).

2.5.4. Cluster 2 recognizes subsets of T cells

Three-color flow cytometry using a 3:1 mix of rHuIL-15 stimulated NK cells and concanavalin A (ConA) stimulated T cell blasts, cultured from PBMCs, was used to analyze the T cell subset being labeled by Cluster 2 mAbs. NK47A and NK29A were compared against several mAbs that recognize common T cell markers including CD3, CD2, CD4, CD8, and the TcR1 δ chain of $\gamma\delta$ T cells. Selective gates were placed on all NK47A⁺ and NK29A⁺ cells to analyze expression of the latter molecules on Cluster 2 subsets. Figure 4 shows that subsets of

the NK47A⁺ cells expressed CD335 (B) or CD3 (C) with half of the CD335⁺ population and all of the CD3⁺ population also expressing CD2. A small population, ~9%, of $\gamma\delta$ T cells expressed the molecule reactive with Cluster 2 mAbs (Fig. 4D-E, H). Twenty-five percent of the TcR1⁺ cells express the NK cell marker CD335 (Fig. 4E). Subsets of cells reactive with NK29A expressed CD4 or CD8 (Fig. 4F-G) with all of the CD4⁺ and CD8⁺ cells also expressing CD2. An average of 42% of the cells labeled by Cluster 2 mAbs were CD2⁻.

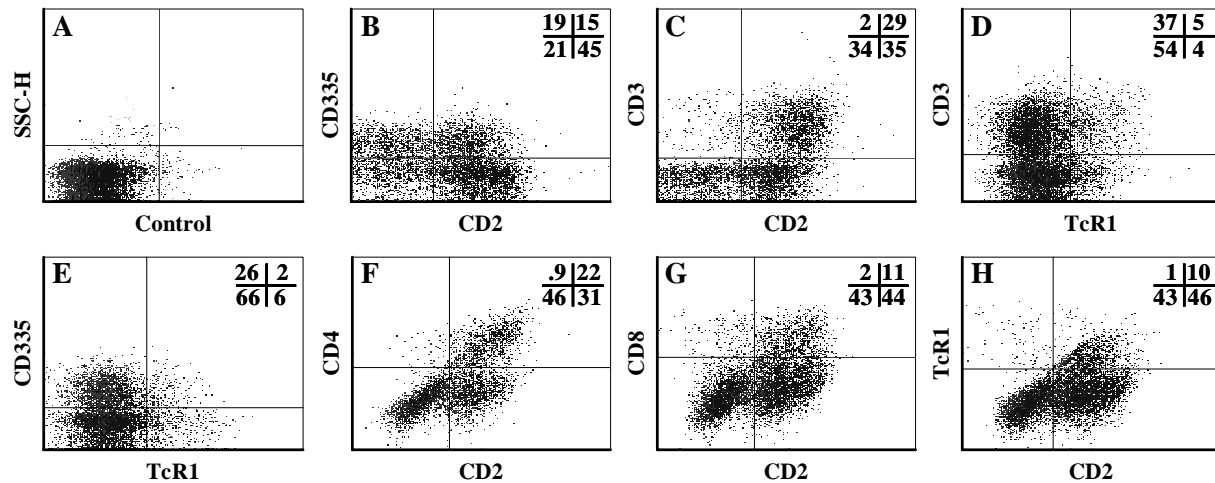


Fig. 4. Phenotypic analysis of Cluster 2 positive cells using three-color FC on a preparation of cells comprised of rHuIL-15 stimulated NK cells and concanavalin A stimulated T cell blasts (3:1 cell ratio respectively). Original SSC vs. FSC gates were set to include all viable cells. Additional gates were set to show only NK47A⁺ (B-E) or NK29A⁺ (F-H) cells. Cluster 2 mAbs labeled CD335⁺CD2⁺, CD335⁺CD2⁻ cells (B) and CD3⁺CD2⁺ (C) cells. Nine percent of $\gamma\delta$ T cells were labeled by Cluster 2 mAbs (D-E, H) and 25% of the TcR1⁺ cells also expressed CD335 (E). Subsets of CD4⁺CD2⁺ (F) and CD8⁺CD2⁺ (G) cells were labeled with Cluster 2 mAbs.

An unique subset of CD3⁺ TcR1⁺ WC1⁻ $\gamma\delta$ T cells expressing the NK cell marker CD335 was recently isolated from bovine splenic leukocytes (Johnson et al., 2008). To determine if Cluster 2 mAbs recognized this new subset, cultures of T cell subsets were made from splenic leukocytes and purified (purity >98%) using MACS and mAbs to CD3 (MM1A) and the TcR1 δ

chain (GB21A). Each subset was cultured for two weeks in medium supplemented with rHuIL-15 and then analyzed using two-color FC for CD335, CD2, CD4, CD8, and the TcR1 δ chain as well as Cluster 2 mAbs NK29A and NK47A. The majority of the CD3 purified rHuIL-15 cultured cells (82-91%) expressed the molecule recognized by Cluster 2 mAbs (Fig. 5A-D, F). Over half (61%) also expressed CD2 (Fig. 5A). All of the CD4⁺ cells from the CD3 purified culture were positive for NK29A but constituted only 8% of the culture (Fig. 5B). Likewise, CD8⁺ cells were also labeled with NK29A but were a much larger population (57%) (Fig. 5C). Roughly 17% of the CD3 purified cell culture was TcR1⁺ with the majority being NK29A⁺ (Fig. 5D). Twenty-two percent of the CD3 purified cell culture expressed the NK cell marker CD335 (Fig. 5E-F). In comparison, only half (41-61%) of the TcR1 purified cell culture expressed the molecule recognized by Cluster 2 mAbs (Fig. 5G-J, L). There were no CD4⁺ cells in the TcR1 purified culture (Fig. 5H). Only 12% were positive for CD8 with the majority again being NK29A⁺ (Fig. 5I). The NK cell marker CD335 was expressed on 11% of the TcR1 purified cell culture (Fig. 5L).

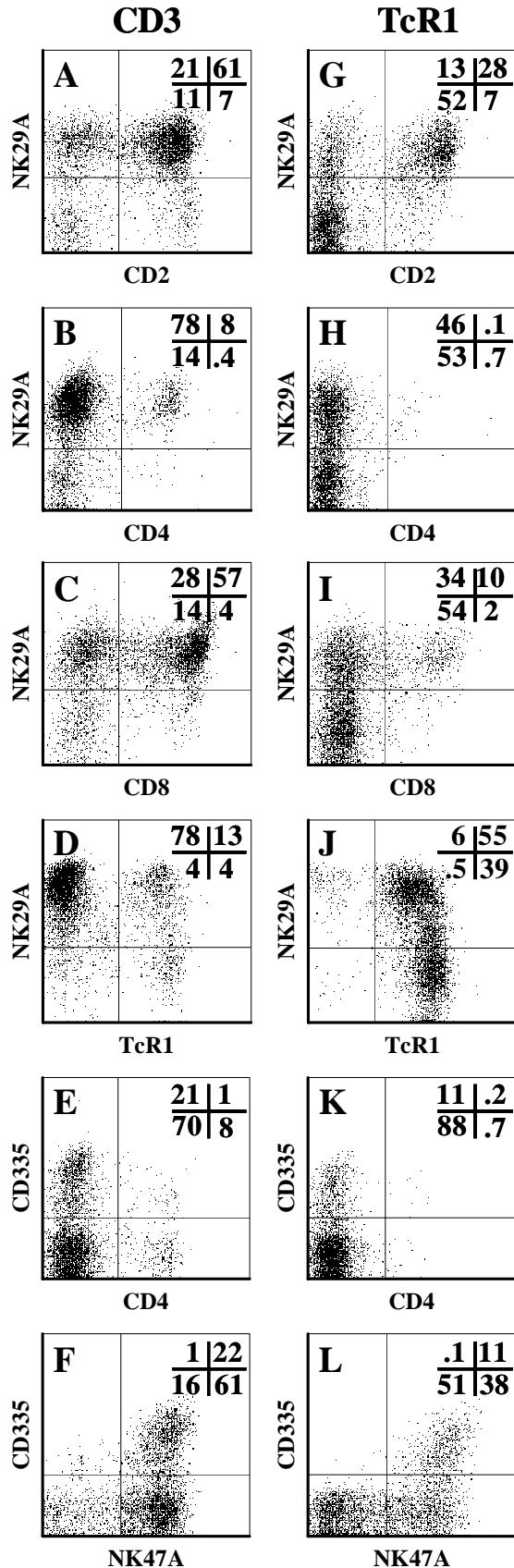


Fig. 5. Further characterization of T cell subsets labeled by Cluster 2 mAbs using purified cultures of CD3⁺ (A-F) or TcR1⁺ (G-L) T cells separated from splenic leukocytes using MACS columns and mAbs to either CD3 (A-F) or the TcR1 δ chain (G-L). Subsets were cultured for two weeks in medium supplemented with 20 ng/mL rHuIL-15. Cluster 2 mAbs labeled the majority of the CD3 purified cultured cells (A-D, F) with 61% being CD2⁺ (A). A small population of CD4⁺ (B) and a large population of CD8⁺ cells (C) were present in the culture and all labeled with NK29A. A subset of $\gamma\delta$ T cells was present in the CD3 purified cells and the majority were reactive with NK29A (D). CD335 is expressed by 22% of the CD3 purified cells (E-F). Approximately half of the TcR1 purified cultured cells were labeled with Cluster 2 mAbs (G-J, L). There were no CD4⁺ cells (H) and only a small population (10%) of CD8⁺ cells (I) in the preparation. CD335 was expressed by 11% of the TcR1 purified cells (K-L).

2.5.5. Cluster 1 mAbs recognize the bovine orthologue of stress protein gp96

Progress was made in characterizing the molecule recognized by Cluster 1 mAbs. 2D gel electrophoresis (2-DE) of a NK cell lysate was used to separate the proteins. A Western blot using the Cluster 1 mAb NK93A identified a protein with a molecular weight of ~92 kDa (Fig. 6). MS/MS analysis of the peptide along with a search of the protein database identified the molecule as the bovine orthologue of the endoplasmic reticulum (ER) heat shock protein gp96 (100% probability). This stress protein is a chaperone molecule used in protein folding and antigen presentation (Hilf et al., 2002; Tsan and Gao, 2004; Wallin et al., 2002).

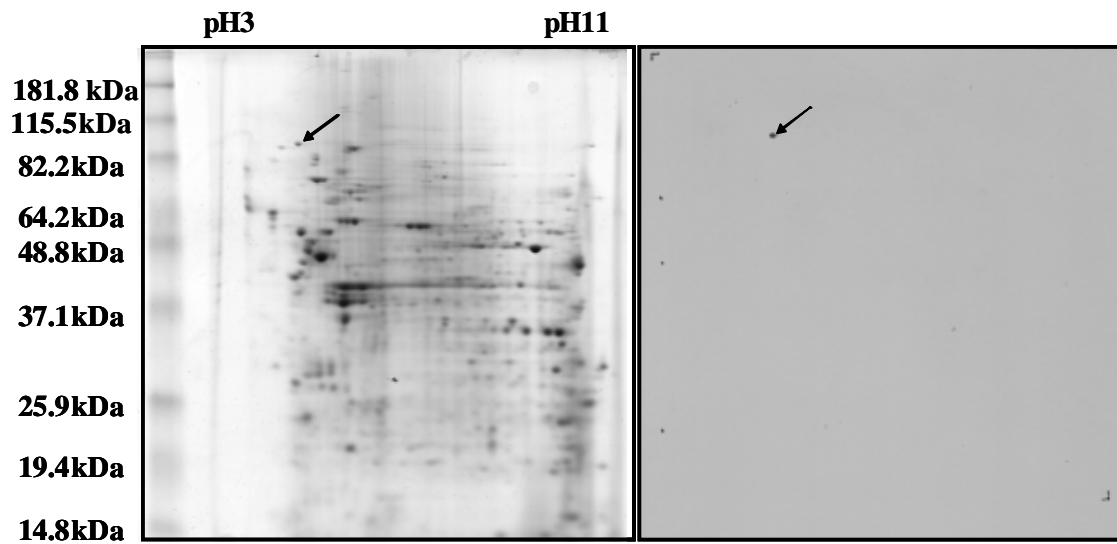


Fig. 6. 2-DE and immunoblot analysis of NK cell lysates. Cell lysates from NK cells were separated by 2-DE in duplicate. One gel was stained with Coomassie Blue (A) and the other was transferred to a PVDF membrane and probed with NK93A mAb (B). Arrows indicate the corresponding spot in both gels.

2.6. Discussion

In this study we successfully used an anti-CD335 mAb and flow cytometry to cluster and characterize new mAbs reactive with molecules expressed on the surface of bovine NK cells. Culturing bovine NK cells with rHuIL-15 was proven to be a very efficient means of obtaining

highly enriched preparations of NK cells from peripheral blood which were then used to immunize mice and produce hybridomas. Flow cytometric analysis, using a suite of mAbs to common T cell markers and the anti-CD335 mAb, allowed us to identify two new mAb clusters. Cluster 1 mAbs, NK64A and NK93A, recognize the bovine orthologue of the ER heat shock protein gp96 expressed by granulocytes and CD335⁺ NK cells. Cluster 2 mAbs, NK29A, NK42A, NK47A, NK86A, NK134A, and NK137A, recognize a yet undetermined molecule expressed on all activated NK cells and subsets of $\alpha\beta$ and $\gamma\delta$ T cells including CD4 and CD8 positive cells.

The development of the anti-CD335 mAb has opened the door for research into the role that NK cells play in the innate immunity of cattle for a milieu of diseases. NK cells are early responders during infection with the protozoan *Neospora caninum* and possess both cytokine and cytotoxic properties. Activation of NK cells is triggered by live or heat-inactivated intact tachyzoites rather than soluble antigens and NK cells themselves can be infected by the protozoan in vitro (Boysen et al., 2006a; Klevar et al., 2007). During infection with *Mycobacterium bovis* and *Mycobacterium avium* subsp. *paratuberculosis* NK cells can be activated by the secreted proteins ESAT-6 and MPP14 and restrict the replication of *M. bovis* in infected macrophages while enhancing the release of IL-12 (Denis et al., 2007; Endsley et al., 2006; Olsen et al., 2005). NK cells were also found to produce IFN- γ in response to supernatants from *Babesia bovis* merozoite-exposed monocytes (Goff et al., 2006). In addition to understanding NK cell functions in infected animals, the anti-CD335 mAb enhances the ability to study NK cells in healthy cattle to gain a better understanding of NK subsets and tissue distribution. In blood NK cells comprise 0.5 – 10% of the total lymphocyte population and show a decrease in number with animal age (Kulberg et al., 2004). Studies have shown that NK cells

reside in the lymph nodes of healthy cattle and have a higher expression of CD44, CD25, and CD8 and relatively no expression of CD2 compared with NK cells in blood. Lymph node derived NK cells express CD16 and CD62L and possess cytotoxic capabilities but are also able to produce INF- γ following stimulation with IL-2 and IL-12 (Boysen et al., 2008).

The Cluster 1 and Cluster 2 mAbs described in this paper will add to the knowledge gained from the anti-CD335 mAb. Cluster 1 mAbs recognize both activated and resting NK cells similar to the anti-CD335 mAb (Storset et al., 2004). However, Cluster 1 mAbs recognize gp96 expressed on the surface of the NK cells rather than an activating receptor. It was recently discovered that a population of CD3⁺ TcR1⁺ WC1⁻ $\gamma\delta$ T cells express CD335 when cultured in rHuIL-15 and are thus labeled with the anti-CD335 mAb (Johnson et al., 2008). Cluster 1 mAbs are shown to have no reactivity with resting/unstimulated $\gamma\delta$ or $\alpha\beta$ T cells and will therefore be more useful in identifying activated NK.

Cluster 2 mAbs recognize a molecule expressed by activated NK cells and subsets of both $\alpha\beta$ and $\gamma\delta$ T cells. The Cluster 2 mAbs do not label resting NK cells as seen by the low expression on PBMCs. This observation has been further confirmed by unsuccessful attempts to use NK29A and NK47A to separate T cell subsets from splenic lymphocytes (personal observation). The resting splenic lymphocytes do not express the molecule recognized by NK29A and NK47A therefore the mAbs were unable to label the cells. After the splenic lymphocytes were separated using anti-CD3 and anti-TcR1 mAbs and cultured for two weeks in medium supplemented with rHuIL-15, the Cluster 2 mAbs labeled 48 – 85% of the cells. Cluster 2 mAbs labeled a subset of CD4⁺ T cells present in the CD3 purified rHuIL-15 cultured splenic cells. Studies of NK receptors on T cell subsets have revealed that subsets of CD4⁺ and CD8⁺ T cells with effector and/or memory phenotype often express NK receptors including members of the KIR, KLR, and

LIR families as well as CD94-NKG2, NKG2D, and Ly49 in mice. CD4⁺ T cell expression of the NK receptors CD94-NKG2 in humans and Ly49 in mice can be induced by stimulation with IL-15 (Snyder et al., 2004; Vivier and Anfossi, 2004).

The molecule recognized by Cluster 1 mAbs was determined by 2-DE and subsequent MS/MS analysis to be the bovine orthologue of the ER heat shock protein gp96. Heat shock proteins serve as molecular chaperones to mediate protein folding and have also been shown to play a role in antigen presentation via the MHC class I pathway (Hilf et al., 2002; Tsan and Gao, 2004; Wallin et al., 2002). Despite containing a carboxy terminal KDEL sequence, which is a retention-retrieval signal from the Golgi to the ER, recent studies have found gp96 to be expressed on the surface of murine tumor cells (Altmeyer et al., 1996), lipopolysaccharide (LPS)-stimulated B cells, thioglycolate-elicited macrophages, bone marrow-differentiated dendritic cells (Banerjee et al., 2002), and a subset of immature thymocytes (Wiest et al., 1997). No information was found on the cell surface expression of gp96 on bovine cells indicating that the development of the Cluster 1 mAbs provides the first evidence of the expression of gp96 on bovine NK cells and granulocytes.

The availability of the anti-CD335 mAb has not only facilitated research into the roles that NK cells play in the innate immunity of cattle but it has also allowed for the development of additional mAbs specific for bovine NK cells. Our newly developed Cluster 1 and Cluster 2 mAbs add to the tools available for NK cell research and make it possible to make more rapid progress in identifying additional mAbs to facilitate further research on bovine NK cells.

2.7. Acknowledgements

This work was supported in part by the National Institutes of Health Grant P20 RR15587, P20 RR016454, and U54AI57141 and the Idaho Agricultural Experiment Station.

2.8. References

- Boysen, P., Gunnes, G., Pende, D., Valheim, M., Storset, A., 2008, Natural killer cells in lymph nodes of healthy calves express CD16 and show both cytotoxic and cytokine-producing properties. *Developmental and Comparative Immunology* 32, 773-783.
- Boysen, P., Klevar, S., Olsen, I., Storset, A., 2006a, The protozoan *Neospora caninum* directly triggers bovine NK cells to produce gamma interferon and to kill infected fibroblasts. *Infection and Immunity* 74, 953-960.
- Boysen, P., Olsen, I., Berg, I., Kulberg, S., Johansen, G., Storset, A., 2006b, Bovine CD2-/NKp46+ cells are fully functional natural killer cells with a high activation status. *BMC Immunology* 7.
- Davis, W., Brown, W., Hamilton, M., Wyatt, C., Orden, J., Khalid, A., Naessens, J., 1996, Analysis of monoclonal antibodies specific for the $\gamma\delta$ TcR. *Veterinary Immunology and Immunopathology* 52, 275-283.
- Delgi-Esposti, M., Smyth, K., 2005, Close encounters of different kinds: dendritic cells and NK cells take centre stage. *Nature Reviews* 5, 112-124.
- Denis, M., Keen, D., Parlane, N., Storset, A., Buddle, B., 2007, Bovine natural killer cells restrict the replication of *Mycobacterium bovis* in bovine macrophages and enhance IL-12 release by infected macrophages. *Tuberculosis* 87, 53-62.
- Diefenbach, A., Raulet, D., 2001, Strategies for target cell recognition by natural killer cells. *Immunological Reviews* 181, 170-184.
- Endsley, J., Endsley, M., Estes, D., 2006, Bovine natural killer cells acquire cytotoxic/effector activity following activation with IL-12/15 and reduce *Mycobacterium bovis* BCG in infected macrophages. *Journal of Leukocyte Biology* 79, 71-79.
- Goff, W., Johnson, W., Parish, S., Barrington, G., Elsasser, T., Davis, W., Valdez, R., 2002, IL-4 and IL-10 inhibition of IFN- γ - and TNF- α -dependent nitric oxide production from bovine mononuclear phagocytes exposed to *Babesia bovis* merozoites. *Veterinary Immunology and Immunopathology* 84, 237-251.
- Goff, W., Storset, A., Johnson, W., Brown, W., 2006, Bovine splenic NK cells synthesize IFN- γ in response to IL-12-containing supernatants from *Babesia bovis*-exposed monocyte cultures. *Parasite Immunology* 28, 221-228.
- Hamilton, M., Davis, W., 1995, Culture conditions that optimize the outgrowth of hybridomas, In: Davis, W. (Ed.) *Monoclonal Antibody Protocols, Methods in Molecular Biology*. The Humana Press, Inc., Totowa, NJ, pp. 17-28.
- Hilf, N., Singh-Jasuja, H., Schild, H., 2002, The heat shock protein Gp96 links innate and specific immunity. *International Journal of Hyperthermia* 18, 521-533.
- Johnson, W., Bastos, R., Davis, W., Goff, W., 2008, Bovine WC1- $\gamma\delta$ T cells incubated with IL-15 express the natural cytotoxicity receptor CD335 (NKp46) and produce IFN- γ in response to exogenous IL-12 and IL-18. *Developmental and Comparative Immunology* 32, 1002-1010.
- Klevar, S., Kulberg, S., Boysen, P., Storset, A., Moldal, T., Björkman, C., Olsen, I., 2007, Natural killer cells act as early responders in an experimental infection with *Neospora caninum* in calves. *International Journal for Parasitology* 37, 329-339.
- Kulberg, S., Boysen, P., Storset, A., 2004, Reference values for relative numbers of natural killer cells in cattle blood. *Developmental and Comparative Immunology* 28, 941-948.

- Lanier, L., 2000, The origin and functions of natural killer cells. *Clinical Immunology* 95, S14-S18.
- Lanier, L., 2005, NK cell recognition. *Annual Review of Immunology* 23, 225-274.
- MacHugh, N., Mburu, J., Hamilton, M., Davis, W., 1998, Characterisation of a monoclonal antibody recognising the CD3 ϵ chain of the bovine T cell receptor complex. *Veterinary Immunology and Immunopathology* 61, 25-35.
- Moretta, A., Marcenaro, E., Parolini, S., Ferlazzo, G., Moretta, L., 2008, NK cells at the interface between innate and adaptive immunity. *Cell Death and Differentiation* 15, 226-233.
- Natarajan, K., Dimasi, N., Wang, J., Mariuzza, R., Margulies, D., 2002, Structure and function of natural killer cell receptors: Multiple molecular solutions to self, nonself discrimination. *Annual Review of Immunology* 20, 853-885.
- Olsen, I., Boysen, P., Kulberg, S., Hope, J., Jungersen, G., Storset, A., 2005, Bovine NK cells can produce interferon in response to the secreted mycobacterial proteins ESAT-6 and MPP14 but not in response to MPB70. *Infection and Immunity* 73, 5628-5635.
- Perkins, D., Pappin, D., Creasy, D., Cottrell, J., 1999, Probability-based protein identification by searching sequence databases using mass spectrometry data. *Electrophoresis* 20, 3551-3567.
- Raulet, D., Vance, R., McMahon, C., 2001, Regulation of the natural killer cell receptor repertoire. *Annual Review of Immunology* 19, 291-330.
- Shevchenko, A., Chernushevic, I., Shevchenko, A., Wilm, M., Mann, M., 2002, "De novo" sequencing of peptides recovered from in-gel digested proteins by nanoelectrospray tandem mass spectrometry. *Molecular Biotechnology* 20, 107-118.
- Storset, A., Kulberg, S., Berg, I., Boysen, P., Hope, J., Dissen, E., 2004, NKp46 defines a subset of bovine leukocytes with natural killer cell characteristics. *European Journal of Immunology* 34, 669-676.
- Tsan, M., Gao, B., 2004, Heat shock protein and innate immunity. *Cellular and Molecular Immunology* 1, 274-279.
- Varma, S., Shatry, A., 1980, A technique for partial marsupialization of the spleen in calves. *The Veterinary Record* 106, 127-128.
- Wallin, R., Lundqvist, A., More, S., von Bonin, A., Kiessling, R., Ljunggren, H., 2002, Heat-shock proteins as activators of the innate immune system. *TRENDS in Immunology* 23, 130-135.
- Zhang, C., Zhang, J., Tian, Z., 2006, The regulatory effect of natural killer cells: Do "NK-reg cells" exist? *Cellular and Molecular Immunology* 3, 241-254.

CHAPTER THREE

EFFECT OF CULTURE TEMPERATURE ON MONOCLONAL ANTIBODY PRODUCTION BY THE NK64A HYBRIDOMA IN BATCH AND HIGH-DENSITY CULTURES

3.1. Introduction

The success of monoclonal antibodies (mAbs) as therapeutic agents coupled with their high dose requirements (≥ 100 mg) has created a need for improved mammalian cell culture processes (Birch and Racher 2006; Jain and Kumar 2008). To keep up with market demands, mAb production must be on the order of 10-100 kg/year requiring reactors to increase in size up to 20,000 L (Birch and Racher 2006; Jain and Kumar 2008; Morrow 2007). To help combat this problem bioreactor systems with increased cell density, that still retain maximum cell viability, are needed.

The two most common bioreactor systems used in industry are the fed-batch and continuous perfusion systems (Birch and Racher 2006; Butler 2005; Dalm et al. 2004; Dalm et al. 2005; Dalm et al. 2007; Farid 2006).

Fed-batch processes involve slow feeding of essential nutrients to maintain nutrient sufficiency, a limiting factor in standard batch cultures (Butler 2005). Fed-batch cultures can reach densities of 10×10^6 cells/mL (Detzel et al. 2008) and have a relatively short production time. However, a short production time leads to more down time and requires larger reactors (up to 20,000L) to meet product demand (Dalm et al. 2005). Perfusion cultures improve on fed-batch cultures because they allow for long-term operation by continuously refreshing the medium and removing harmful waste products (Birch and Racher 2006; Butler 2005; Dalm et al. 2005). Perfusion systems are smaller and have less down time than fed-batch cultures but require cell retention devices to maintain high cell densities (10^7 cells/mL) (Butler 2005; Dalm et

al. 2005). Cell retention devices include spinfilters, hollow fibers, centrifuges, settlers, and acoustic cell separators and are mostly external devices which expose the cells to uncontrolled conditions and nutrient gradients (Birch and Racher 2006; Dalm et al. 2005; Detzel et al. 2008).

In an effort to improve on the existing high density bioreactors, a new continuous centrifugal bioreactor (CCBR) capable of sustaining densities up to 3.2×10^8 cells/mL has been developed (Detzel et al. 2008; Mason 2004; Van Wie et al. 1991; Van Wie et al. 1986). The CCBR eliminates the problems associated with other perfusion bioreactors by its unique cell immobilization method that employs balancing centrifugal forces with opposing drag and buoyant forces (Detzel et al. 2008; Mason 2004). A kinetic growth model has also been derived which accurately predicts the CCBR environment including variables such as substrate and product concentrations and cell growth (Detzel et al. 2008). This model, however, does not take into account the effect cell culture temperature has on growth rate and mAb production.

The standard temperature for mammalian cell culture is 37°C which is physiological temperature. Increasing temperature to 39°C has been shown to increase cellular metabolism thus increasing glucose consumption and metabolite production as well as increasing mAb production in certain cell lines (Bloemkolk et al. 1992; Sureshkumar and Mutharasan 1991). A further increase in temperature to 42°C resulted in no proliferation (Sureshkumar and Mutharasan 1991). Decreasing the cell culture temperature has been shown to decrease cell metabolism and increase cell viability (Bloemkolk et al. 1992; Chuppa et al. 1997; Sureshkumar and Mutharasan 1991; Yoon et al. 2004). Specific mAb production has also been found to increase with a decrease in cell culture temperature. Studies with recombinant Chinese hamster ovary cells have revealed cell lines that show a 2- to 25-fold increase in specific mAb production at 32°C (Chuppa et al. 1997; Fox et al. 2004; Yoon et al. 2004). The effect of cell culture

temperature on specific mAb production has proven to be cell line dependent (Chuppa et al. 1997; Yoon et al. 2004) thus creating a need to study the effect of temperature on each cell line in order to maximize mAb production while still minimizing total cost.

3.2. Theory

3.2.1. Kinetic modeling

A generalized Monod expression developed by Han and Levenspiel was modified to account for product inhibition by lactate and ammonium and substrate inhibition by glucose to determine cellular growth rate (Equation 1) (Han and Levenspiel 1988). Concentrations of cells, glucose, mAb, lactate, and ammonium are denoted as C_{Cells} , C_G , C_{mAb} , C_L , and C_A respectively. $C_{L_{\text{max}}}$ and $C_{A_{\text{max}}}$ represent the maximum inhibitor concentration, for lactate and ammonium respectively, where zero growth rate is observed and/or cell death occurs. The Monod constant is represented by C_M and is defined as the value of glucose concentration that results in a growth rate of half of the maximum value. The observed growth rate is μ while μ_{max} is the maximum specific growth rate that can be obtained at high substrate concentrations. D is the dilution rate and is defined as F/V where F is the flow rate of fresh medium into the reactor and V is the volume of the reactor. When the reactor is filled to capacity a certain number of cells must leave the reactor, represented by the term $C_{\text{Cell}_{\text{out}}}$, to accommodate for additional cell growth. The powers n , m , p , and q are orders of inhibition and vary depending on the type of observed inhibition. Equations 2-5 employ the use of yield coefficients, Y_{iC} , to relate cell growth to substrate and product concentrations. C_{i0} is the feed concentration of glucose, mAb, lactate or ammonium (Detzel et al. 2008).

$$\frac{\partial C_{Cell}}{\partial t} = \mu_{\max} \cdot \frac{\left(1 - \frac{C_L}{C_{L_max}}\right)^n \cdot \left(1 - \frac{C_A}{C_{A_max}}\right)^m \cdot C_G \cdot C_{Cell}}{C_G + C_M \cdot \left(1 - \frac{C_L}{C_{L_max}}\right)^q \cdot \left(1 - \frac{C_A}{C_{A_max}}\right)^p} - (D \cdot C_{Cell_out}) \quad (1)$$

$$\frac{\partial C_G}{\partial t} = D(C_{G0} - C_G) - Y_{GC} \cdot \left(\frac{\partial C_{Cell}}{\partial t}\right) \quad (2)$$

$$\frac{\partial C_{mAb}}{\partial t} = D(C_{mAb0} - C_{mAb}) + Y_{mAbC} \cdot \left(\frac{\partial C_{Cell}}{\partial t}\right) \quad (3)$$

$$\frac{\partial C_A}{\partial t} = D(C_{A0} - C_A) + Y_{AC} \cdot \left(\frac{\partial C_{Cell}}{\partial t}\right) \quad (4)$$

$$\frac{\partial C_L}{\partial t} = D(C_{L0} - C_L) + Y_{LC} \cdot \left(\frac{\partial C_{Cell}}{\partial t}\right) \quad (5)$$

These expressions were solved simultaneously in Mathcad version 14 (Parametric Technology Corp., Needham, MA) to predict all concentrations as a function of time and dilution rate, and then used to compare model values with experimental results. Once it is determined that the model can produce accurate values it may be used to make predictions about cell growth and mAb production rates for a host of cell concentrations and dilution rates. Such predictions can help the researcher determine optimal operating conditions for very high population density cultures in a flow through system.

3.2.2. Bioreactor settling velocities and porosities

Cells are retained in the CCBR by balancing centrifugal forces with the opposing buoyant forces and drag forces imposed on the cells by medium fluid as it passes the cells. Figure 1 depicts these forces and their relative directions in the bioreactor.

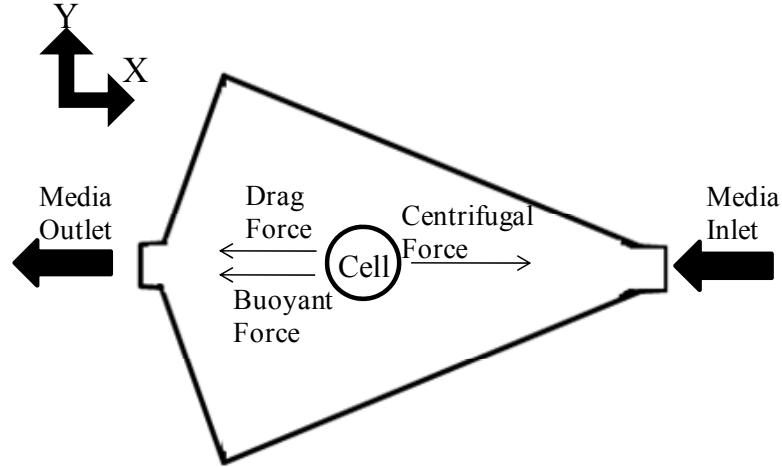


Figure 1: Schematic of bioreactor and direction of forces acting on the cells.

A hindered settling model for dense suspensions was adopted from Van Wie and Hustvedt and modified to describe the settling forces present in the bioreactor (Van Wie and Hustvedt 1988). The settling force (F_s) at any point (r) in the reactor is a function of the radius of the cell (R), the density of the particle (ρ_p), the density of the fluid (ρ_f), and the angular velocity (ω) as seen in Eq. 6.

$$F_s = \frac{4}{3}\pi R^3(\rho_p - \rho_f)\omega^2 r \quad (6)$$

The drag force that opposes the settling velocity can be modeled by the Stokes Drag equation for a particle in a laminar stream shown in Eq. 7; where F_d is the drag force on the cell, μ_f is the viscosity of the fluid, R is the radius of the cell, and V_0 is the velocity of the fluid stream.

$$F_d = 6\pi\mu_f R V_0 \quad (7)$$

The equation used to describe the particle settling velocity was derived by Detzel et al. and is shown in Eq. 8 where ε is the porosity of the bed which can be related to angular velocity by comparing one set of conditions versus another as seen in Eq. 9 (Detzel et al. 2008).

$$v = \frac{2}{9} R^2 (\rho_p - \rho_f) \omega^2 r \frac{\varepsilon^{4.7}}{\mu_f} \quad (8)$$

$$\varepsilon_2 = \varepsilon_1 \cdot \left(\frac{\omega_1}{\omega_2} \right)^{\frac{2}{4.7}} \quad (9)$$

3.3. Materials and Methods

3.3.1. Culture medium

The culture medium used in all batch and CCBR experiments was full DMEM solution containing Dulbecco's Modified Eagle Medium (DMEM) supplemented with 10% Calf Bovine Serum (CBS) from Hyclone, 2 mM L- glutamine, 100 units/mL penicillin, 100 μ g/mL streptomycin, 10 mM HEPES buffer, and 3×10^{-5} M 2-mercapto-ethanol. All medium ingredients were purchased from Gibco unless stated otherwise. DMEM was purchased in powdered form and contains 4,500 mg/L D-glucose and L-glutamine but no sodium pyruvate or sodium bicarbonate. The powdered DMEM was dissolved in NANOpure water prepared to a resistivity level of 18 M Ω -cm in a Barnstead NANOpure Infinity Laboratory Water System (Dubuque, IA) along with sodium bicarbonate and HEPES buffer. The pH was adjusted to 7.4 using 1 M NaOH. Four liters of this base DMEM were made per batch and sterile filtered into 500 mL bottles using a Nalgene® bottle top vacuum filter with a 2 μ m polyethersulfone (PES) membrane. CBS, penicillin, streptomycin, and 2-mercapto-ethanol were added to the base DMEM to make full DMEM.

3.3.2. *Cell line*

A newly developed NK64A hybridoma cell line was used in all experiments. The development of this new cell line is described in Godwin et al. (manuscript in preparation for submission, Chapter 2). The cell line was stored in CBS supplemented with 10% dimethylsulfoxide (DMSO) under liquid nitrogen.

3.3.3. *Batch cultures*

To begin a culture, a cell vial was removed from the liquid nitrogen tank and placed on ice to avoid a sudden change in temperature before being immersed in a 37°C water bath. The vial was continuously moved while in the water bath and removed as soon as all ice crystals were thawed to avoid over-heating the cells. The thawed cell suspension was then moved to a sterile 15 mL conical tube using a sterile glass pipette. Full DMEM was added drop-wise until a volume of 6 mL was reached. The cells were centrifuged at 1500 rpm for 10 minutes and the supernatant removed. Full DMEM was used to resuspend the cells and they were placed in 25 mL Petri dishes and incubated in a Forma Steri-Cult incubator at 37°C with 5% CO₂ and 95% humidity.

Batch culture experiments were performed to determine the effect of temperature on cell growth rate, glucose consumption, and lactate, ammonium ion and mAb production. Initial cell concentrations were low, 1×10^5 cells/mL, and the experiments were performed over a short period of time to ensure that only temperature, and not substrate and product concentrations, would affect cell growth. A total of five different experiments were performed each at a different temperature: 31, 33, 35, 37, and 39°C. Each experiment consisted of five 25 mL cell culture plates containing 25 mL of full DMEM. Every 18 hours a 1 mL sample was taken from one plate, spun down to remove the cells, and frozen for later analysis. The plate was then flushed using a 10 mL vacuum pipette to ensure an even distribution of the cells and a sample

was taken to count using a Neubauer Hemocytometer and the Trypan-Blue exclusion method to distinguish between live and dead cells. After a plate was used for sampling and counting it was thrown away; in other words every plate was really a separate experiment run under differing conditions and for different amounts of time. This was done to prevent the removal of medium from affecting the results of the experiment. However, this technique also has its challenges to inter-plate consistency as each might be inoculated with slightly differing amounts of cells or percent viabilities, and there may be temperature and O₂/CO₂ gradients within the incubator. To compensate for these problems all experiments were performed in duplicate. All five temperature experiments were performed in the same incubator one right after the other. The incubator was set to control the temperature to within 0.5°C of the set value and during all cultures, except the 37°C culture, there were no other experiments being performed in the incubator thus the incubator was only opened when the plates were removed for sampling. The cells used to inoculate the cultures were kept in the exponential growth phase in a separate incubator, which was always set at 37°C.

3.3.4. Inhibition studies

The inhibition studies were performed by culturing the NK64A hybridomas in 12-well plates with medium containing varying concentrations of either ammonium chloride or sodium lactate. Each well of the 12-well plate contained a different metabolite concentration obtained by diluting a concentrated stock solution with full DMEM. The stock solution was made by adding an appropriate amount of ammonium chloride to 50 mL of full DMEM to reach the desired stock concentration, 22 or 36 mM, or the appropriate amount of sodium lactate to 100 mL of full DMEM for a stock concentration of 2200 mg/dL. The wells were then inoculated with 5×10^4 cells/mL and incubated. The cells were counted every 12-13 hours using the Trypan Blue dye

exclusion method. A total of five counts were performed over the course of three days. Each well was mixed thoroughly before counting and a 50 μ L sample was removed for each cell count. When a cell count of zero was obtained for a given well, that well was no longer counted. Two separate experiments were performed for each metabolite and each experiment consisted of duplicate plates.

Cell growth rate, instead of cell viability, was used to determine the maximum ammonium and lactate concentrations because the maximum concentration is the point at which no cell growth occurs. Cells may still be viable at high metabolite concentrations even though they are not duplicating. Also cell counts obtained from the Trypan Blue dye exclusion method are unable to give accurate values for dead cells due to the fact that most cells lyse after death and are therefore unable to be counted. Growth rates were obtained from a linear fit of the natural log of the cell concentration versus time.

3.4. CCBR

3.4.1. Construction

The CCBR is easily constructed by making a few changes to the COBE® Spectra™ Apheresis System (Gambro BCT Inc., Lakewood, CA) which was originally manufactured as a blood separation unit. First, the cell purging sets that come with the Spectra™ must be altered to fit the purpose of this research. The only necessary parts are the 11.4 mL chamber, the anti-twister mechanism, and enough tubing to have one feed line, one product line, and one recycle line. All excess pieces are cut away and discarded with the exception of excess tubing, which is stored in case a replacement piece is needed. The tubing is reconnected into the proper configuration, as depicted in Figure 2, using polypropylene fittings. Only two of the four peristaltic pumps are used in this system; one for the feed line and one for the product line. The

inoculation line is added to the feed line before the feed pump by the addition of a three-way stainless steel valve. Another stainless steel three-way valve is used to add the sampling line to the recycle line. A piece of gas permeable seven-lumen silicone tubing is added to the feed line before the reactor chamber. To help oxygenate the medium it is passed through the middle lumen while air is passed through one of the outside lumens using a RAININ Instrument Company Inc. Rabbit™ model peristaltic pump (Woburn, MA).

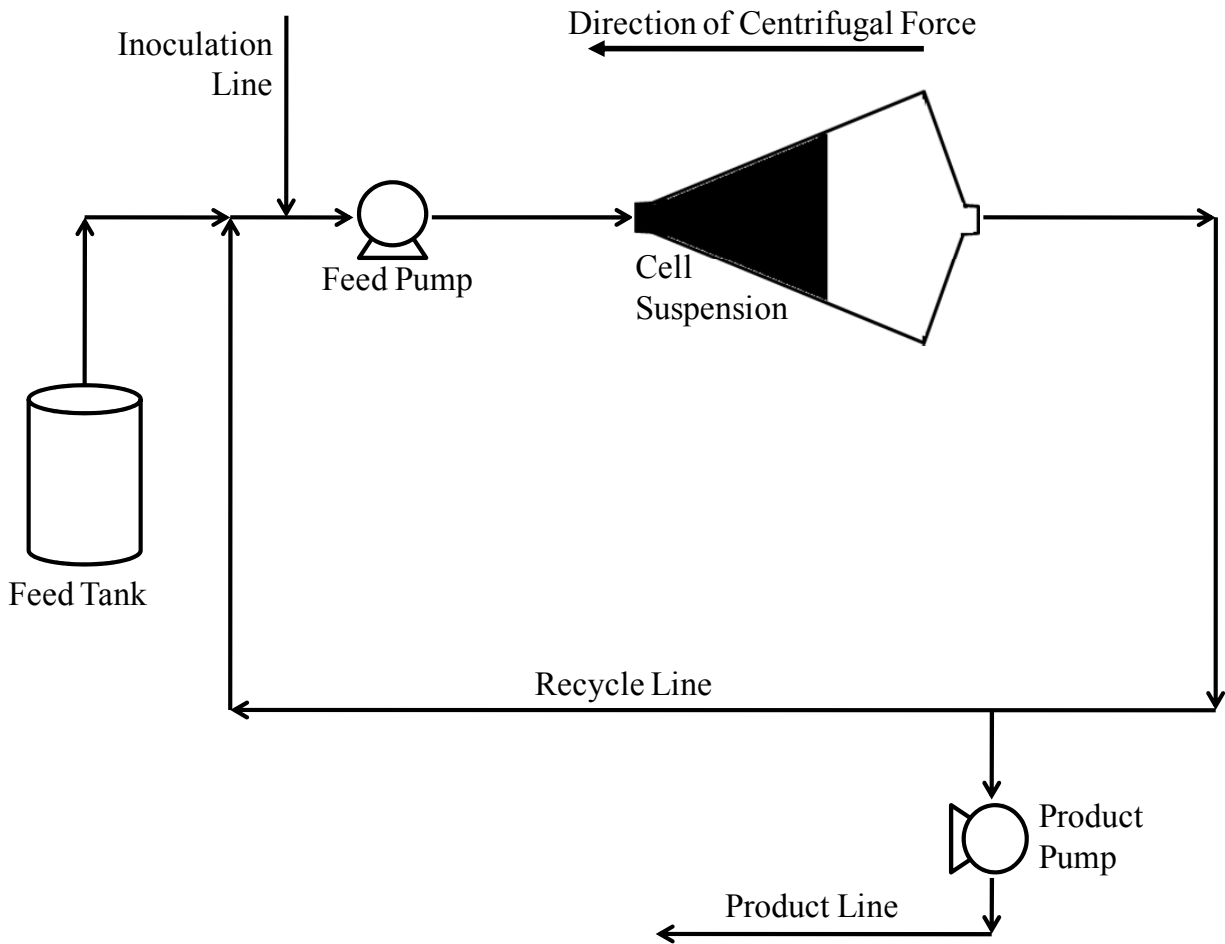


Figure 2: Flow profile of the CCBR cell culture system.

The tubing set is sterile when it is removed from the package. However, to insure there is no contamination the system is flushed with 70% ethanol for 24 hours prior to inoculation. Autoclaving the tubing set is not an option because it is made of polyethylene which is damaged

at high temperatures. The feed and product reservoirs are 1 L polypropylene bottles which are autoclaved before use. Each bottle contains three ports that are inserted into the screw-on cap. For the feed bottle, one port is connected to the feed line and the other two are connected to short tubes with sterile 2 μm filters for displacement of medium by filtered air. For the product bottle, one port is used to connect to the product line and the other two are left open since there was no need to keep the product reservoir sterile.

3.4.2. Startup

Before each run in the CCBR, a new tubing set is removed from its package, modifications made to remove excess tubing and provide the correct valving arrangement, and mounted onto the system. The CCBR is then turned on and the pumps are loaded by pressing the CONTINUE button. Next, the CCBR is put in Super Manual mode by pressing the CHANGE MODE button followed by the PERIOD button. The user must confirm this change by pressing the ENTER/YES button. The entire system is then filled with 70% ethanol and allowed to operate in a total recycle mode for 24 hours. The ethanol is then removed from the system through the sampling valve and the sterile feed bottle is filled with full DMEM and attached to the tubing set along with the empty product bottle. The tubing lines are flushed with medium and the sampling valve is left open to allow this medium to be discarded to ensure that all the ethanol has been removed from the system. The sampling valve is then closed, the tubing set is filled with fresh medium, and all air bubbles are removed.

3.4.3. Sampling

Samples were taken from the CCBR approximately every 12 hours through the sample valve. The first sample was collected in a microcentrifuge tube and spun down to remove any cells or debris present and then transferred to a new microcentrifuge tube and frozen for later analysis. A

second sample was also taken at this time in a small glass bottle and was used to determine the pH of the reactor medium through the use of a pH meter.

To determine the number of cells present in the CCBR, a cell count was also performed every 12 hours. The rotation of the centrifuge was stopped and the feed flow rate was increased to 20 mL/min to allow the cells to become completely mixed throughout the system. The product pump was turned off at this time to prevent cells from being pumped out of the system. Cells were allowed to cycle through the lines in this manner for approximately 20 minutes before a sample was collected in a microcentrifuge tube through the sampling valve. The feed flow rate was then reset at 6.5 mL/min and the centrifuge was restarted. The product pump was kept off for a couple of minutes after the CCBR was restarted to allow all of the cells to become suspended in the reactor chamber. It was then set to its previous value.

3.4.4. Reactor runs

Reactor Run 1 (Run 1) was performed with the CCBR in a closed positive pressure room and two oil-filled space heaters were used to maintain the temperature of the room at 37°C. The run was seeded with 2.53×10^8 cells. Cell counts and samples were taken every twelve hours and the samples were spun down and frozen for later analysis. The room temperature was also monitored closely and the heaters were adjusted so as to maintain a constant temperature. The average temperature for Run 1 was $36.7^\circ\text{C} \pm 0.8$. The pH of the medium was tested at the time of sampling and the product flow rate was adjusted throughout the runs to maintain a pH around 7-7.2. The average pH for Run 1 was 7.06 ± 0.08 .

Reactor Run 2 (Run 2) was performed in the same manner as Run 1 except the temperature was decreased to 33°C and the reactor was seeded with 2.50×10^8 cells/mL. The average temperature for Run 2 was $33.7^\circ\text{C} \pm 1.1$ and the average pH was 7.04 ± 0.08 .

3.5. Analysis

3.5.1. Cell concentration and viability assay

Cell concentration and viability was determined using a Neubauer Hemocytometer and the Trypan-Blue dye exclusion method, which allows the investigator to distinguish between live and dead cells as only dead cells take up the dye.

3.5.2. Glucose assay

Glucose concentrations were determined using the RAICHEM (San Diego, CA) Glucose Color Reagent Assay Kit (product number 80038), which relies on the glucose oxidase-Trinder color reaction where glucose is oxidized to form D-gluconate and hydrogen peroxide (H_2O_2). In the presence of peroxidase, 4-aminoantipyrine and p-hydroxybenzene sulfonate are oxidatively coupled by H_2O_2 to form a quinoneimine dye with a maximum absorption at 500 nm. A standard curve was created using known glucose concentrations ranging between 0 and 4000 mg/L.

Absorbance was read using a SLT Laboratories Spectra Rainbow ELISA plate reader.

3.5.3. Lactate assay

Lactate concentrations were determined by using either the Sigma Diagnostics (St. Louis, MO) Lactate Assay Kit (product number 735), which relies on the lactate oxidase reaction, or the BioAssay Systems (Hayward, CA) EnzyChrom™ Lactate Assay Kit (product number ECLC-100), which relies on the lactate dehydrogenase reaction. In the lactate oxidase reaction, lactic acid is converted to pyruvate and hydrogen peroxide (H_2O_2), which then allows peroxidase to catalyze the oxidative condensation of chromagen precursors. This reaction produces a colored dye with maximum absorption at 540 nm. Samples were diluted 1/15 and analyzed using a standard curve ranging between 0.69 and 40 mg/dL. In the lactate dehydrogenase reaction, the oxidation of lactate forms NADH which is coupled to the formazan (MTT)/phenazine

methosulfate (PMS) reagent forming a colored product with an absorption maximum at 565 nm. Samples were diluted 1/10 and analyzed using a standard curve ranging between 0 and 2 mM and created using the standard samples provided with the kit. Absorbances were read at the appropriate wavelengths using a SLT Laboratories Spectra Rainbow ELISA plate reader.

3.5.4. *Ammonium assay*

Ammonium ion concentrations were determined by using the RAICHEM Ammonia Assay Kit (product number 85446), which relies on the glutamate dehydrogenase reaction. A standard curve was created using known ammonium ion concentrations between 0 and 0.5 mM. Samples were diluted to fit onto the standard curve. Absorbances were read at 340 nm using a VICTOR³ Wallac 1420 Multilabel Counter.

3.5.5. *Monoclonal antibody assay*

Monoclonal antibody concentrations were determined using the Mouse IgG – LL NANORID plate (product number GT272.3) from The Binding Site Ltd. (Birmingham, UK). The NANORID plates are coated with an agarose gel containing mouse IgG antibody. Samples are placed in cylindrical wells on the gel and the antigen in the sample (in this case the NK mAb) diffuses radially into the gel forming antigen-antibody complexes. These antigen-antibody complexes will form a precipitin ring, which will increase in size until equilibrium is met between the formation and breakdown of these complexes. At equilibrium, or completion, there is a linear relationship between the square of the ring diameter and the antigen concentration. One mAb standard was used per RID plate and the mAb samples were not diluted. Ring diameters were read using a light box and mAb concentrations were determined using the RID Reference Table, based on the ideal standard curve, provided in the kit.

3.6. Results and Discussion

3.6.1. Inhibition studies

Ammonium ion and lactate inhibition studies were performed to determine C_{A_max} and C_{L_max} for the growth rate model. The results of each experiment can be seen in Figure 3.

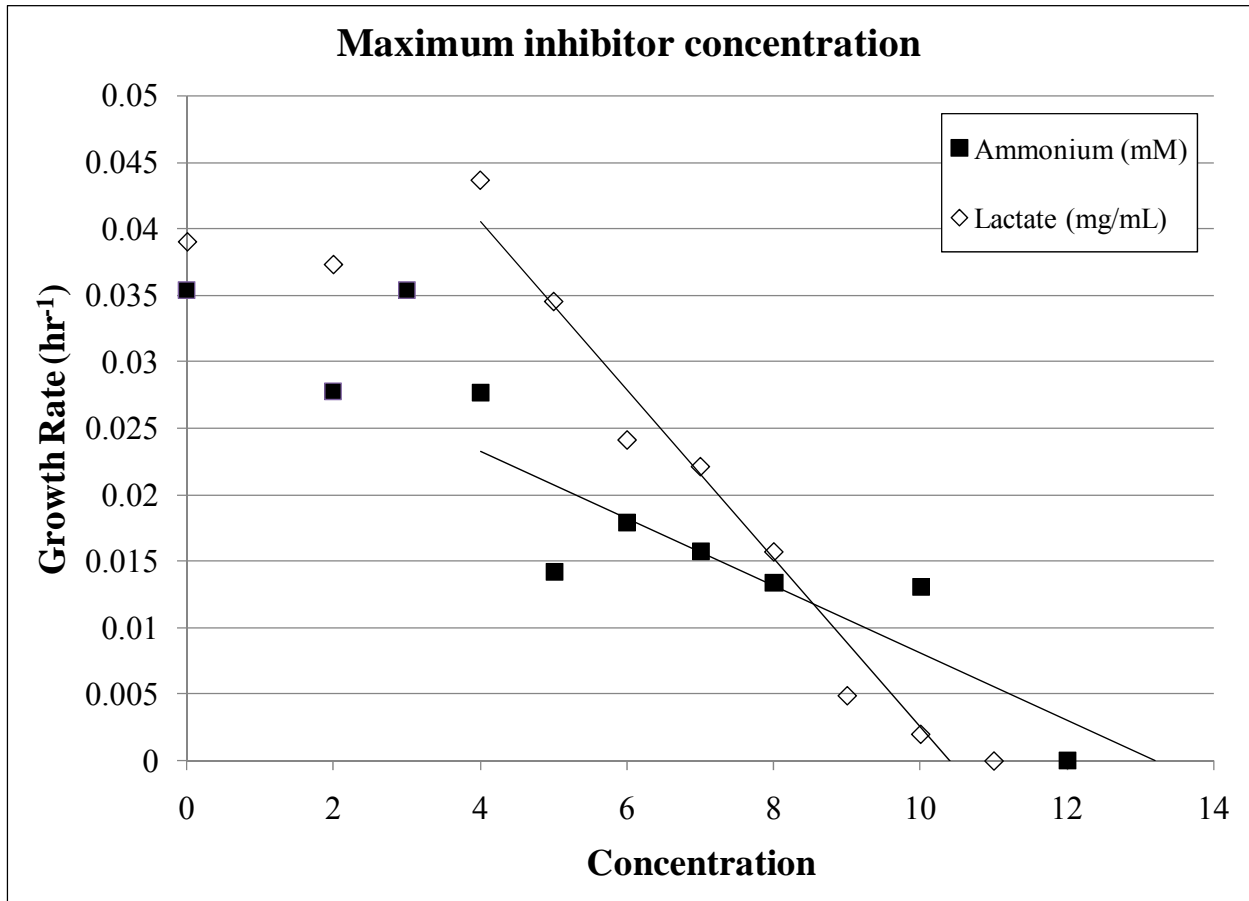


Figure 3: Results of ammonium ion and lactate inhibition experiments.

Graphing the growth rates versus the ammonium ion and lactate concentrations shows that growth rates slow and become zero at high concentrations. At even higher concentration, growth rates become negative indicating cell death associated with the increasing concentrations of the metabolite; there is no need to model for concentrations above these values however, because further growth associated production of metabolite cannot occur above this limiting maximum

concentration. Concentrations below 4 mM for ammonium and 4 mg/mL for lactate showed no inhibition and were therefore not included in the linear fit. This bimodal effect introduces error into the model at low inhibitor concentrations with maximum errors of 17 and 10% occurring at 4 mM for ammonium and 4 mg/mL for lactate respectively. The error decreases at lower concentrations because as the inhibitor concentration approaches zero the inhibition factor approaches a value of 1. The experiment displayed for ammonium yields a maximum concentration of 13.3 mM and that for the lactate 10.4 mg/mL. These values were used as C_{A_max} and C_{L_max} in the kinetic model.

3.6.2. *Temperature studies*

Modeling the reactor conditions at different temperatures requires knowledge of cell growth and metabolism at the temperatures of interest. Batch studies were performed at temperatures of 31, 33, 35, 37, and 39°C to determine growth rate, μ , and yield coefficients, Y_{iC} 's, for the NK64A hybridoma as a function of temperature. The results of the five temperature experiments for each parameter can be seen in Figures 4 – 8.

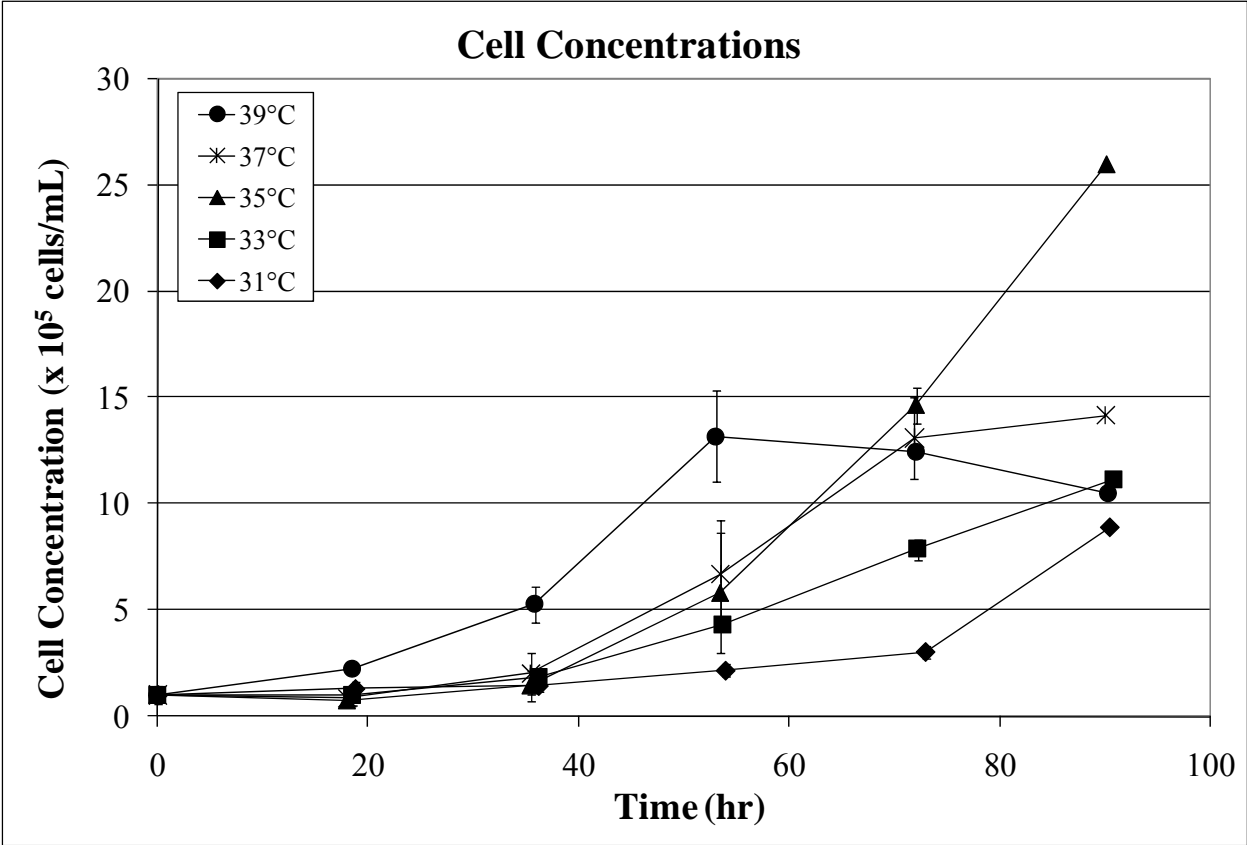


Figure 4: Live cell concentration profiles for the five temperature experiments.

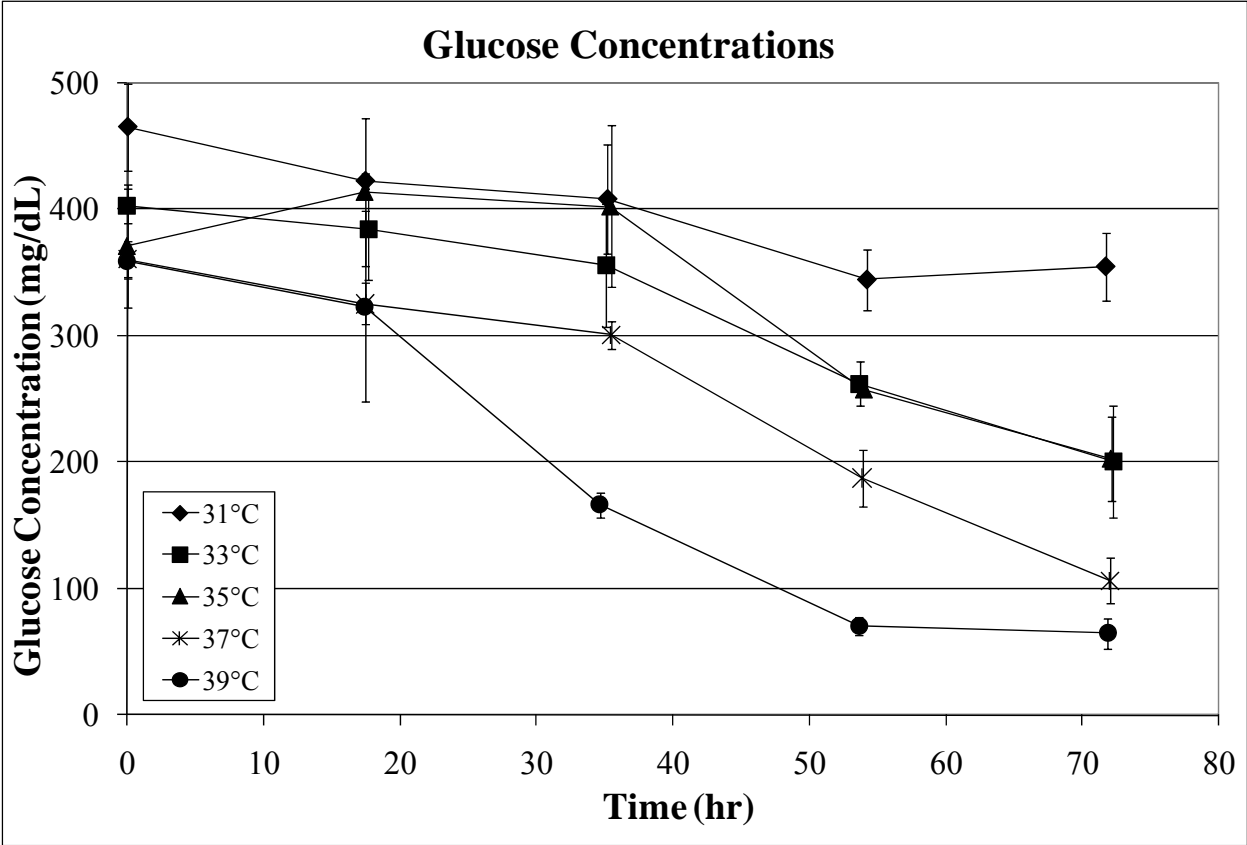


Figure 5: Glucose concentrations for the five temperature experiments.

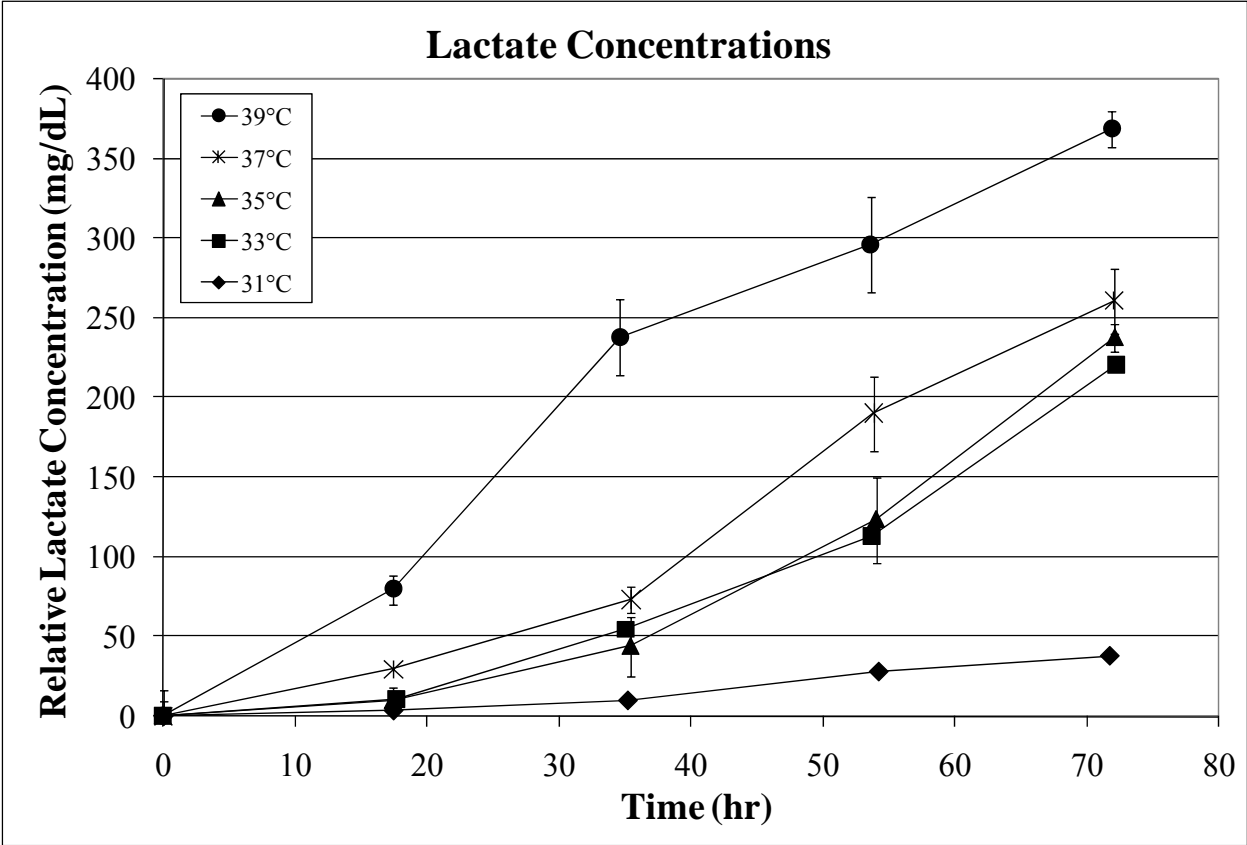


Figure 6: Lactate concentrations for the five temperature experiments.

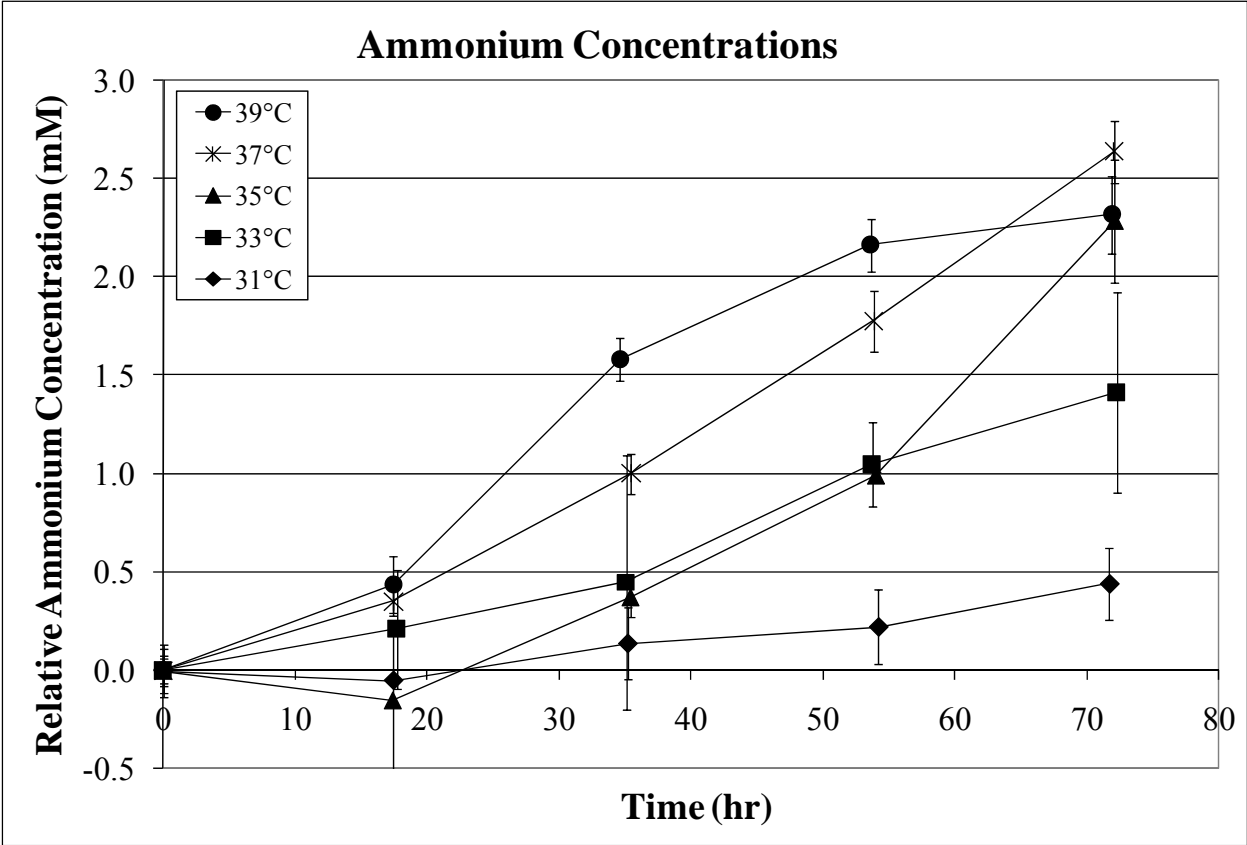


Figure 7: Ammonium ion concentrations for the five temperature experiments.

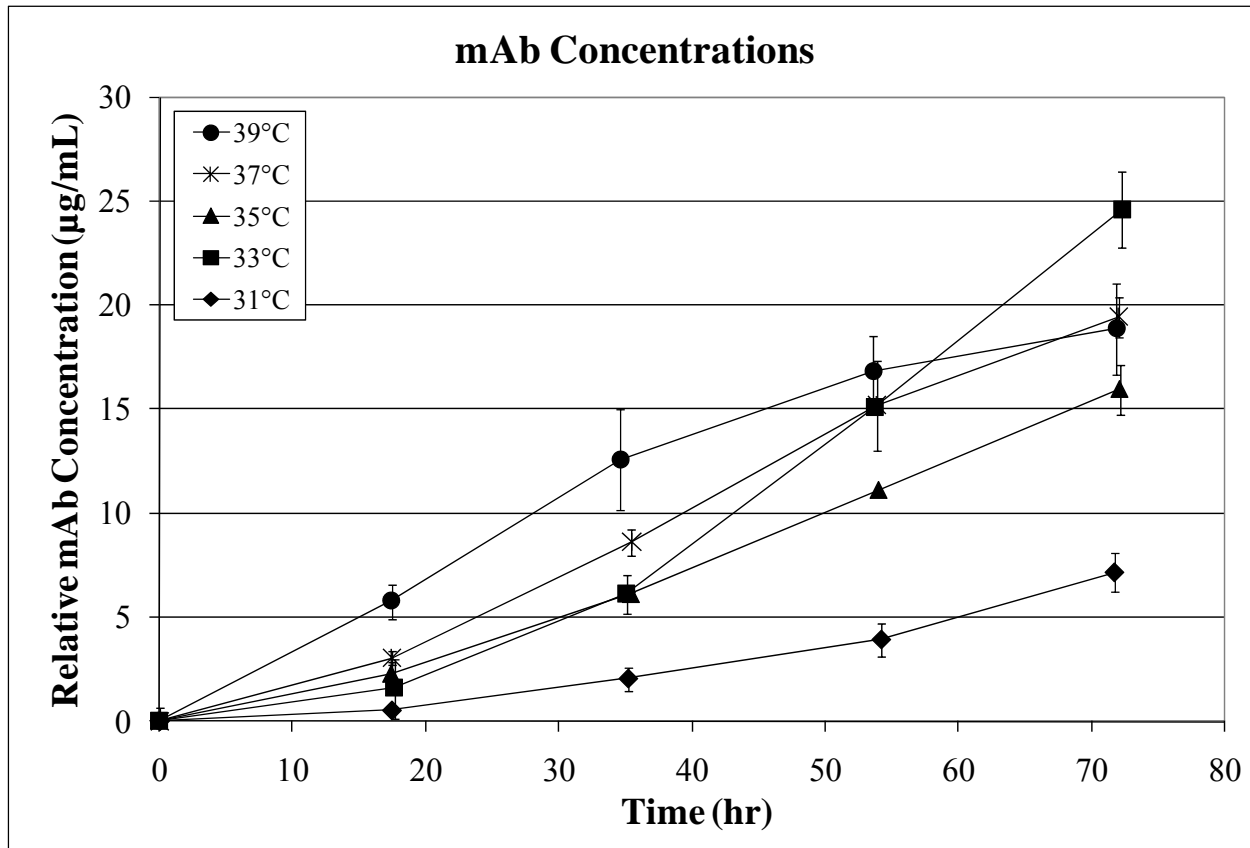


Figure 8: Monoclonal antibody concentrations for the five temperature experiments.

The cell concentration profiles in Figure 4 show that cell growth increases with increasing temperature. At 54 hours the highest cell concentration is 1.3×10^6 cells/mL at a temperature of 39°C and the lowest is 0.22×10^6 cells/mL at 31°C. The drop in cell concentration observed at the end of the 37 and 39°C cultures is due to either a drop in pH, from 7.4 at the start of the culture to 6.6 at the end, or a build-up of lactate and ammonium which can inhibit cell growth and even result in cell death (Detzel et al. 2008; Doyle and Butler 1990). Figures 6 and 7 show that 37 and 39°C have the highest concentrations of both lactate and ammonium. For 37°C the final lactate and ammonium concentrations are at 27 and 32% of the maximum concentrations at which cell death occurs and for 39°C they are at 35 and 28% respectively. Glucose consumption

is also higher at these higher temperatures as seen in Figure 5. By the end of the experiment both 37 and 39°C cultures have consumed 75% of the initial glucose concentration whereas the 33 and 35°C cultures have consumed 50% and the 31°C culture has only consumed 12.5%. To determine the main cause of the growth inhibition seen in the 37 and 39°C cultures the individual contributions of each metabolite were calculated, where a value of 1 indicates no inhibition (Detzel et al. 2008). For each culture the individual contributions of lactate and ammonium were >0.82. However, the glucose inhibition contributions for the 37 and 39°C cultures were 0.65 and 0.49 respectively, indicating that substrate inhibition was a major factor in the decline in cell growth seen at the end of the cultures. Temperatures 31, 33, and 35°C had lactate and ammonium contributions >0.85 and glucose contributions >0.79 indicating little inhibition in cell growth as seen in Figure 5. The pH in the 37 and 39°C cultures could also have an inhibiting effect on cell growth. Detzel et al. has shown that optimal pH for the MM1A hybridoma cell line is 7.2 and a drop in pH to 6.8 results in a 20% decrease in viability (Detzel et al. 2008). The pH at the end of the 37 and 39°C cultures was 6.6 which would correlate to a growth rate that is 70% of the maximum.

MAB production has a slightly different temperature profile than the other metabolites as seen in Figure 8. There is some indication that total mAb production increases with an increase in temperature with 31°C having the lowest mAb concentration followed by 35, 37, and 39°C. However by the end of the experiment the 33°C culture has the highest mAb concentration at a value of 25 µg/mL. The final mAb concentration for both the 37 and 39°C cultures is not far behind the 33°C culture at 20 µg/mL. It can also be seen that mAb production slows down at the end of the 37 and 39°C cultures, which is due to the decrease in live cell concentration and growth rate inhibition, as discussed earlier, and hence growth related mAb production.

The specific growth rate, μ , for each temperature was determined by plotting $\ln[\text{Cell}]$ vs. time and taking the slope of the line (Table 1). All correlations coefficients were >0.88 for growth rate determination. The value of μ was essentially constant at an average value of $0.052 \text{ hr}^{-1} \pm 0.001$ in the temperature range of 35 to 39°C but decreased to 0.036 hr^{-1} for 33°C and 0.026 hr^{-1} for 31°C; this is consistent with the μ values reported by Suershkumar et al. for their hybridoma cell line, an average value of $0.046 \text{ hr}^{-1} \pm 0.002$ for the temperature range of 35 to 39°C and a value 0.034 hr^{-1} for 33°C (Sureshkumar and Mutharasan 1991).

Yield coefficients for glucose consumption, lactate, ammonium ion, and mAb production were determined by plots of metabolite concentration vs. cell concentration. Table 1 lists the yield coefficients per 10^5 cells per mL. Sureshkumar and Mutharasan (1991) (Sureshkumar and Mutharasan 1991) showed a 130% increase in glucose consumption, a 440% increase in lactate production and a 110% increase in mAb production at increasing temperature for the 14-4-4S hybridoma cell line, the trends found for the NK64A hybridoma cell line are shown in Figure 9.

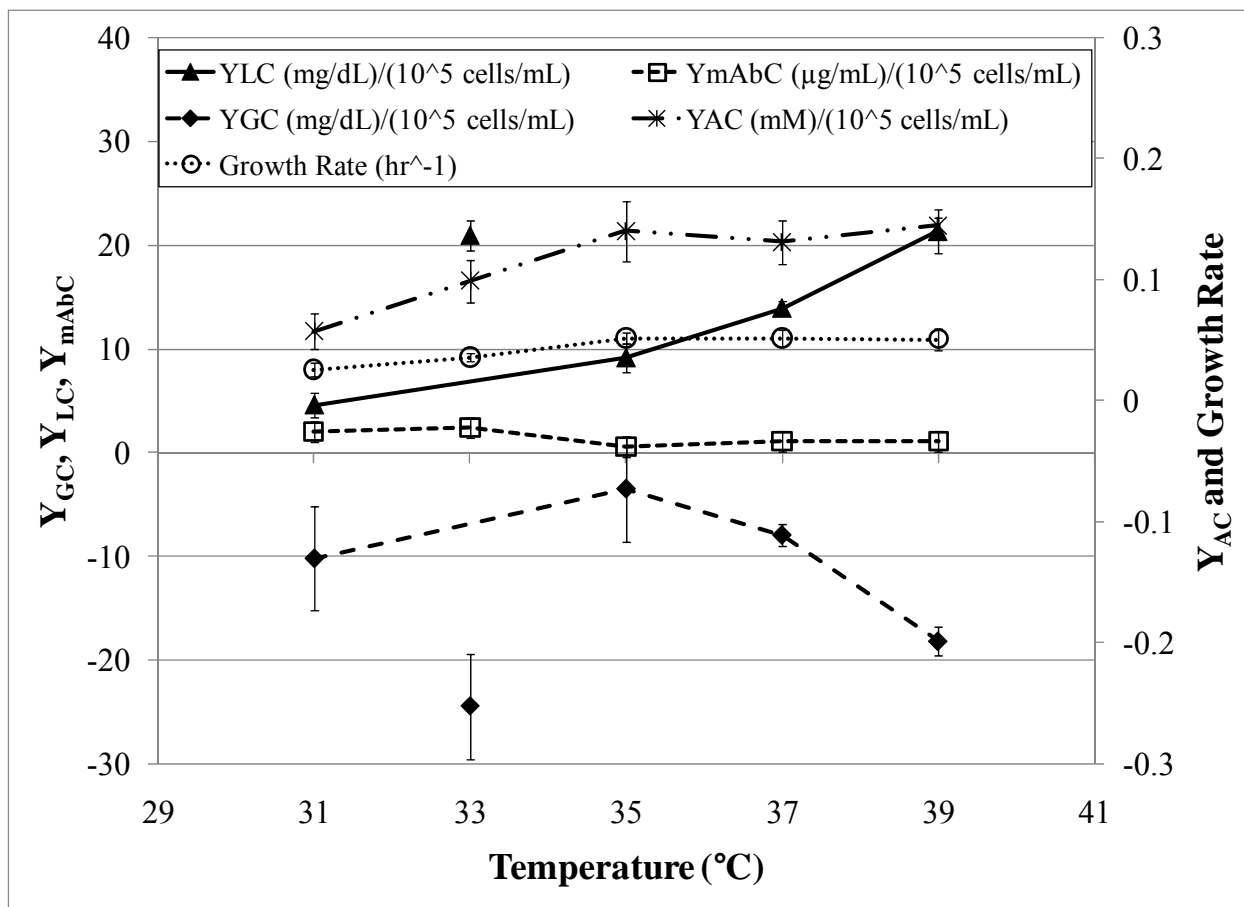


Figure 9: Yield coefficients and growth rate as a function of cell culture temperature.

Ammonium production increases from 31 to 35°C then becomes constant at a value of 0.14 as temperature increases to 39°C, an overall increase of 130%. Specific mAb production is highest at 31 and 33°C with a value that is twice that of the cultures at the higher temperatures. This is consistent with results from temperature studies on recombinant hamster ovary cells producing mAb (Fox et al. 2004; Yoon et al. 2004) where results show anywhere between a 2- and 25-fold increase in specific mAb production rate at 32°C compared to 37°C depending on the cell line. Glucose consumption and lactate production show an overall trend of increasing as temperature increases, by 80 and 370% respectively, omitting the values obtained at 33°C. It is

possible that the values at 33°C are in error; however, it is important to note that both values are increased in agreement with the fact that glucose consumption is coupled to lactate production.

Temperature (°C)	μ (hr ⁻¹)	Y_{GC}	Y_{LC}	Y_{AC}	Y_{mAbC}
31	0.026	10.1	4.6	0.06	2.2
33	0.036	24.4	21.0	0.10	2.4
35	0.052	3.5	9.2	0.14	0.6
37	0.052	7.9	14.0	0.13	1.1
39	0.051	18.1	21.4	0.14	1.1

Table 1: Cell growth parameters determined from batch temperature studies.

3.6.3. Temperature dependencies of yield coefficients

Recent studies by Sureshkumar et al. on a murine hybridoma cell line have shown that culture temperature greatly affects cell growth rate, glucose consumption, and lactate and mAb production. Cells cultured at 29 and 42°C showed no growth while cells cultured at 33, 35, 37, and 39°C showed increasing growth rate with increasing temperature. Glucose consumption as well as lactate and mAb production was also increased with temperature (Sureshkumar and Mutharasan 1991). Data was extrapolated from their work and used to determine Arrhenius parameters for growth rate and yield coefficients as a function of temperature. The corresponding graph is shown in Figure 10. The Arrhenius rate equation used is given in Eq. 10 where Y_i is the yield coefficient for the metabolite, Y_i^0 is the Arrhenius constant for the metabolite, E is the activation energy, R is the ideal gas constant, and T is the absolute temperature in degrees Kelvin.

$$Y_i = Y_i^0 \times e^{-E/RT} \quad \text{Eq.10}$$

Ammonium production was not investigated by Sureshkumar et al. Values for ammonium production as a function of temperature were estimated by assuming a linear relationship between lactate production and ammonium production for a hybridoma cell line (Mason 2004); for this we assumed a proportionality constant of 0.008. Assuming a linear relationship between ammonium and lactate production allowed for an easy but rough calculation of the ammonium produced by the cell line used by Sureshkumar et al. and therefore may not be accurate.

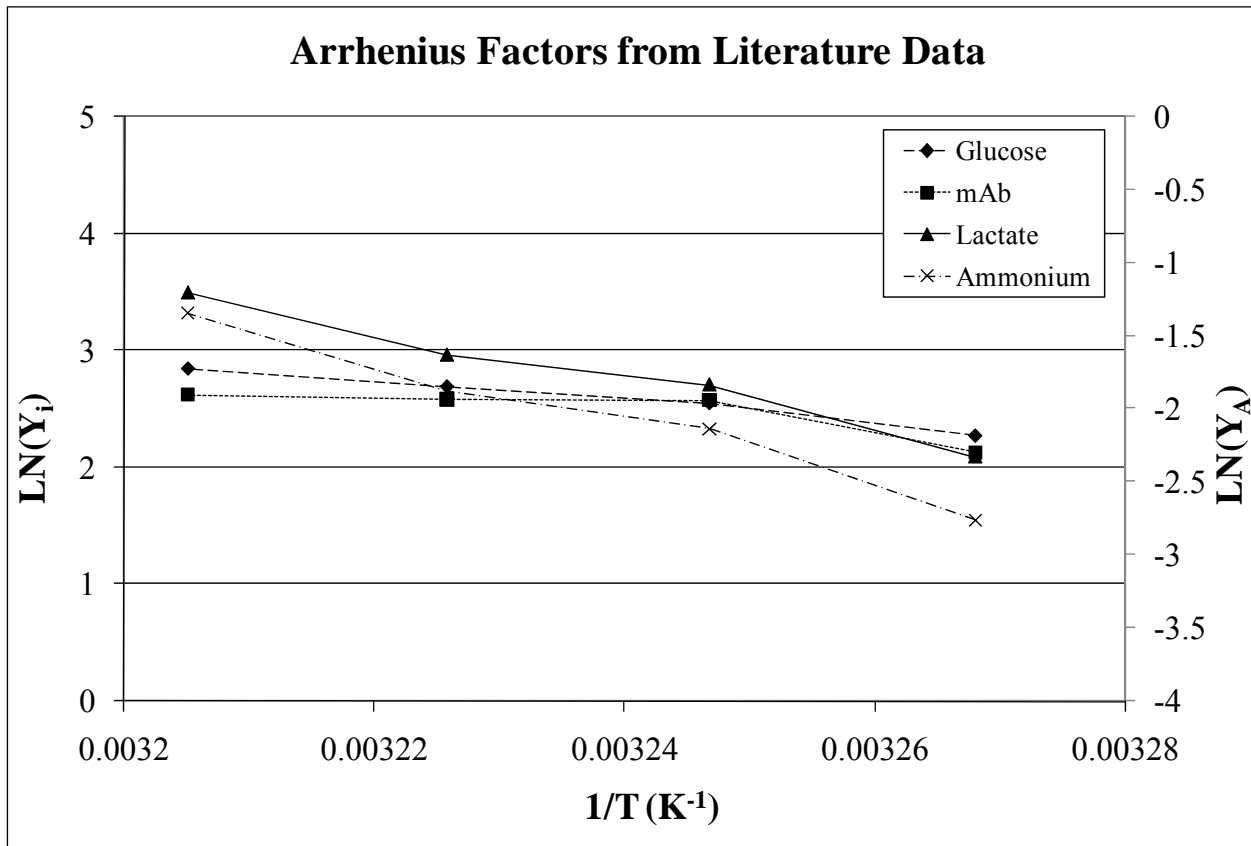


Figure 10: Arrhenius plot for literature values.

Taking a similar approach with the data collected for the NK64A hybridoma cell line, Figure 11 indicates a possible Arrhenius dependency of yield coefficients for this new cell line. Omitting the values at the lower temperatures for lactate and glucose yield coefficients reveals an

Arrhenius trend for these species. Ammonium shows a bimodal trend with an apparent Arrhenius dependency for the 31-35°C temperature range. Specific mAb production shows an overall increase at lower culture temperatures, omitting the value at 35°C. These preliminary results indicate a possible Arrhenius dependency of the yield coefficients for the NK64A hybridoma. However, additional experiments should be performed to confirm these trends.

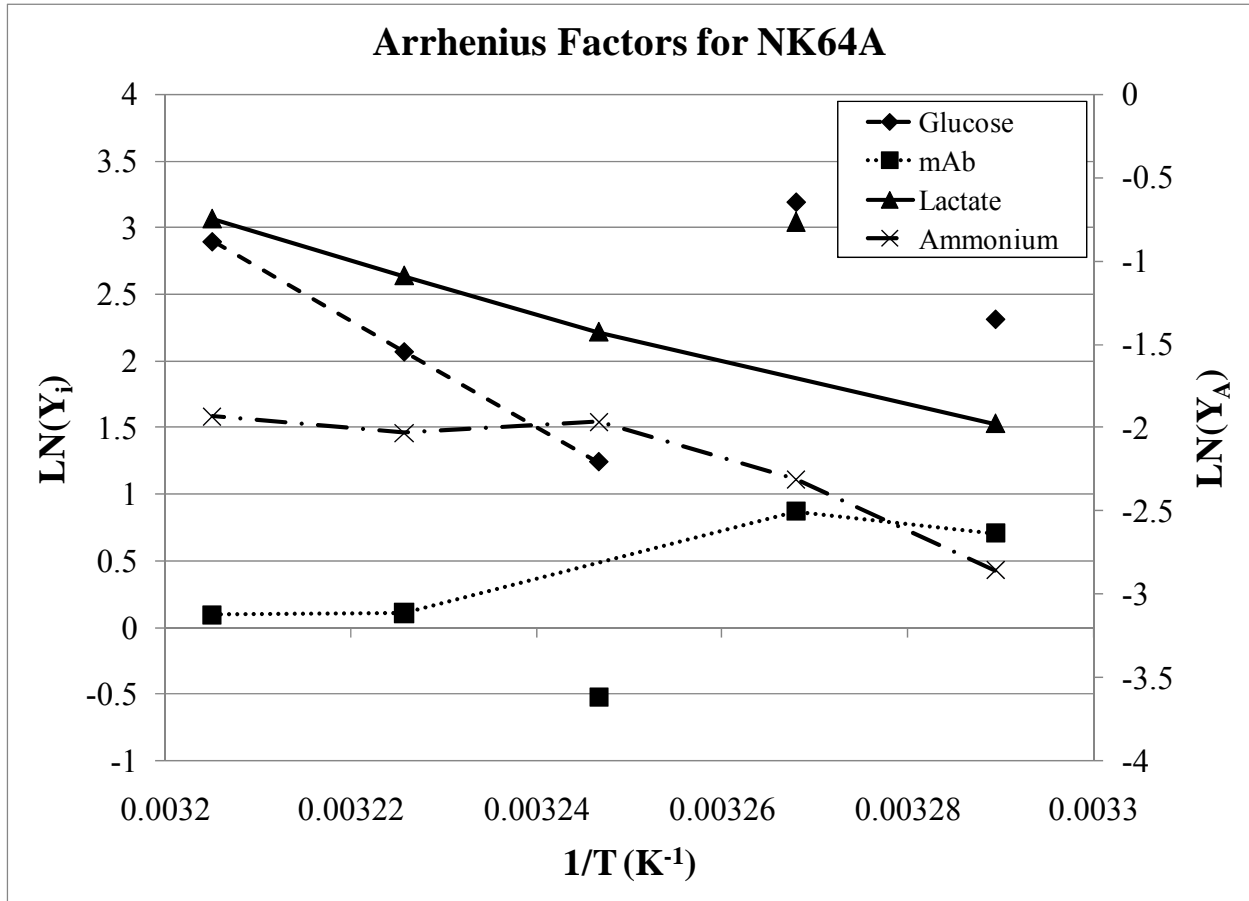


Figure 11: Arrhenius plot for NK64A hybridoma.

3.6.4. Modeling of batch culture

The validity of the model was first tested by fitting the model to the results obtained from a batch culture at 37°C in 75 mL tissue culture plates. The culture was seeded with 1.5×10^5 cells/mL and maintained for 3 days in an incubator set at $37^\circ\text{C} \pm 0.5$ with 5% CO₂. Cell counts

were performed every 12 hours and sample were taken and frozen for later analysis. At approximately 48 hours post inoculation, 5 mL of fresh medium was added to help maintain the culture pH at 7.2. The parameters used in the model were taken from the results of the 37°C batch temperature study performed in 25 mL tissue culture plates. The values for n, m, p, and q in Eq. 1 were taken from the work of Detzel et al. on the MM1A hybridoma and are 0.22, 0.52, -1.16, and 0.55 respectively (Detzel et al. 2008). The assumption was made that the values for the inhibition exponents would not change drastically for the new NK64A hybridoma; however, experiments to determine the actual values for the NK64A cell line should be performed to confirm this assumption. Results for the batch culture and model fit can be seen in Figures 12 and 13.

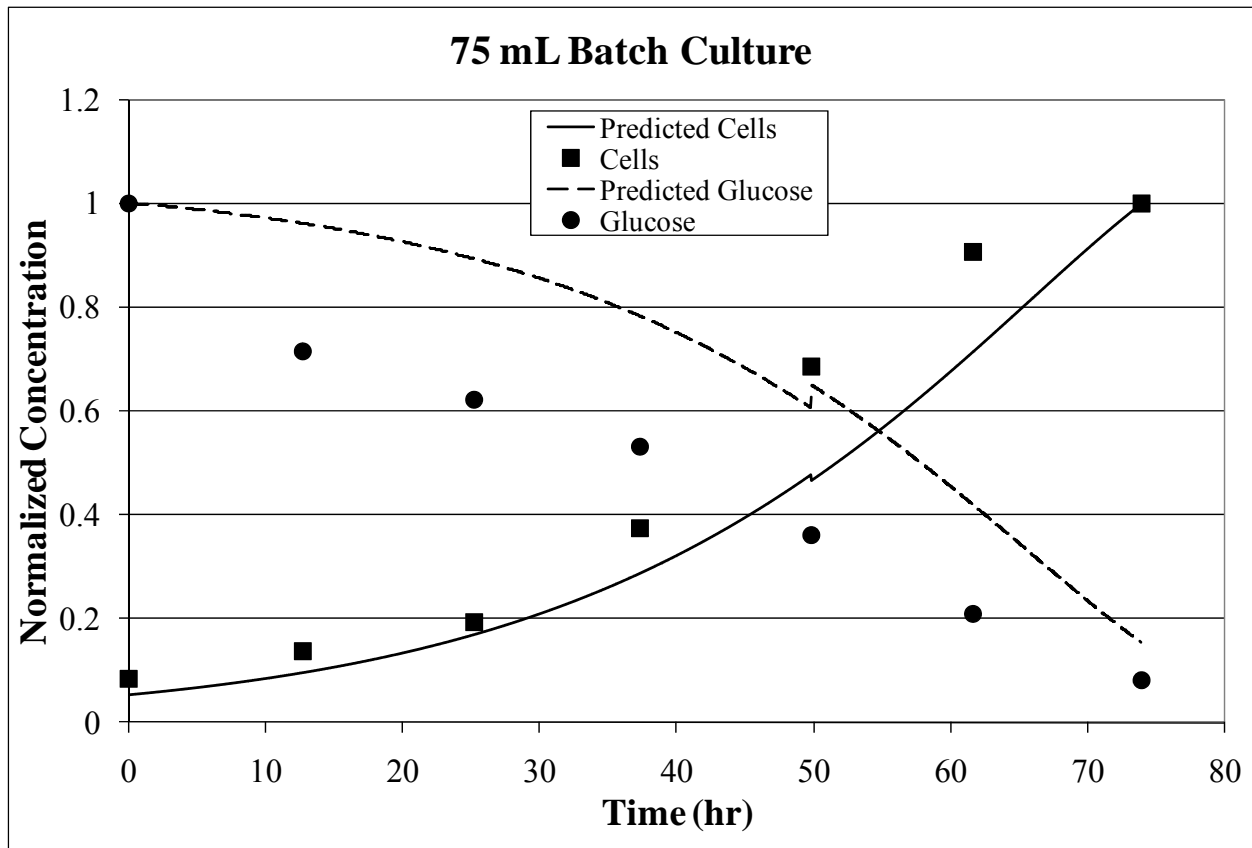


Figure 12: Model fit for cell and glucose concentration in 75 mL batch culture.

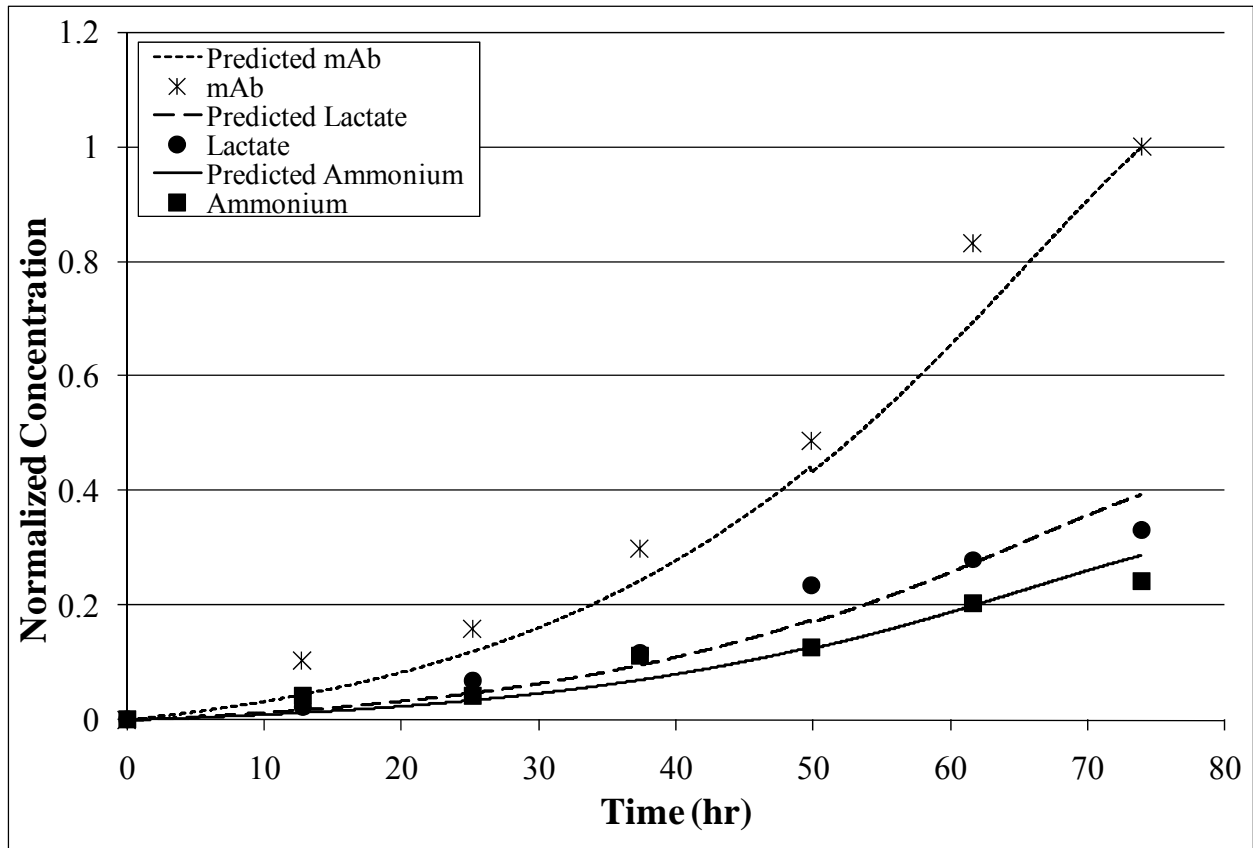


Figure 13: Model fit for mAb, lactate, and ammonium ion concentration in 75 mL batch culture.

The model is able to predict mAb, lactate, and ammonium production with a slight under prediction of an average of 16, 10, and 8% for each respective species. The case is slightly more severe for the cell concentration with an average cell concentration that is 26% above the predicted values. This in part accounts for the under prediction in glucose utilization with an average deviation of 62%. It is possible that the large deviation in the glucose concentration is due to an error in the glucose assay and it would be beneficial to re-run the assay to confirm these results.

Model of CCBR culture

Based on the results of the temperature batch studies, it was expected that higher mAb production would result when cells are cultured at lower temperatures due to the enhanced yield coefficient. However, one must also include the effective concentrations of the substrate and all metabolites as the collective set of values results in an overall inhibition coefficient defined by all the terms multiplying the $\mu_{\max} \cdot C_{\text{cell}}$ term in Eq. 1. To get an understanding of how the NK64A hybridomas will grow when cultured in the CCBR under high density conditions the model was adapted to fit the conditions used in the bioreactor culture. The values used for μ_{\max} and the yield coefficients in Eqs. 1-6 were the values obtained in the batch temperature study found in Table 1. The initial cell concentration was set at 2.50×10^7 cells/mL and the cells were allowed to grow until a concentration of 8.98×10^7 cells/mL, which was considered the steady state concentration (Detzel et al. 2008). After the steady state cell concentration was reached the cell growth was turned off by setting the cellular growth rate and the rate at which the cells leave the system in Eq. 1 equal to zero (Detzel et al. 2008). The model also includes the initial lag phase often seen in CCBR culture (Detzel et al. 2008). The dilution rate was increased step-wise over the course of the run from an initial value of 1.84 hr^{-1} to a final value of 3.23 hr^{-1} to ensure that the concentrations of ammonium and lactate remain below inhibiting levels. This also allows control of pH during the CCBR culture. The total inhibition was calculated by normalizing Eq. 1 to the maximum specific growth rate observed during the batch study (Detzel et al. 2008). A value of 1 indicates no inhibition. Figures 14-17 show the results of the model for 37°C and 33°C cultures. All concentrations were normalized to their maximum values; 400 mg/dL for glucose, 1040 mg/dL for lactate, 13.3 mM for ammonium. Cell concentration was normalized to a maximum of 1.0×10^8 cells/mL to allow comparison of each temperature to a

maximum concentration and mAb was normalized to the highest concentration as predicted by the 33°C model.

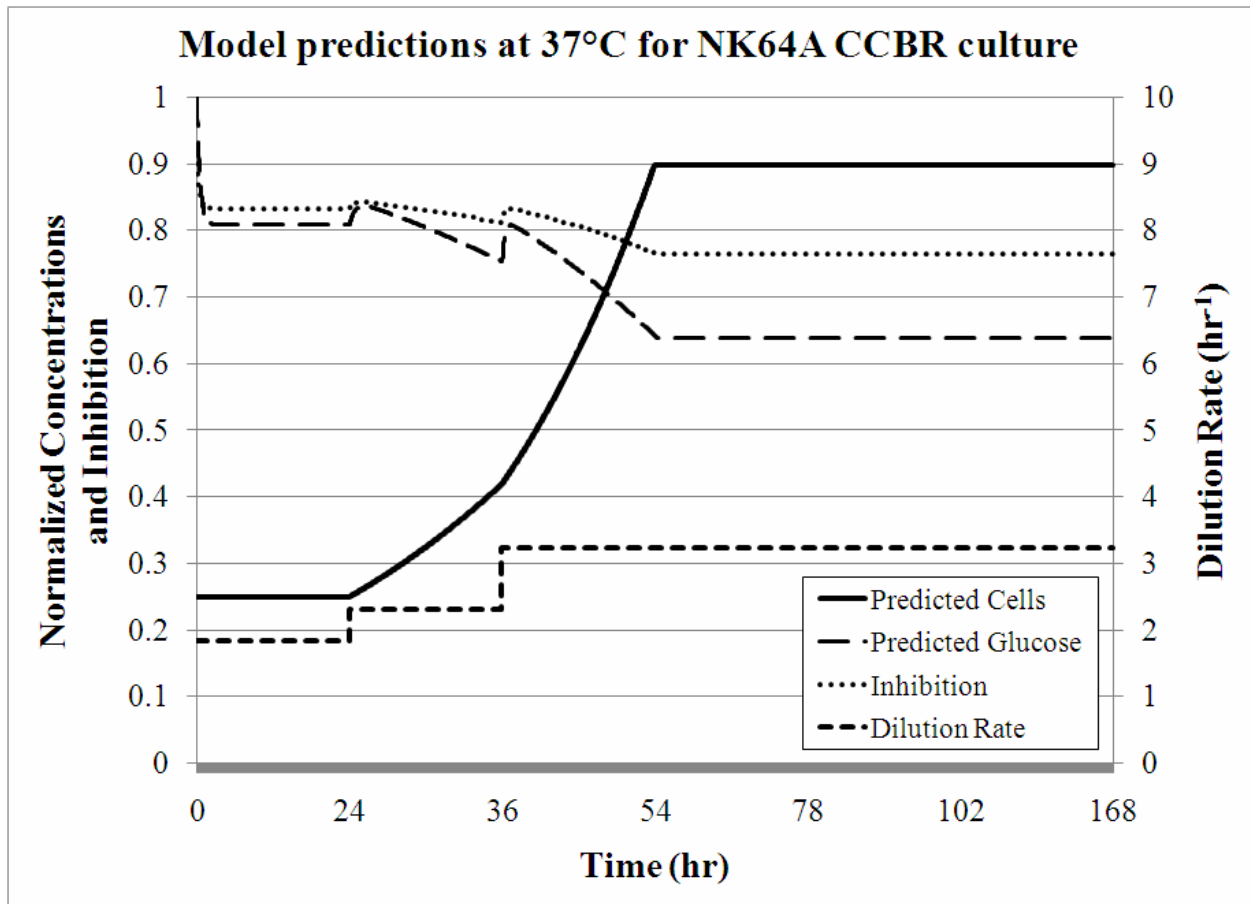


Figure 14: Model predictions for cell and glucose concentrations and collective inhibition effects during NK64A culture in the CCBR at 37°C with an initial cell concentration of 2.50×10^7 cells/mL.

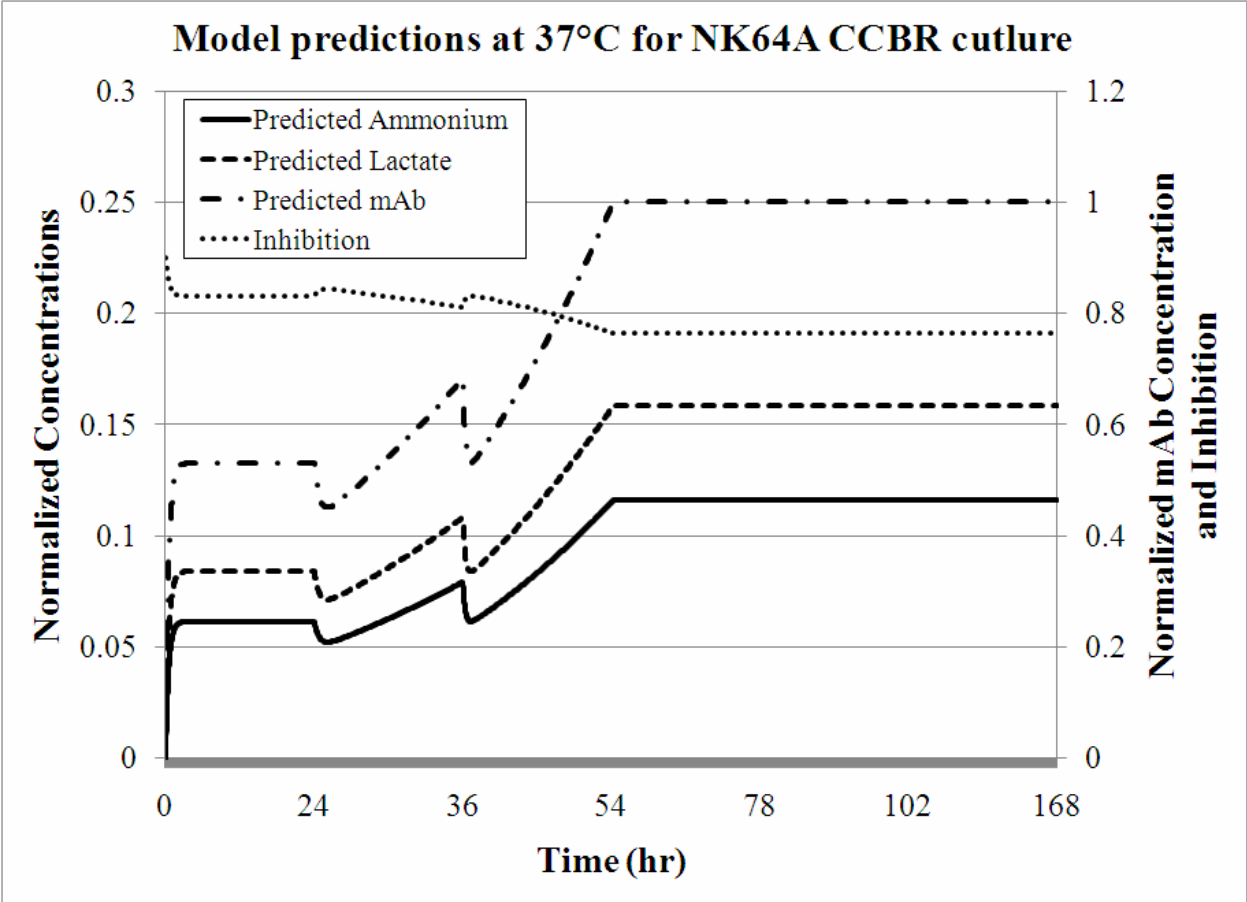


Figure 15: Model predictions for ammonium, lactate, and mAb production and collective inhibition effects during NK64A culture in the CCBR at 37°C with an initial cell concentration of 2.50×10^7 cells/mL.

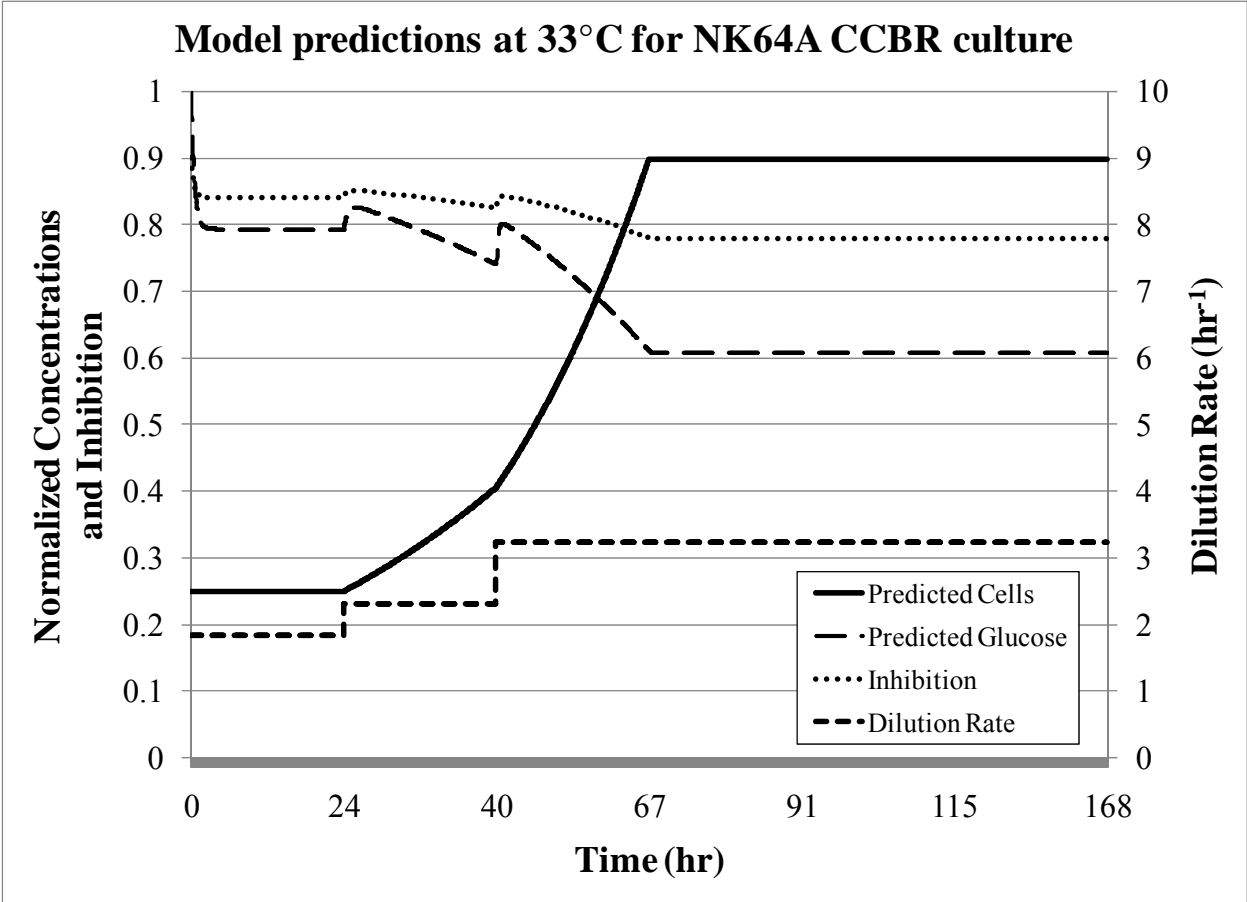


Figure 16: Model predictions for cell and glucose concentrations and collective inhibition effects during NK64A culture in the CCBR at 33°C with an initial cell concentration of 2.50×10^7 cells/mL.

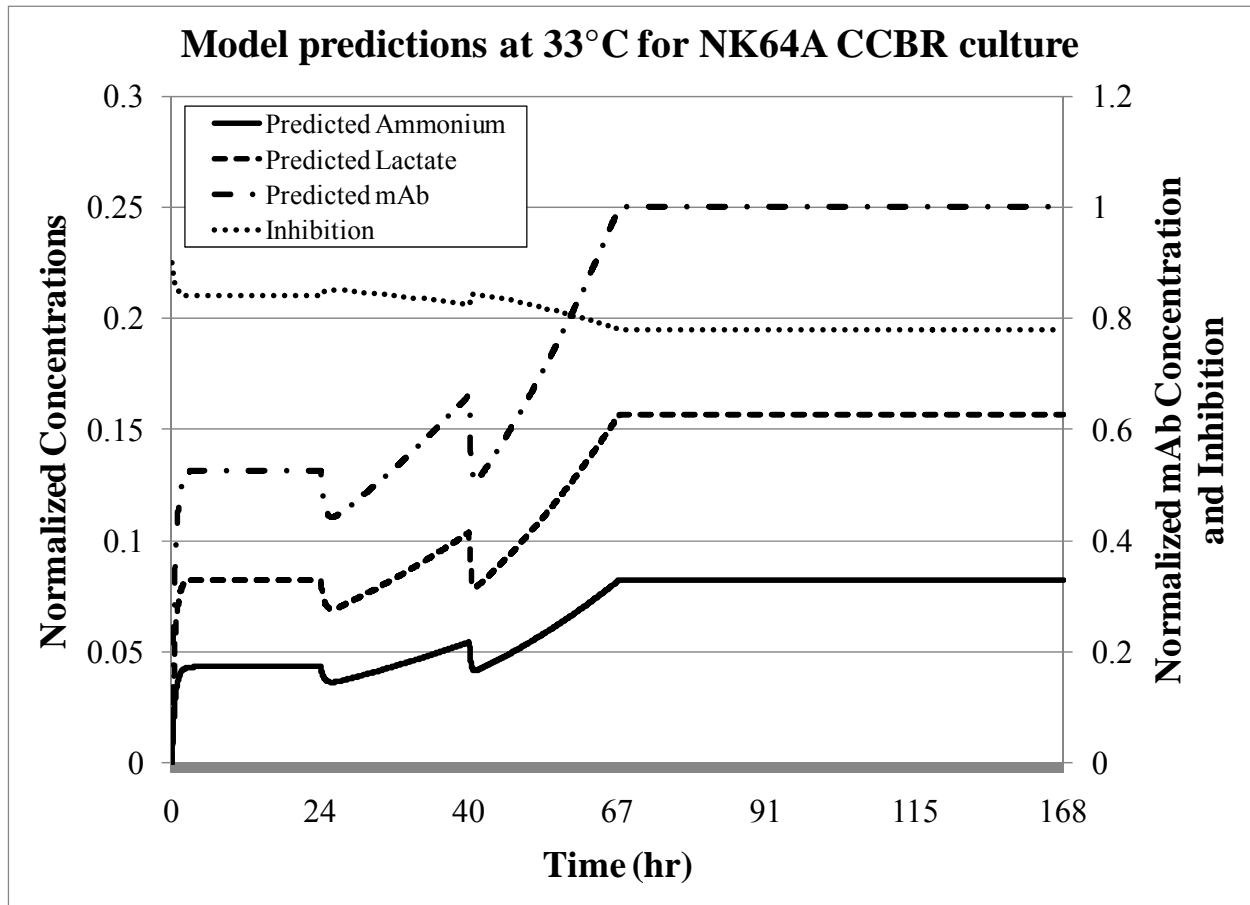


Figure 17: Model predictions for ammonium, lactate, and mAb production and collective inhibition effects during NK64A culture in the CCBR at 33°C with an initial cell concentration of 2.50×10^7 cells/mL.

The time it takes to reach the steady state cell concentration is increased by 13 hours for the 33°C culture compared to the 37°C culture due to the growth rate for the 33°C culture being 67% smaller than the growth rate at 37°C. The model predicts that for the 37°C culture the glucose concentration will drop to 64% of its initial concentration at the end of the exponential growth phase and remains at this concentration for the duration of the culture. For the 33°C culture the minimum glucose concentration is 61% of the initial concentration which is also reached at the end of the exponential growth phase. More glucose is consumed during the 33°C culture

because Y_{GC} for this culture is 20.1×10^{-5} (mg/dL)/(cells/mL) compared to 13.1×10^{-5} (mg/dL)/(cells/mL) for 37°C. The peak concentrations of ammonium and lactate are 12 and 16% of their maximum concentrations for the 37°C culture and 8 and 16% for the 33°C culture respectively. The ammonium yield coefficient is the same at 33°C as it is at 37°C however a higher ammonium concentration is predicted in the 37°C culture. However, even though Y_{LC} is 68% higher at 33°C the model predicts that the same concentration of lactate is produced during both cultures. The maximum mAb concentration reached was 18.6 $\mu\text{g/mL}$ in the 33°C culture compared to 13.3 $\mu\text{g/mL}$ for the 37°C culture. This difference is not as high as expected considering that Y_{mAbC} for 33°C is 2 times higher than the Y_{mAbC} at 37°C. The inhibition factor reached a low of 0.76 for the 37°C culture and a low of 0.78 for the 33°C culture. These results show that culturing the NK64A hybridomas in the CCBR at 33°C results in more mAb production and less inhibition compared to the same culture at 37°C. The only disadvantage is the increase in the time it takes to reach steady state concentration in the reactor for the 33°C culture. This increase in time does not result in a lower mAb production as the total mAb produced at the start of steady state is 42% higher in the 33°C culture than it is in the 37°C culture.

3.6.5. *Model fit to reactor runs*

The pH and temperature profiles for Run 1 are shown in Figure 18. The average pH for the run was 7.06 ± 0.08 .

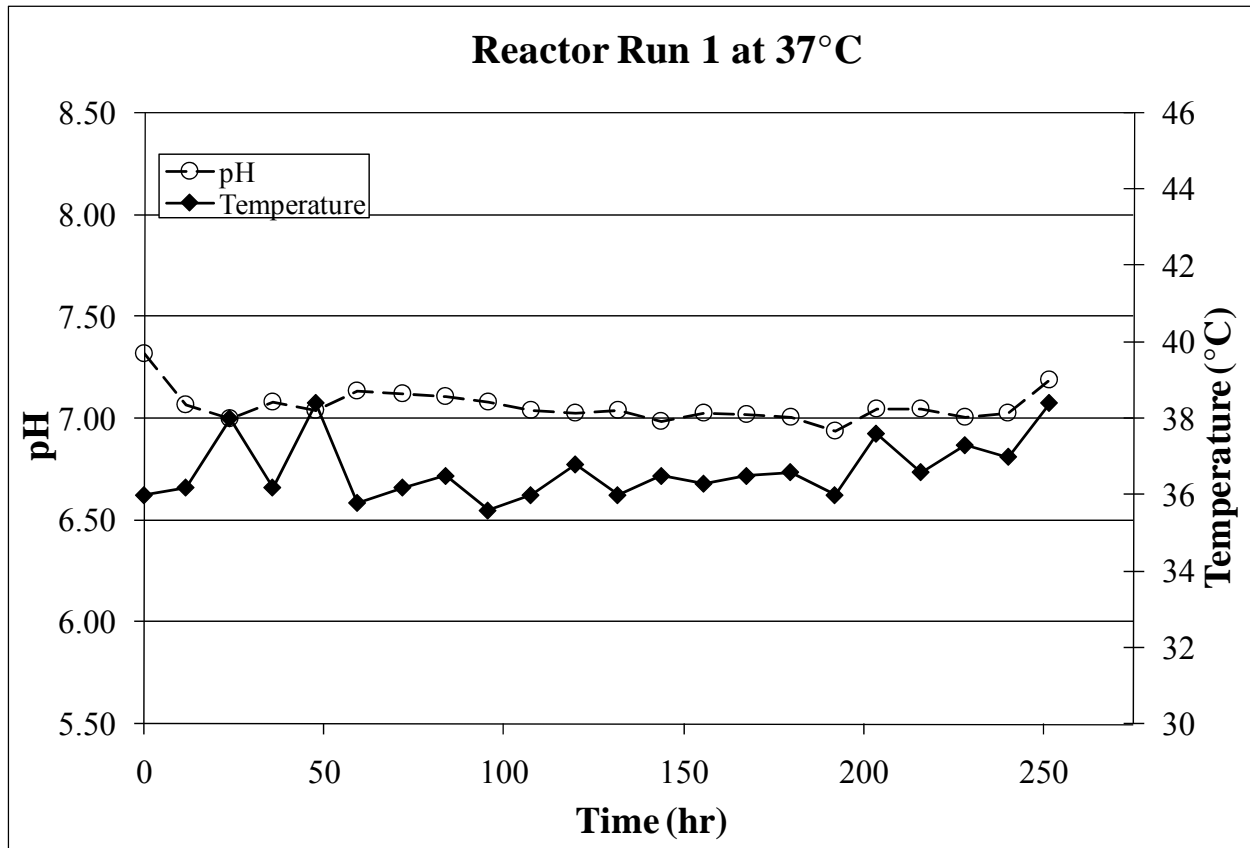


Figure 18: pH and temperature profiles for Run 1 at 37°C.

The growth rate determined by plotting the $\text{Ln}[\text{Cell}]$ vs. time for the reactor is observed to be 0.0039 hr^{-1} about 8% of the 0.052 hr^{-1} value observed for batch cultures at 37°C. The decrease in growth rate could be a result of the high density environment where cell-cell contact, signaling factors, or high localized concentrations of ammonium and lactate due to inefficient mixing cause a decrease in cell growth rate. To adjust for this, the model was re-run using the actual experimental growth rate found for the reactor process. Using the same yield coefficients obtained during the batch study at 37°C predicted reaction progress is plotted in Figures 19 and 20. The inhibition factor was calculated using the model predicted values and remained above 0.83 for the duration of the run. The concentrations were normalized to their maximum values;

400 mg/dL for glucose, 1040 mg/dL for lactate, 13.3 mM for ammonium, and 4.95×10^7 cells/mL for cells.

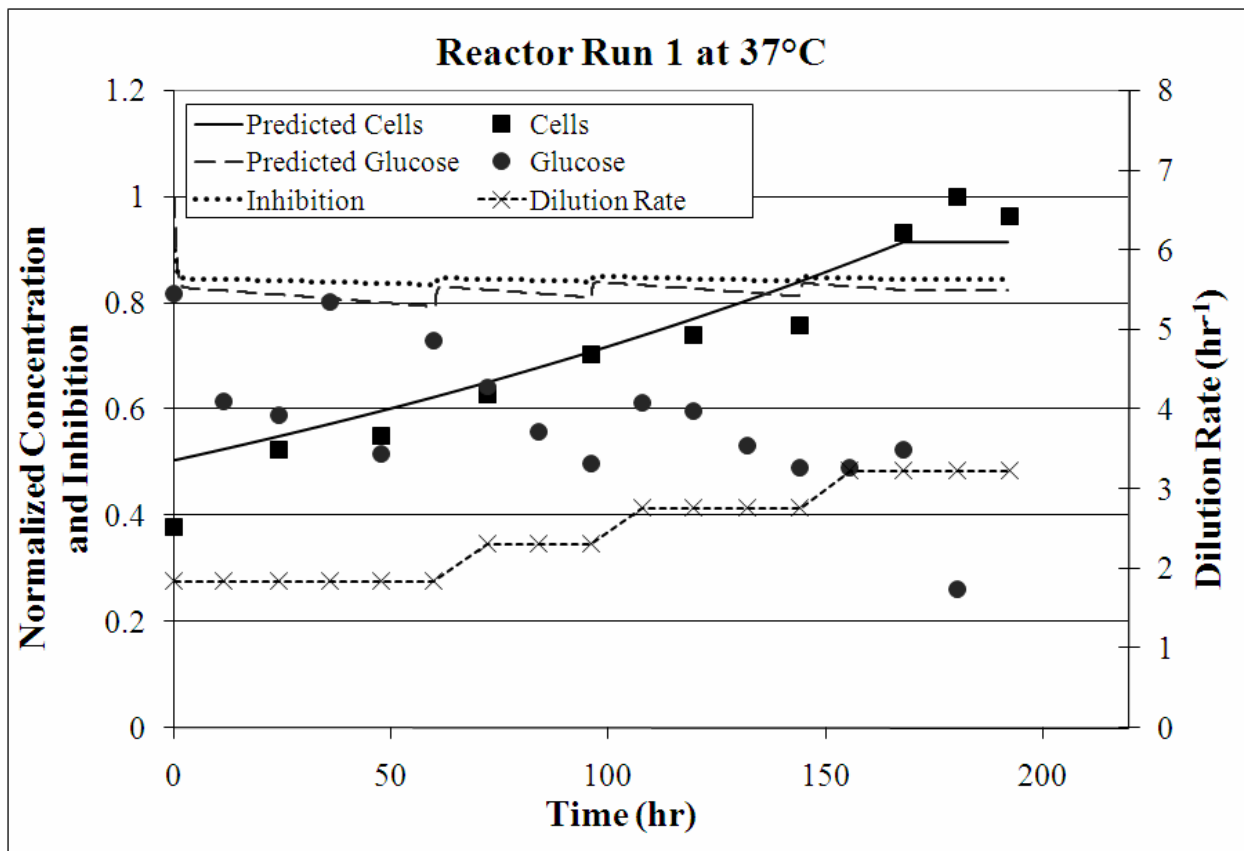


Figure 19: Model fit to the cell and glucose concentration data obtained from Run 1 at 37°C using the growth rate observed in the reactor and the yield coefficients from the 37°C batch study.

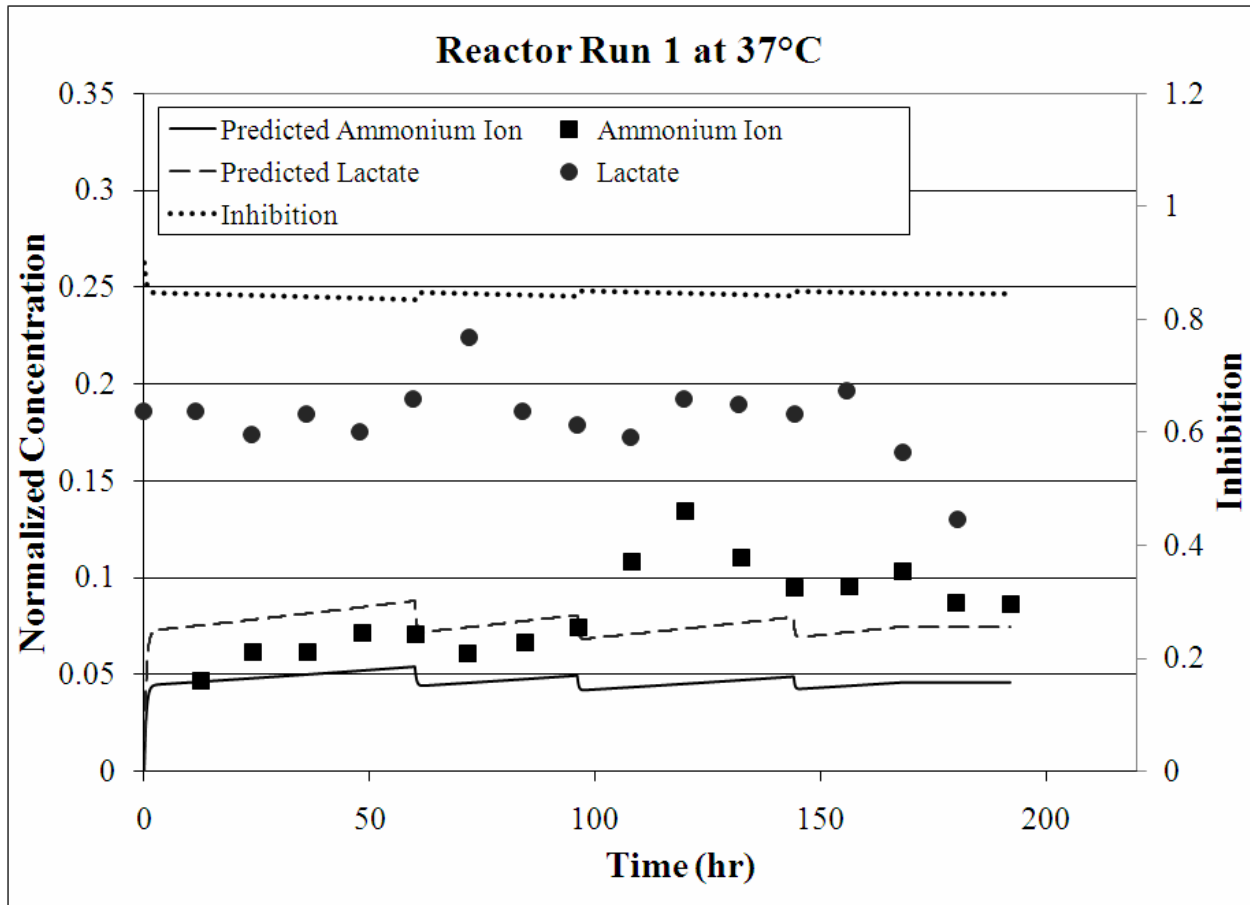


Figure 20: Model fit to the lactate and ammonium concentration data obtained from Run 1 at 37°C using the growth rate observed in the reactor and the yield coefficients from the 37°C batch study.

Even though the model was able to fit the cell growth, with an average deviation of 16%, it was not able to accurately predict the concentrations of glucose, lactate, or ammonium. Since the growth rate was affected by the high density culture it is reasonable to assume that the yield coefficients could be affected in a similar manner. Adjusting the yield coefficients for glucose and lactate by a factor of 2.5 and adjusting the yield coefficient for ammonium by a factor of 2 results in a better fit with average deviations of 21, 12, and 29% of the glucose, lactate, and ammonium data respectively, as illustrated in Figures 21 and 22. For this the inhibition factor

decreases to 0.74 due to an increase in glucose consumption and an increase in the production of lactate and ammonium. This alters the fit of the model to the cell concentration data, however, not significantly as the model and data agree within an average of 13%.

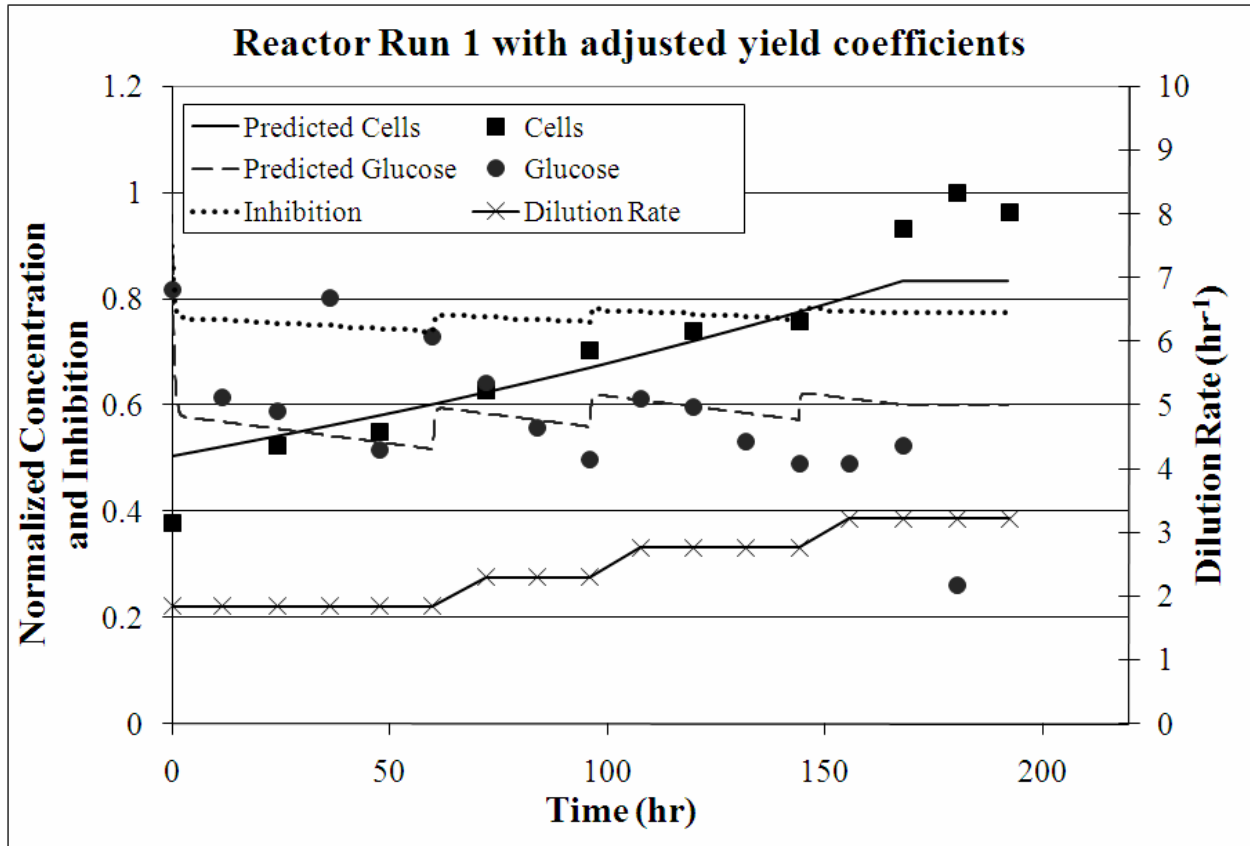


Figure 21: Model fit to the cell and glucose concentration data obtained from Run 1 using the growth rate observed in the reactor and adjusted yield coefficients for glucose, lactate, and ammonium.

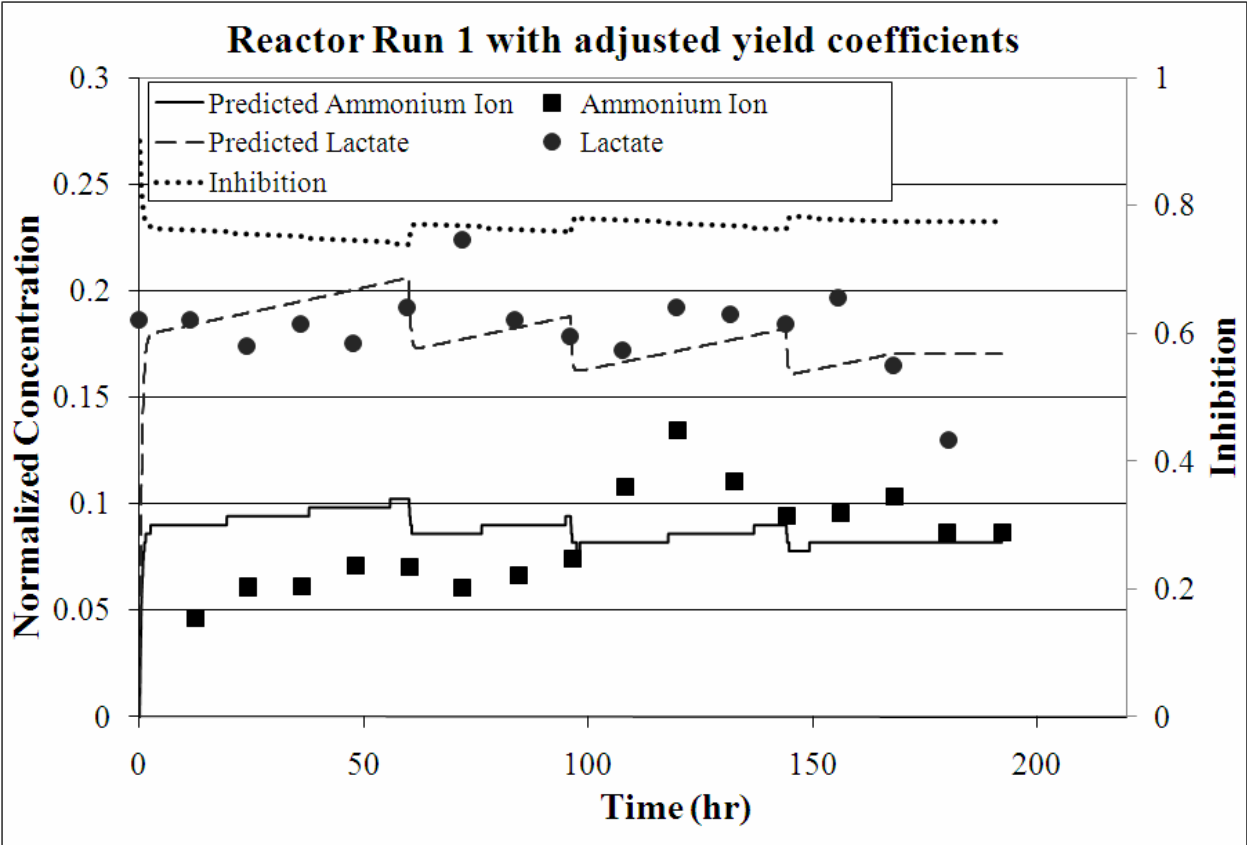


Figure 22: Model fit to the lactate and ammonium concentration data obtained from Run 1 using the growth rate observed in the reactor and adjusted yield coefficients for glucose, lactate, and ammonium.

A second CCBR run was conducted at 33°C and the pH and temperature profiles for Run 2 are shown in Figure 23.

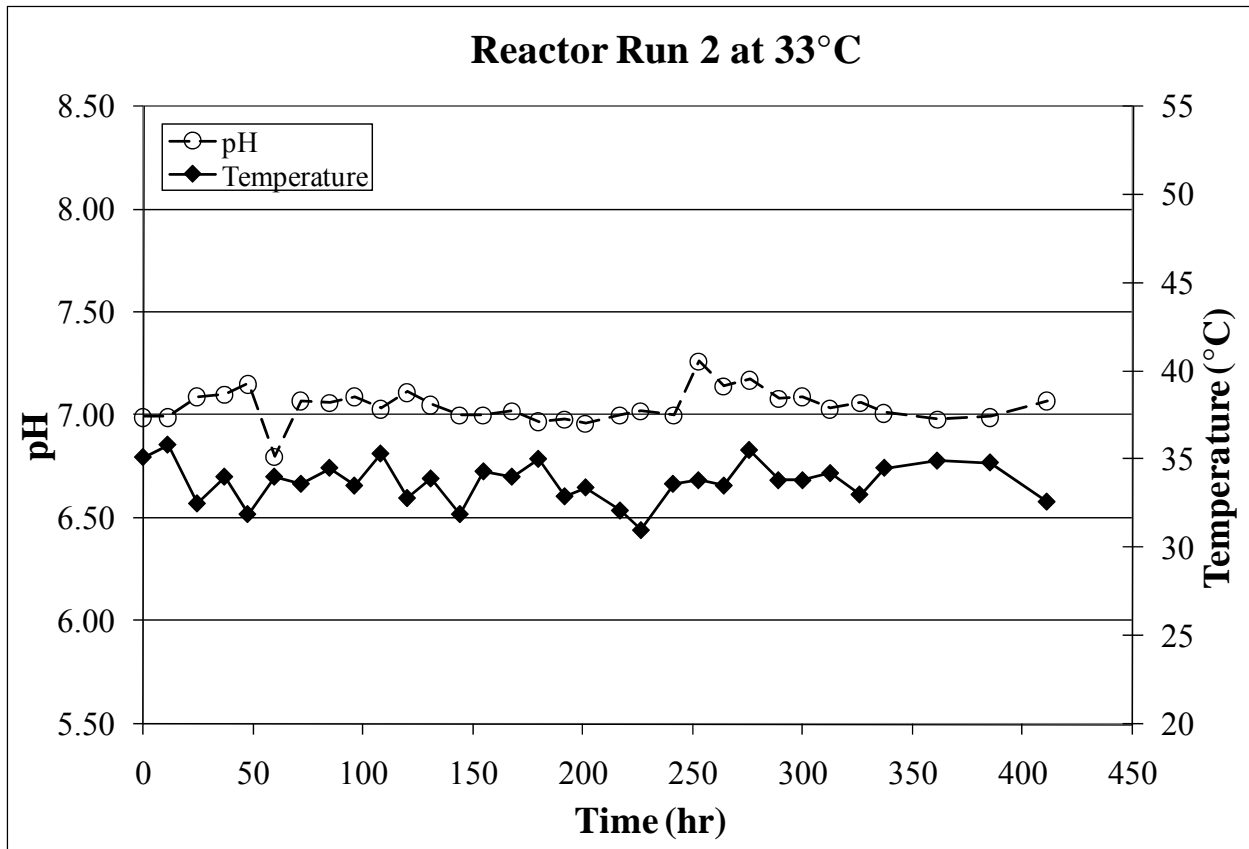


Figure 23: pH and temperature profiles for Run 2 at 33°C.

The growth rate in the reactor was observed to be 0.011 hr^{-1} about 30% of the 0.036 hr^{-1} value observed for the batch culture for 33°C but 65% higher than the 0.0039 hr^{-1} value observed in the CCBR culture at 37°C. Thus it seems that there is some benefit to the lower culture temperature that helps counteract the negative impact of the high density culture. The model was again run using the actual experimental growth rate found for the reactor process. Using the yield coefficients obtained during the batch study at 33°C predicted reaction progress is plotted in Figures 24 and 25. The inhibition factor was calculated using the model predicted values and

remained above 0.88 for the entire run. The concentrations were normalized to their maximum values; 400 mg/dL for glucose, 1040 mg/dL for lactate, 13.3 mM for ammonium, and 5.27×10^7 cells/mL for cells.

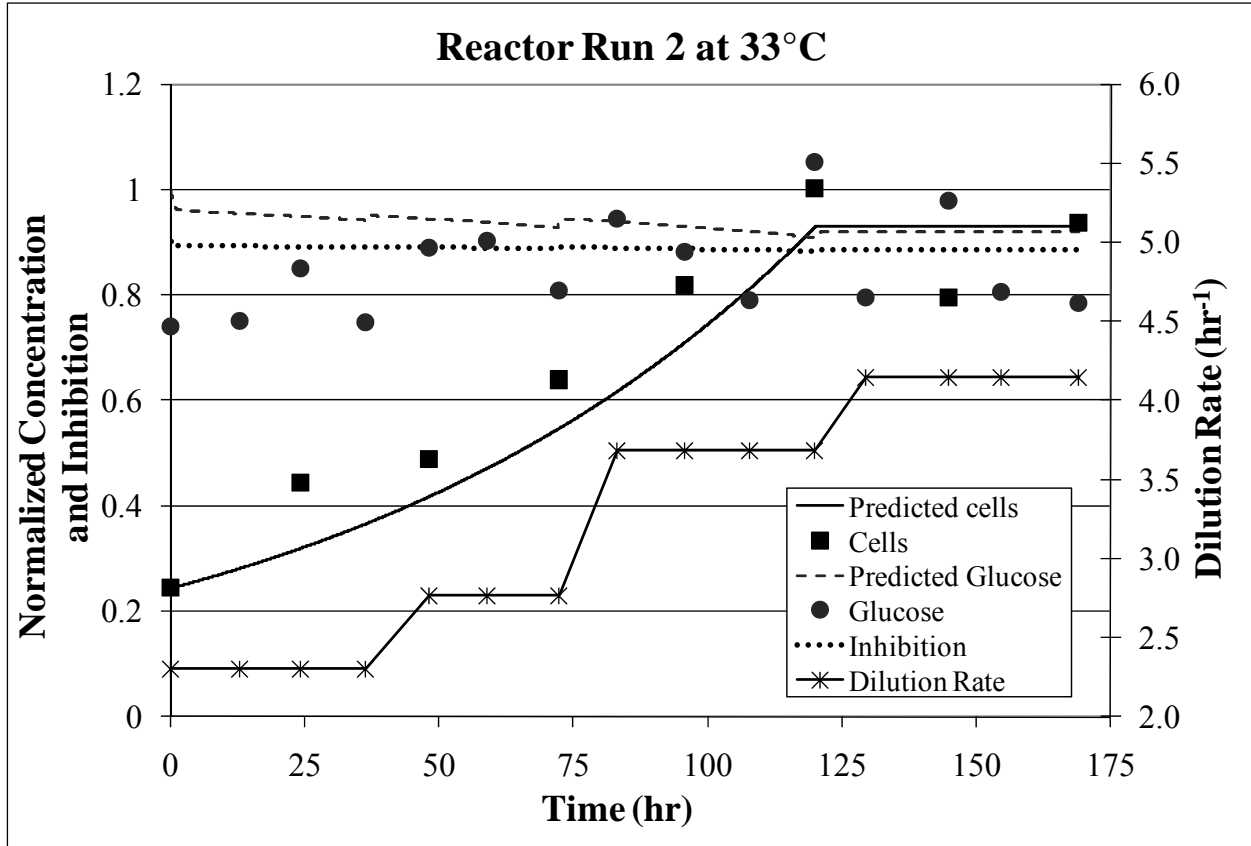


Figure 24: Model fit to the cell and glucose concentration data obtained from Run 2 at 33°C using the growth rate observed in the reactor and the yield coefficients from the 33°C batch study.

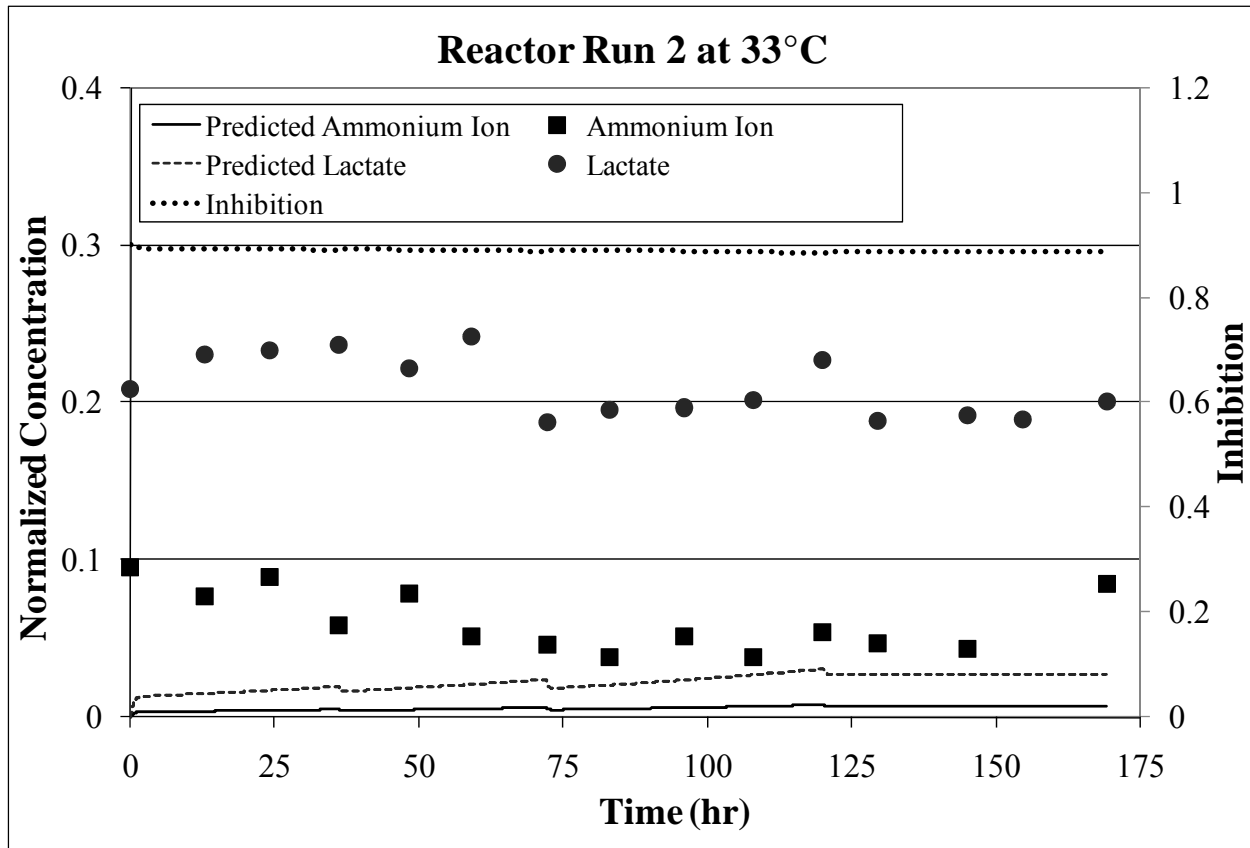


Figure 25: Model fit to the lactate and ammonium concentration data obtained from Run 2 at 33°C using the growth rate observed in the reactor and the yield coefficients from the 33°C batch study.

Once again the model was able to fit the cell growth, with an average deviation of 9%, but it was not able to accurately predict the concentrations of glucose, lactate, or ammonium.

Adjusting the yield coefficient for glucose by a factor of 1.5 and adjusting the yield coefficients for lactate and ammonium by a factor of 10 results in a better fit with average deviations of 11, 22, and 31% of the glucose, lactate, and ammonium data respectively, as illustrated in Figures 26 and 27. For this the inhibition factor decreases to 0.81 for the adjusted yield coefficients due to an increase in glucose consumption and an increase in the production of lactate and ammonium.

This alters the fit of the model to the cell concentration data, however, not significantly as the model and data agree within an average of 16%.

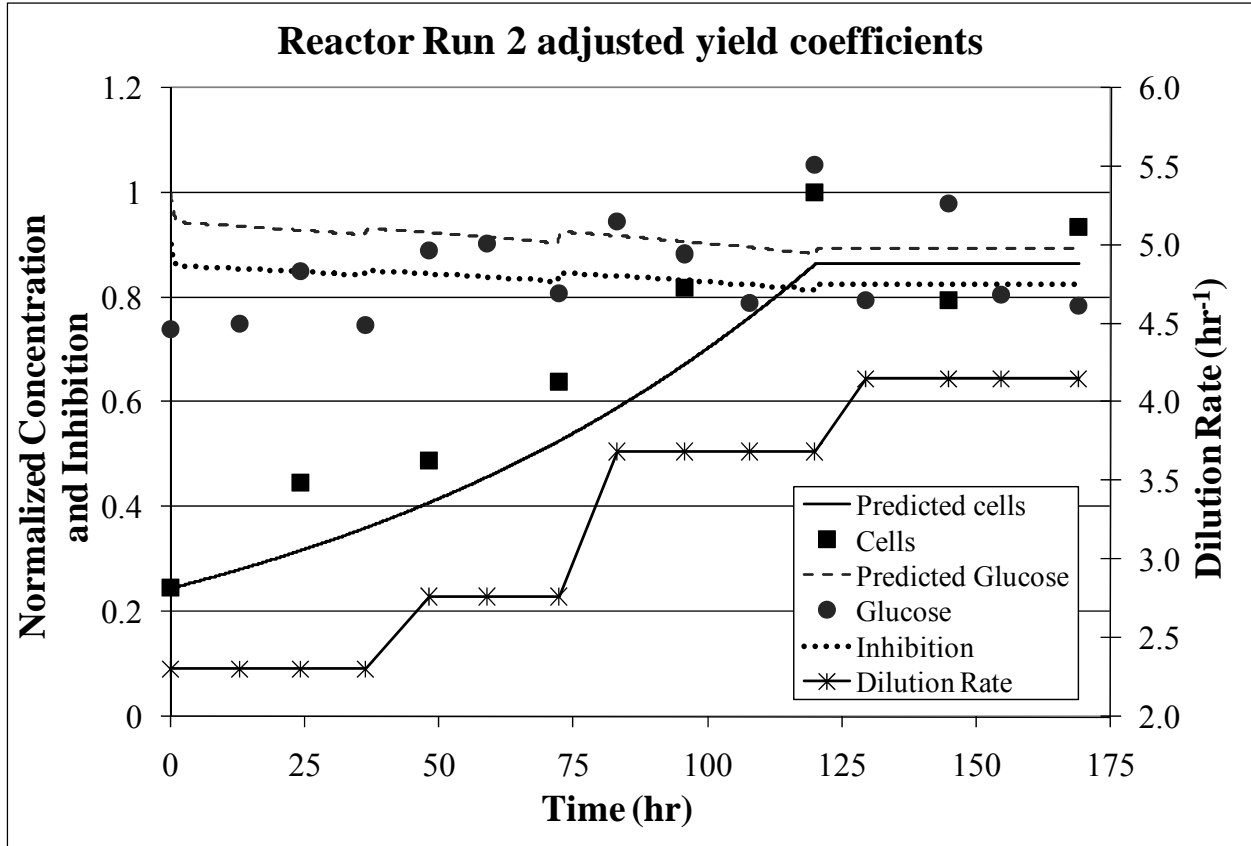


Figure 26: Model fit to the cell and glucose concentration data obtained from Run 2 using the growth rate observed in the reactor and adjusted yield coefficients for glucose, lactate, and ammonium.

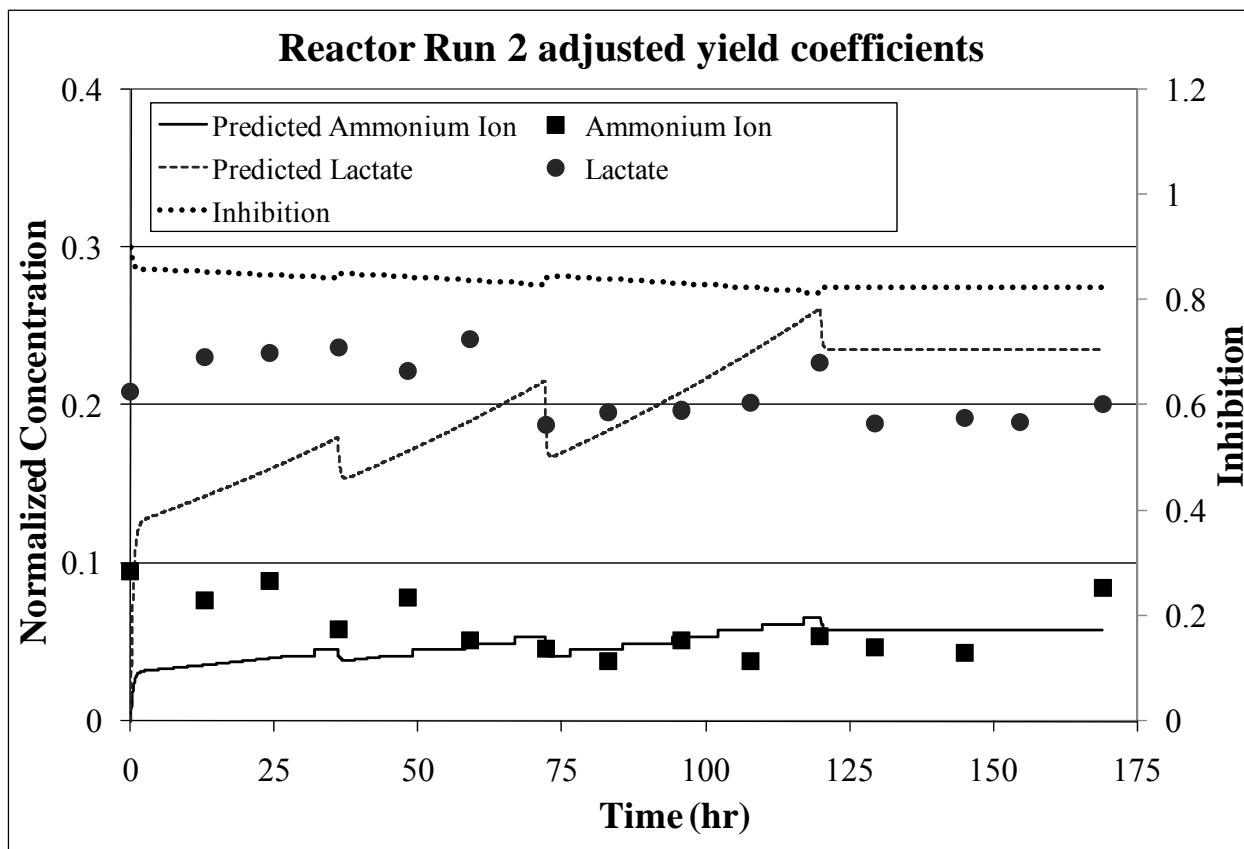


Figure 27: Model fit to the lactate and ammonium concentration data obtained from Run 2 using the growth rate observed in the reactor and adjusted yield coefficients for glucose, lactate, and ammonium.

3.7. Conclusions

In this research, the effect of cell culture temperature on cell growth rate and specific mAb production was studied on the newly developed NK64A hybridoma cell line. From batch studies at temperatures ranging from 31 to 39°C it was determined that the cell growth rate was unchanged between 35 and 39°C with an average value of $0.052 \text{ hr}^{-1} \pm 0.001$, but decreased to a value of 0.036 hr^{-1} for 33°C and 0.026 hr^{-1} for 31°C cultures. The yield coefficients of glucose and lactate increased with an increase in temperature from 31 to 39°C while ammonium

increased from 31 to 35°C and then remained constant up to 39°C. The highest specific mAb production rate was found at 33°C with a value of 2.4 ($\mu\text{g}/\text{mL}$)/(10^5 cells/mL); a 120% increase compared to 37°C with a value of 1.1 ($\mu\text{g}/\text{mL}$)/(10^5 cells/mL). The parameters obtained from the batch studies were used to create a kinetic model to predict glucose, ammonium, lactate, and mAb concentrations during batch and CCBR cultures. Fitting the model to batch data obtained from a 75 mL tissue plate culture resulted in an accurate fit of the cell, lactate, and mAb concentrations but had an error of 62 and 8% for the glucose and ammonium concentrations respectively. Culturing the NK64A hybridoma in the CCBR at temperatures of 37 and 33°C resulted in observed growth rates that were 8 and 30%, respectively, of the observed growth rates in the batch data. Adjusting for this observed growth rate in the kinetic model did not result in an accurate fit of the CCBR data for either run. Additional adjustments of the yield coefficients for glucose, ammonium, and lactate brought the model into agreement with the data. For 37°C the yield coefficients for glucose and lactate were increased by a factor of 2.5 and the yield coefficient for ammonium was increased by a factor of 2. For the 33°C culture the yield coefficient for glucose was increased by a factor of 1.5 and the yield coefficients for ammonium and lactate were increased by a factor of 10. Based on these results it can be concluded that the NK64A hybridoma is highly stressed under the conditions present in the CCBR resulting in an inhibited growth rate and an increased metabolism, indicating that the NK64A hybridoma is not suitable for culture in the CCBR.

When compared to the MM1A hybridoma used in studies by Detzel et al., which is not inhibited by the conditions present in the CCBR, these results indicate that optimum conditions for cell culture are cell line dependent. Future studies on additional NK hybridoma cell lines should be performed to find a cell line that is not inhibited when cultured in the CCBR.

Evaluation of the effect of temperature on this cell line could then be useful in determining the optimum cell culture strategy necessary to obtain maximum mAb production in the high density environment of the CCBR.

3.8. References

- Birch J, Racher A. 2006. Antibody production. *Advanced Drug Delivery Reviews* 58:671-685.
- Bloemkolk J, Gray M, Merchant F, Mosmann T. 1992. Effect of temperature on hybridoma cell cycle and mAb production. *Biotechnology and Bioengineering* 40:427-431.
- Butler M. 2005. Animal cell cultures: recent achievements and perspectives in the production of biopharmaceuticals. *Applied Microbiology and Biotechnology* 68:283-291.
- Chuppa S, Tsai Y, Yoon S, Shackelford S, Rozales C, Bhat R, Tsay G, Matanguihan C, Konstantinov K, Naveh D. 1997. Fermentor temperature as a tool for control of high-density perfusion cultures of mammalian cells. *Biotechnology and Bioengineering* 55(2):328-338.
- Dalm M, Cuijten S, van Grunsven W, Tramper J, Martens D. 2004. Effect of feed and bleed rate on hybridoma cells in an acoustic perfusion bioreactor: Part I. Cell density, viability, and cell-cycle distribution. *Biotechnology and Bioengineering* 88(5):547-557.
- Dalm M, Jansen M, Keijzer T, van Grunsven W, Oudshoorn A, Tramper J, Martens D. 2005. Stable hybridoma cultivation in a pilot-scale acoustic perfusion system: Long-term process performance and effect of recirculation rate. *Biotechnology and Bioengineering* 91(7):894-900.
- Dalm M, Lamers P, Cuijten S, Tjeerdsma A, van Grunsven W, Tramper J, Martens D. 2007. Effect of feed and bleed rate on hybridoma cells in an acoustic perfusion bioreactor: Metabolic analysis. *Biotechnology Progress* 23:560-569.
- Detzel C, Mason D, Davis W, Van Wie B. 2008. Optimization of a centrifugal bioreactor for high population density hybridoma culture. *Biotechnology Progress* Submitted.
- Doyle C, Butler M. 1990. The effect of pH on the toxicity of ammonia to a murine hybridoma. *Journal of Biotechnology* 15(1-2):91-100.
- Farid S. 2006. Established bioprocesses for producing antibodies as a basis for future planning. *Advances in Biochemical Engineering/Biotechnology* 101:1-42.
- Fox S, Patel U, Yap M, Wang D. 2004. Maximizing interferon- γ production by chinese hamster ovary cells through temperature shift optimization: Experimental and modeling. *Biotechnology and Bioengineering* 85(2):177-184.
- Han K, Levenspiel O. 1988. Extended Monod kinetics for substrate, product, and cell inhibition. *Biotechnology and Bioengineering* 32:430-437.
- Jain E, Kumar A. 2008. Upstream processes in antibody production: Evaluation of critical parameters. *Biotechnology Advances* 26:46-72.
- Mason D. 2004. Hybridoma culture and modeling in a centrifugal bioreactor. Pullman: Washington State University.
- Morrow KJ. 2007. Advances in antibody manufacturing using mammalian cells. *Biotechnology Annual Review* 13:95-113.
- Sureshkumar G, Mutharasan R. 1991. The influence of temperature on a mouse-mouse hybridoma growth and monoclonal antibody production. *Biotechnology and Bioengineering* 37:292-295.
- Van Wie B, Brouns T, Elliott M, Davis W. 1991. A novel continuous centrifugal bioreactor for high-density cultivation of mammalian and microbial cells. *Biotechnology and Bioengineering* 38:1190-1202.
- Van Wie B, Elliott M, Lee J. 1986. Development and characterization of a continuous centrifugal bio-reactor. *Biotechnology and Bioengineering Symposium* 17:335-344.

- Van Wie B, Hustvedt E. 1988. Particle interaction effects on blood cell sedimentation and separations. *Biorheology* 25:651-662.
- Yoon S, Hwang S, Lee G. 2004. Enhancing effect of low culture temperature on specific antibody productivity of recombinant chinese hamster ovary cells: Clonal variation. *Biotechnology Progress* 20:1683-1688.

CHAPTER FOUR

GENERAL CONCLUSIONS AND FUTURE WORK

The availability of the anti-CD335 mAb facilitated the development of additional mAbs to molecules expressed on the surface of bovine NK cells. Flow cytometric analysis using the anti-CD335 mAb and mAbs to common T cell markers resulted in the identification of two new mAb clusters. Cluster 1, containing mAbs NK64A and NK93A, recognizes the bovine orthologue of the stress protein gp96 expressed by bovine granulocytes and NK cells. Cluster 2, containing mAbs NK29A, NK42A, NK47A, NK86A, NK134A, and NK137A, recognizes a yet undetermined molecule expressed by activated NK cells and subsets of $\alpha\beta$ and $\gamma\delta$ T cells including both CD4 and CD8 positive cells. Cluster 1 and Cluster 2 mAbs add to the tools available for bovine NK cell research and will aid in developing additional mAbs to further understand these valuable cells and the role they play in the innate immunity of cattle. Further work must be done to identify the molecule recognized by Cluster 2 and help understand the role it plays when expressed by activated NK cells and subsets of T cells.

Kinetic studies performed on the newly created NK64A hybridoma cell line facilitated the development of a kinetic model to describe cell growth in both batch and high-density CCBR cultures. Inhibition studies determined the maximum ammonium and lactate concentrations at which no cell growth occurs to be 13.3 mM and 10.4 mg/mL respectively. Batch cultures performed over a range of temperatures, 31 to 39°C, resulted in a constant growth rate between 35 and 39°C with an average value of $0.052 \text{ hr}^{-1} \pm 0.001$ and a decrease in growth rate to 0.036 hr^{-1} for 33°C and 0.026 hr^{-1} for 31°C. Yield coefficients showed a possible Arrhenius trend with the yield coefficients for glucose and lactate increasing with an increase in temperature from 31 to 39°C. The ammonium yield coefficient increased from 31 to 35°C then was constant at an

average value of $0.14 \text{ mM}/10^5 \text{ cells/mL}$ up to 39°C . The yield coefficient for mAb was highest at 31 and 33°C then decreased by a factor of 2 for 37 and 39°C .

Applying the kinetic model to a 75 mL batch culture at 37°C resulted in a fit for cell, lactate, ammonium, and mAb concentrations with average deviations of 26, 10, 16, and 8% respectively. Glucose concentrations were not accurately modeled having an average deviation as high as 62%. CCBR cultures performed at 37°C (Run 1) and 33°C (Run 2) showed a decrease in the observed growth rate to values that were 8 and 30% of the growth rates observed in the batch cultures. Adjusting the models for each culture to the new observed growth rates for the reactor resulted in fits for the cell concentrations with deviations of 13 and 16% for Run 1 and Run 2 respectively but fits to glucose, lactate, and ammonium concentrations were off in some cases by more than 100%. Adjusting the yield coefficients for each species improved the fit of the model for both runs. Average deviations for Run 1 were less than 29% and for Run 2 less than 31% with the adjusted yields.

These preliminary results indicate that a 100% increase in mAb production for batch cultures can be obtained for the NK64A hybridoma cell line by decreasing the culture temperature from 37°C to 33°C . The results obtained for the 35°C culture are skeptical and much benefit would be gained by repeating this experiment at all temperatures to obtain consistent data that will allow accurate conclusions to be drawn. Since several new hybridoma cell lines were developed that produce mAbs to bovine NK cells, it would be interesting to evaluate more of these cell lines to determine if there is a consistent trend of an increase in mAb production with a decrease in culture temperature. It would be especially interesting to study the NK93A cell line due to the fact that it produces the same mAb as the NK64A hybridoma. Perhaps the NK93A hybridoma

would be more conducive to culture in the high-density environment of the CCBR than the NK64A hybridoma.